

THE INHIBITION OF MAMMARY EPITHELIAL CELL GROWTH BY THE LONG
ISOFORM OF ANGIOMOTIN

Jacob J. Adler

Submitted to the faculty of the University Graduate School
in partial fulfillment of the requirements
for the degree
Doctor of Philosophy
in the Department of Biochemistry and Molecular Biology,
Indiana University

December 2013

Accepted by the Graduate Faculty, of Indiana University, in partial fulfillment of the requirements for the degree of Doctor of Philosophy.

Doctoral Committee

Clark D. Wells, Ph.D., Chair

Maureen A. Harrington, Ph.D.

Harikrishna Nakshatri, Ph.D.

November 1, 2013

Ronald C. Wek, Ph.D.

© 2013

Jacob J. Adler

DEDICATION

I dedicate this dissertation to my family, especially my wife, Emily C. Adler, and to my parents, Jeffrey and Cynthia Adler. Their dedication to my education, through many avenues, including prayers and love, supported me in the completion of this work.

ACKNOWLEDGMENTS

I would like to acknowledge those whose support and guidance helped finish this work. Specifically, Dr. Clark Wells was always present and supported ideas and thoughts, even when they seemed counter to a present logical pathway in the scientific community. I give him gratitude for keeping me motivated and engaged, including going as far as helping me obtain external funding for this work through the National Science Foundation's GK-12 Program.

I am also thankful to the members of my committee, whose support was essential for my focus. Specifically, I wish to thank Dr. Harikrishna Nakshatri for sharing his expertise in mammary tissue architecture and his many gifts of reagents, Dr. Maureen Harrington for her encouragement and help with identifying important project themes and reagents, and Dr. Ronald Wek for his expertise with transcriptional assays, enthusiasm about the project, encouragement, and reagents.

I am very grateful for the encouragement and active collaboration on this work from my lab mates Dr. Bill Ranahan, Lauren Bringman, Brandon Lane, Brigitte Heller, and Whitney Smith-Kinnaman. Further, this work would not be complete without active help from scientists like Derrick Johnson and Drs. Robert Ingham, Mark Goebel, Ross Cocklin, and Andy Hudmon, and all who made major discoveries within the context of this work. I also appreciate other students and scientists for their constant help throughout, especially those involved with the GK-12 Program. Additionally, my high school students were invaluable for allowing me to expand my research into their classrooms and development of my professional scientific skills.

I would like to thank the entire Biochemistry Department office staff, especially Jack Arthur, who provided key computer-related solutions to numerous problems, helpful career advice, and a kind ear for listening.

This work was funded through Department of Defense and National Institute of Health grants to Clark D. Wells and a National Science Foundation grant to me and Kathleen A. Marrs.

ABSTRACT

Jacob J. Adler

THE INHIBITION OF MAMMARY EPITHELIAL CELL GROWTH BY THE LONG ISOFORM OF ANGIOMOTIN

Mammary ductal epithelial cell growth is controlled by microenvironmental signals in serum under both normal physiological settings and during breast cancer progression. Importantly, the effects of several of these microenvironmental signals are mediated by the activities of the tumor suppressor protein kinases of the Hippo pathway. Canonically, Hippo protein kinases inhibit cellular growth through the phosphorylation and inactivation of the oncogenic transcriptional co-activator Yes-Associated Protein (YAP). This study defines an alternative mechanism whereby Hippo protein kinases induce growth arrest via the phosphorylation of the long isoform of Angiomotin (Amot130). Specifically, serum starvation is found to activate the Hippo protein kinase, Large Tumor Suppressor (LATS), which phosphorylates the adapter protein Amot130 at serine-175. Importantly, wild-type Amot130 potently inhibits mammary epithelial cell growth, unlike the Amot130 serine-175 to alanine mutant, which cannot be phosphorylated at this residue. The growth-arrested phenotype of Amot130 is likely a result of its mechanistic response to LATS signaling. Specifically, LATS activity promotes the association of Amot130 with the ubiquitin ligase Atrophin-1 Interacting Protein 4 (AIP4). As a consequence, the Amot130-AIP4 complex amplifies LATS tumor suppressive signaling by stabilizing LATS protein steady state levels via preventing AIP4-targeted degradation of LATS. Additionally, AIP4 binding to Amot130 leads to the ubiquitination and stabilization of Amot130. In turn, the Amot130-AIP4 complex signals the ubiquitination and degradation of YAP. This inhibition of YAP activity by Amot130 requires both AIP4 and the ability of Amot130 to be phosphorylated by LATS. Together, these findings significantly modify

the current view that the phosphorylation of YAP by Hippo protein kinases is sufficient for YAP inhibition and cellular growth arrest. Based upon these results, the inhibition of cellular growth in the absence of serum more accurately involves the stabilization of Amot130 and LATS, which together inhibit YAP activity and mammary epithelial cell growth.

Clark D. Wells, Ph.D., Chair

TABLE OF CONTENTS

List of Figures	x
List of Abbreviations	xii
 Chapter 1	
Introduction	1
1.1. Organization of the Mammary Organ, Mammary Organogenesis, and the Origins of Breast Cancer	2
1.2. Serum Factors and Their Roles in Epithelial Cell Growth.....	8
1.3. Hippo Signaling and Its Role in Epithelial Cell Growth.....	11
1.4. The Angiotensins and Their Roles Epithelial Cell Growth and Hippo Signaling	19
1.5. The Nedd4 Ubiquitin Ligases and Their Roles in Epithelial Cell Growth.....	24
1.6. Cell Lines and Model Systems Used in This Study	31
1.7. Rationale and Central Focus.....	35
 Chapter 2	
Materials and Methods	37
 Chapter 3	
The Long Isoform of Angiotensin is Phosphorylated by the LATS1 and LATS2 Protein Kinases and Inhibits Growth in Mammary Epithelial Cells.....	53
3.1. Introduction	54
3.2. Results	55
3.2.1. Serum Deprivation and LATS1 Protein Impact the Protein Levels of Amot130 ...	55
3.2.2. Amot130 is Phosphorylated by LATS1 and LATS2 at Serine Residue 175	60
3.2.3. The Mutant Amot130 (S175A) Lacks the Ability of Wild-type Amot130 to Inhibit the Growth of Breast Cancer Cells and Mammary Acini	64
3.3. Discussion	68
3.3.1. A Novel Substrate for LATS1/2 in Hippo Signaling	68
3.3.2. Proposed Mechanism of Amot130 Inhibition of Mammary Epithelial Cell Growth in Response to LATS1/2 Activity	69
 Chapter 4	
Serum Deprivation and LATS1 Protein Kinase Activity Lead to Increased Steady State Protein Levels of the Long Isoform of Angiotensin via the Nedd4 Ubiquitin Ligase AIP4 ...	71
4.1. Introduction	72
4.2. Results	73
4.2.1. Amot130 Directly Binds AIP4.....	73
4.2.2. Serum Starvation and LATS1 Activity Enhances the Association of AIP4 with Amot130	77
4.2.3. Amot130 is Ubiquitinated by AIP4	79
4.2.4. Amot130 is Ubiquitinated at Lysine Residue 481	84
4.2.5. Amot130 Protein Levels are Stabilized by AIP4	86
4.3. Discussion	92
4.3.1. Stabilization of Amot130 by AIP4	92

4.3.2. Amot130 Phosphorylation by LATS1 Increases the Stability of Amot130 by Promoting AIP4 Binding and Ubiquitination of Amot130.....	94
Chapter 5	
The Long Isoform of Angiotensin and AIP4 Cooperatively Inhibit the Transcription of YAP-Dependent Genes	96
5.1. Introduction	97
5.2. Results	98
5.2.1. Amot130 Repurposes AIP4 from LATS1 Degradation to the Ubiquitination of YAP.....	98
5.2.2. The Ability of Amot130 to be Phosphorylated at Serine Residue 175 Allows for Amot130 to Reduce the Stability of YAP	105
5.2.3. The Amot130-AIP4 Complex Mediates the Inhibition of YAP by LATS	109
5.3. Discussion	113
5.3.1. The YAP-Amot130-AIP4 Complex Formation and Its Inhibition of YAP Activity	113
5.3.2. The Essential Role of Amot130 in Reinforcing YAP Inhibition	113
5.3.3. Phosphorylation of Serine Residue 127 on YAP is not Sufficient for YAP Inhibition via Serum Starvation.....	116
Chapter 6	
Concluding Remarks on the Role of the Long Isoform of Angiotensin in Growth Signaling in Mammary Epithelial Cells	118
6.1. Introduction	119
6.2. Influencing Angiotensins and Their Impact on Signaling	119
6.2.1. The Role of Serum Factors in Angiotensin Signaling.....	119
6.2.2. The Similarities and Differences Between the Angiotensins.....	122
6.2.3. The Role of Angiotensin in Mammary Tissue	123
6.2.4. The Involvement of the Angiotensins in Viral Signaling	124
6.2.5. Promoting <i>AMOT</i> Transcription via Microenvironmental Elements in Mammary Tissue	125
6.2.6. Regulation of the Angiotensins into the Nucleus.....	128
6.3. The Dual Role of AIP4 in Mammary Epithelial Cell Growth.....	132
6.4. The Multiple Mechanisms of YAP Ubiquitination	133
6.5. Conclusion.....	134
Appendix – Nucleotide Sequences and Cloning Strategies	135
References.....	138
Curriculum Vitae	

LIST OF FIGURES

Figure 1-1	Organization of the Breast	5
Figure 1-2	Normal Mammary Gland Organogenesis	6
Figure 1-3	Progression of Invasive Ductal Carcinoma in the Breast	7
Figure 1-4	Brief Overview of Serum Factors LPA, S1P, and EGF Signaling Pathways	10
Figure 1-5	Overview of Hippo Signaling in Mammals	16
Figure 1-6	The Functional Regions of the Transcriptional Co-activators YAP and TAZ	17
Figure 1-7	Comparison of Upstream Effectors of Canonical Hippo Signaling in <i>Drosophila</i> Versus Mammals	18
Figure 1-8	A Schematic Diagram of the Angiotensin Family	22
Figure 1-9	The Role of Angiotensin in the Inhibition of YAP and TAZ Nuclear Activity	23
Figure 1-10	Overview of the Process of Ubiquitination of a Target Protein	28
Figure 1-11	Conserved Domains of the Nedd4 Family of Ubiquitin Ligases in Humans	29
Figure 1-12	Adapter Proteins Increase the Activity of Nedd4 Ubiquitin Ligases	30
Figure 1-13	Growth Conditions of Mammary Epithelial Cells	34
Figure 3-1	Correlation of Amot130 Protein and Hippo Signaling Components Under Serum Starvation Conditions	57
Figure 3-2	Serum Starvation Conditions Increase Amot130 Steady State Protein Levels	58
Figure 3-3	Loss of LATS1 Protein Decreases Amot130 Steady State Protein Levels	59
Figure 3-4	LATS1 and LATS2 Phosphorylate Amot130 at Serine-175	62
Figure 3-5	LATS1 Phosphorylation of Amot130 at Serine-175 Promotes Binding of the 14-3-3 γ Protein	63
Figure 3-6	Ability of Amot130 to be Phosphorylated at Serine-175 is Essential for Amot130 to Inhibit the Growth of Cancer Cells	66
Figure 3-7	Ability of Amot130 to be Phosphorylated at Serine-175 is Essential for Amot130 to Regulate the Growth of Mammary Acini	67
Figure 3-8	Working Model for Serum Starvation Inhibition of Cell Growth	70
Figure 4-1	Nedd4 Family of Ubiquitin Ligases Differentially Bind Amot130	75
Figure 4-2	WW Domains of AIP4 Directly Bind Amot130 Specific P-Y Motifs	76
Figure 4-3	Amot130 Binding to AIP4 is Enhanced by Serum Starvation and Requires LATS1 Activity	78
Figure 4-4	AIP4 Ubiquitinates Amot130	81
Figure 4-5	LATS1 Activity Enhances AIP4 Ubiquitination of Amot130	82
Figure 4-6	Amot130 Binding to AIP4 Activates the AIP4 Ligase	83
Figure 4-7	Amot130 is Ubiquitinated at Lysine-481 by AIP4	85
Figure 4-8	Amot130 Stability is Increased by AIP4	89
Figure 4-9	Two Amot130 Mutants, (K481R) and (S175A), Have Similarly Reduced Protein Stability	90
Figure 4-10	Two Amot130 Mutants, (K481R) and (S175A), Have Similarly Altered Subcellular Localization	91
Figure 4-11	Working Model for Serum Starvation Inhibition of Cell Growth	95
Figure 5-1	Amot130 Prevents AIP4-Mediated LATS1 Degradation	101
Figure 5-2	YAP is in a Complex with AIP4 and Amot130	102
Figure 5-3	YAP is Ubiquitinated by the Amot130-AIP4 Complex	103
Figure 5-4	Serum Starvation and Ability of Amot130 to be Phosphorylated at Serine-175 Enhances YAP Ubiquitination by the Amot130-AIP4 Complex	104
Figure 5-5	Amot130 Expression Induces YAP Degradation	107

Figure 5-6	Wild-type Amot130 and Mutant Amot130 (S175A) Promote Different Subcellular Distributions of YAP	108
Figure 5-7	Amot130 Inhibits YAP-Dependent Transcription Cooperatively with AIP4	111
Figure 5-8	Amot130 Mediates the Inhibition of YAP-Dependent Transcription by LATS	112
Figure 5-9	Proposed Cyclic Model for Amot130 and LATS1 Inhibition of YAP-Dependent Transcription	115
Figure 5-10	An Alternative Mechanism for Serum Starvation Inhibition of Cellular Growth	117
Figure 6-1	Serum Starvation Increases Amot80 Steady State Protein Levels	121
Figure 6-2	Possible Transcription Factor Binding Sites for Promoting <i>AMOT</i> Transcription	127
Figure 6-3	The Role of Nuclear Amot130 in YAP-Dependent Transcription	131

LIST OF ABBREVIATIONS

ACCH	Amot coiled-coil homology
AIP4	Atrophin-1 Interacting Protein 4
Amot	Angiomotin
Amot80	80-kDa Angiomotin protein isoform
Amot130	130-kDa Angiomotin protein isoform
AmotL1	Angiomotin-like 1
AmotL2	Angiomotin-like 2
ATCC	American Type Culture Collection
ATP	Adenosine triphosphate
BCA	Bicinchoninic acid
BCL10	B-cell lymphoma/leukemia 10 protein
BSA	Bovine serum albumin
C2	Ca ²⁺ -regulatory
cDNA	Complimentary DNA
CFP	Cerulean fluorescent protein
CHX	Cycloheximide
Crb	Crumb
C-terminus	Carboxyl terminus
CTGF	Connective tissue growth factor
Cyr61	Cysteine-rich angiogenic inducer 61
DACHS	Dachsous protein
DAPI	4', 6-diamidino-2-phenylindole
DCIS	Ductal carcinoma in situ
DEPC	Diethylpyrocarbonate
DMEM	Dulbecco's Modified Eagle Medium
DMSO	Dimethyl sulfoxide
DNA	Deoxyribonucleic acid
DTT	Dithiothreitol
E1	Ubiquitin activating enzyme
E2	Ubiquitin conjugating enzyme
E3	Ubiquitin ligase enzyme
Ed	Echinoid protein
EDTA	Ethylenediaminetetraacetic acid
EGF	Epidermal growth factor
EGTA	Ethylene glycol tetraacetic acid
ER	Estrogen receptor
Ex	Expanded protein
FBS	Fetal bovine serum
GAPDH	Glyceraldehyde 3-phosphate dehydrogenase
GFP	Green fluorescent protein
GPCR	G-protein couple receptor
GST	Glutathione s-transferase
HECT	Homologous to the E6-AP carboxyl-terminus
HEK	Human embryonic kidney
HEPES	4-(2-hydroxyethyl)-1-piperazineethanesulfonic acid
HER2	Human epidermal growth factor receptor 2
IB	Immunoblot
IDC	Invasive ductal carcinoma

IGEPAL	Octylphenoxypolyethoxyethanol
IL-6	Interleukin-6
IP	Immunoprecipitation
K0	Containing no lysine residues (Lysine-0, all 7 lysines mutated to arginines)
LATS	Large tumor suppressor
lrECM	Laminin-rich extracellular matrix
LPA	Lysophosphatidic acid
Mer	Merlin protein
MOPS	3-(N-morpholino)propanesulfonic acid
MST	Mammalian Ste20-like protein kinase
NDFIP2	Nedd4 family interacting protein 2
Nedd4	Neural-precursor-cell-expressed developmentally down-regulated protein 4
NFκB	Nuclear factor-κB
N-terminus	Amino terminus
PALS1	Protein associated with Lin Seven 1
Par	Partitioning defective
PATJ	PALS1-associated tight junction protein
PBS	Phosphate-buffered saline
PCR	Polymerase chain reaction
PDZ	Post-synaptic density, Discs large, Zonula occludens
PEI	Polyethylenimine
PLC	Pregnancy lactation cycle
PLC	Phospholipase C
PP1	Serine/threonine protein phosphatase 1
PSL	Photostimulated luminescence
PR	Progesterone receptor
P-Y	Proline and tyrosine-rich motif
qRT-PCR	Quantitative real time polymerase chain reaction
RIPA	Radioimmunoprecipitation assay
RPMI	Roswell Park Memorial Institute
RNA	Ribonucleic acid
RT	Reverse transcriptase
RTK	Receptor tyrosine kinase
RUNX	Runt-box related
S1P	Sphingosine 1-phosphate
SCF-(β)-TRCP	Skp1/Cdc53/Cullin/F-box receptor/β-transducin repeat-containing protein
SDS-PAGE	Sodium-dodecyl sulfate polyacrylamide gel electrophoresis
shRNA	short hairpin ribonucleic acid
siRNA	small interfering ribonucleic acid
snRNP70	70-kDa small nuclear ribonucleoprotein
STAT	Signal transducers and activators of transcription
TAZ	Transcriptional co-activator with PDZ-binding motif
tBid	truncated BH3 interacting-domain death agonist
TEAD	TEA-domain
Ub	Ubiquitin
WT	Wild-type
WW	Containing two conserved tryptophans
YAP	Yes-associated protein
YFP	Yellow fluorescent protein
ZO	Zona occludens

CHAPTER 1. INTRODUCTION

Some text in this chapter was originally published in *The American Biology Teacher*. Adler et al. Day as a Pathologist: Utilization of Technology to Guide Students in Exploring Careers in Breast Cancer Pathology. *The American Biology Teacher*. 2013; Vol: 75, 8: 559-565. © the National Association of Biology Teachers.

1.1. Organization of the Mammary Organ, Mammary Organogenesis, and the Origins of Breast Cancer

Human body systems contain many growth control mechanisms that help regulate and maintain cellular homeostasis and tissue-specific function (Xu et al., 2009). Many of these mechanisms are biochemical or biophysical cues, working through cellular architecture and biochemical signals, which modify tissue function via physiological perturbations. The mammary organ is an example of such, containing tissue that is highly sensitive to a wide-variety of growth control mechanisms (Bissell et al., 2003). Thus, studying normal and cancerous mammary cell models is useful to dissect growth control signaling that is likely relevant to the functions of the mammary organ.

The breast, while composing a basic overall structure during fetal and infant growth, undergoes remodeling events during puberty, pregnancy, lactation, and menopause that require cells to move, change size and to divide or conversely to die (Hassiotou and Geddes, 2013; Russo and Russo, 2004). The composition of the mature breast is mainly deposits of adipose tissue, glandular tissue, blood vessels, and muscle that are embedded into fibrous connective tissue called the stroma (Figure 1-1). The glandular tissue, in turn, is composed of hollow tubes called ducts that are formed by luminal cuboidal epithelial cells. These epithelial cells are surrounded by a layer of myoepithelial cells, which have properties of smooth muscle cells and are able to squeeze the ducts for milk movement during lactation. This glandular tissue develops and grows during puberty and upon its maturation is a crucial element in the function of the breast (Neville MC, 2002; Russo J, 1992). Such glandular tissue forms a tree-like branching system that arises from clusters of 10-100 alveoli comprising lobules (Going and Moffat, 2004; Hartmann, 2007). During lactation, milk is produced by lactocytes in the lobules and travels through the lumens of the ducts to reach the nipple (Hassiotou and Geddes, 2013).

Importantly, key remodeling events in the mammary gland during pregnancy and lactation promote healthy physiological changes during the woman's life cycle (Figure 1-2). Termed together as the *pregnancy lactation cycle* (PLC) (Russo and Russo, 2004), these physiological changes are important for the development of a functional milk-secreting organ. Within this cycle, growth and remodeling events occur followed by massive cell death and whole organ involution. These remodeling events include ductal branching, alveolar morphogenesis, secretory differentiation, and post-lactation involution (Hassiotou and Geddes, 2013). The PLC requires major changes in the organization and the size of the mammary organ, involving changes in the epithelial cells and surrounding stromal tissue. For example, during involution, the final step of the PLC, the breast is completely reorganized. Involution begins with massive cell death and then clearing of cell debris. A complete redevelopment of the ductal network and surrounding tissue follows, which is maintained until the next gestation (Stein et al., 2007). These steps are partially regulated by estrogen, progesterone, and prolactin hormones (Pang and Hartmann, 2007). While hormones play a large role in this process, many details controlling this process are ambiguous. The capacity of this organ to undergo large remodeling events throughout adulthood may explain why abnormal changes leading to pathogenic conditions like cancer are so prevalent.

Abnormal changes may occur anywhere and at any time in the breast to initiate cancer at that location. Breast cancer is one of the most frequently diagnosed cancers and one of the leading causes of cancer deaths in women (Ferlay et al., 2007; Ferlay et al., 2010). These cancers are categorized into particular types based on the origin of the tissue from which they arise and by their invasive capacity. For instance, ductal tumors arise out of ducts whereas lobular tumors arise from lobules. Even though cancer can occur in any cell, it is frequently seen in the epithelial cells that line the ducts. The pathological event of cancer begins when these epithelial cells, due to environmental or genetic cues, begin to divide and grow inappropriately, undergoing hyperplasia, and fail to form normal breast structures (Figure 1-3). This typically is observed by cells growing into the lumen of the duct in a process termed *intra-ductal hyperplasia*, also known as benign

proliferative breast disease (Hussein and Hassan, 2006). As benign hyperplastic cells undergo deregulated cell growth, they have an increased probability of acquiring cancer-initiating mutations that further drive higher rates of cell growth and loss of ductal morphology. When these cells remain within the confines of the duct, this is termed *ductal carcinoma in situ* (DCIS). DCIS is not diagnosed as breast cancer, but can be detected by a mammogram. However, if these cells break through the ductal layer and invade into the surrounding stroma and adipose tissue, they are then recognized as cancer and are termed *invasive ductal carcinoma* (IDC). These cancer cells are frequently able to migrate into the bloodstream and vasculature to be deposited elsewhere in the body, creating a highly lethal metastasized breast cancer.

Many of the factors involved in breast cancer remain elusive and treatments consequently often do not result in a cure. Thus, early detection is still the best way to prevent breast cancer (Erbas et al., 2006; Key et al., 2001; Wren, 2007). Research into the natural history of breast cancer is therefore essential to understand the microenvironmental, genetic, and molecular factors that will serve as the targets for better therapeutics (Xu et al., 2009).

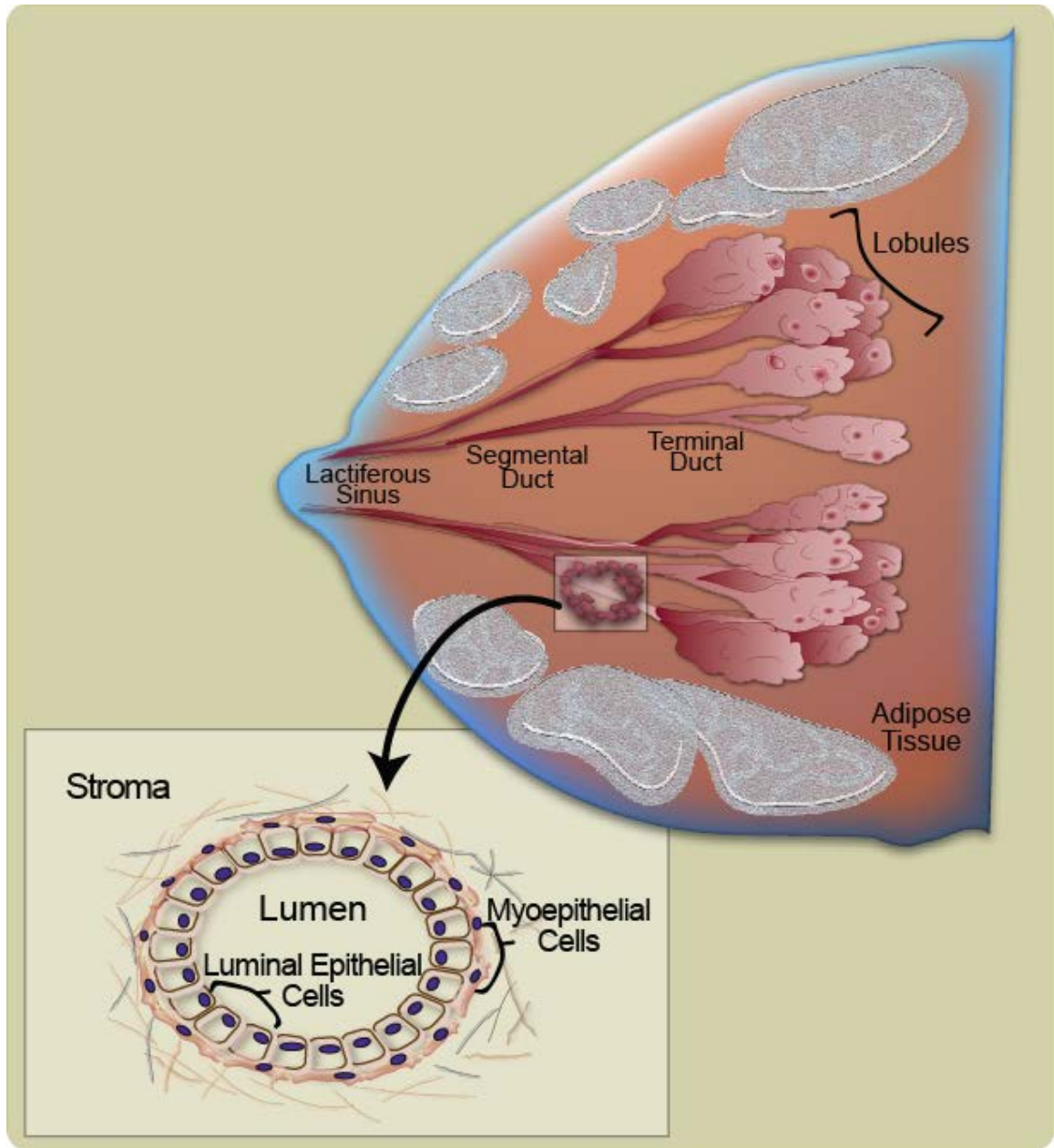


Figure 1-1 Organization of the Breast.

The breast is composed of adipose tissue and the stroma, a network of connective tissue, both of which surround the secretory ductal tissue. The ductal tissue presents as a tree-like branching path, where milk is stored and secreted from in lobules and is transported to the nipple (lactiferous sinus). A cross-section of the duct is presented, indicating two layers of epithelial cells lining the mammary ducts. A layer of simple cuboidal epithelial cells faces the inner hollow lumen. In the lobules, these epithelial cells can differentiate into secretory cells for milk production. The second layer is the myoepithelial cells, which surround and help hold the luminal epithelial cells in place. Overall, these epithelial cells are very important for the structure and function of the mammary organ. Figure adapted from (Adler et al., 2013c).

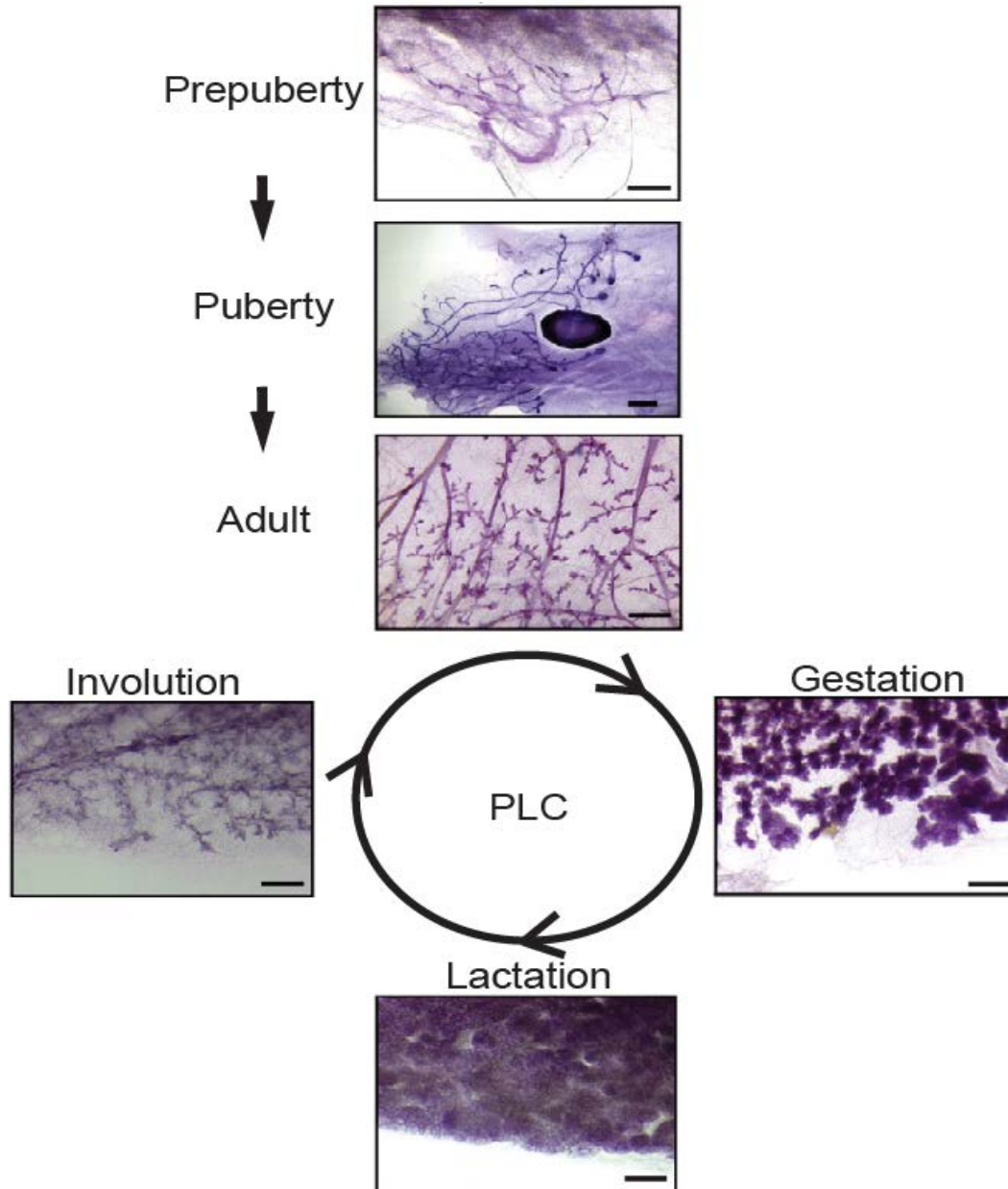


Figure 1-2 Normal Mammary Gland Organogenesis.

A selected series of mouse mammary tissue whole mounts, illustrating morphological changes at selected phases of development. This particular series highlights the embryonic through adult mammary gland. It begins with a postnatal, prepuberty gland (2-week old), a rapidly growing pubertal mammary gland (5-week old), and a developed adult ductal gland (10-week old). Upon gestation, the ductal system undergoes rapid changes in structure and function. These changes occur as a cycle, termed the *pregnancy lactation cycle* (PLC). Initially, remodeling occurs during pregnancy (gestation day 18.5). This is followed by lactation, in which the gland is functionally differentiated and milk is being produced. Then, during post-lactation the ductal tissue undergoes rapid cell death followed by whole organ involution (day 8 post-lactation). This is followed by a reorganization of the breast until the next PLC. Scale bars = 1 mm (Prepuberty-Adult); 50 μ m (PLC). Figure designed by William Ranahan. Figure adapted from (Khokha and Werb, 2011).

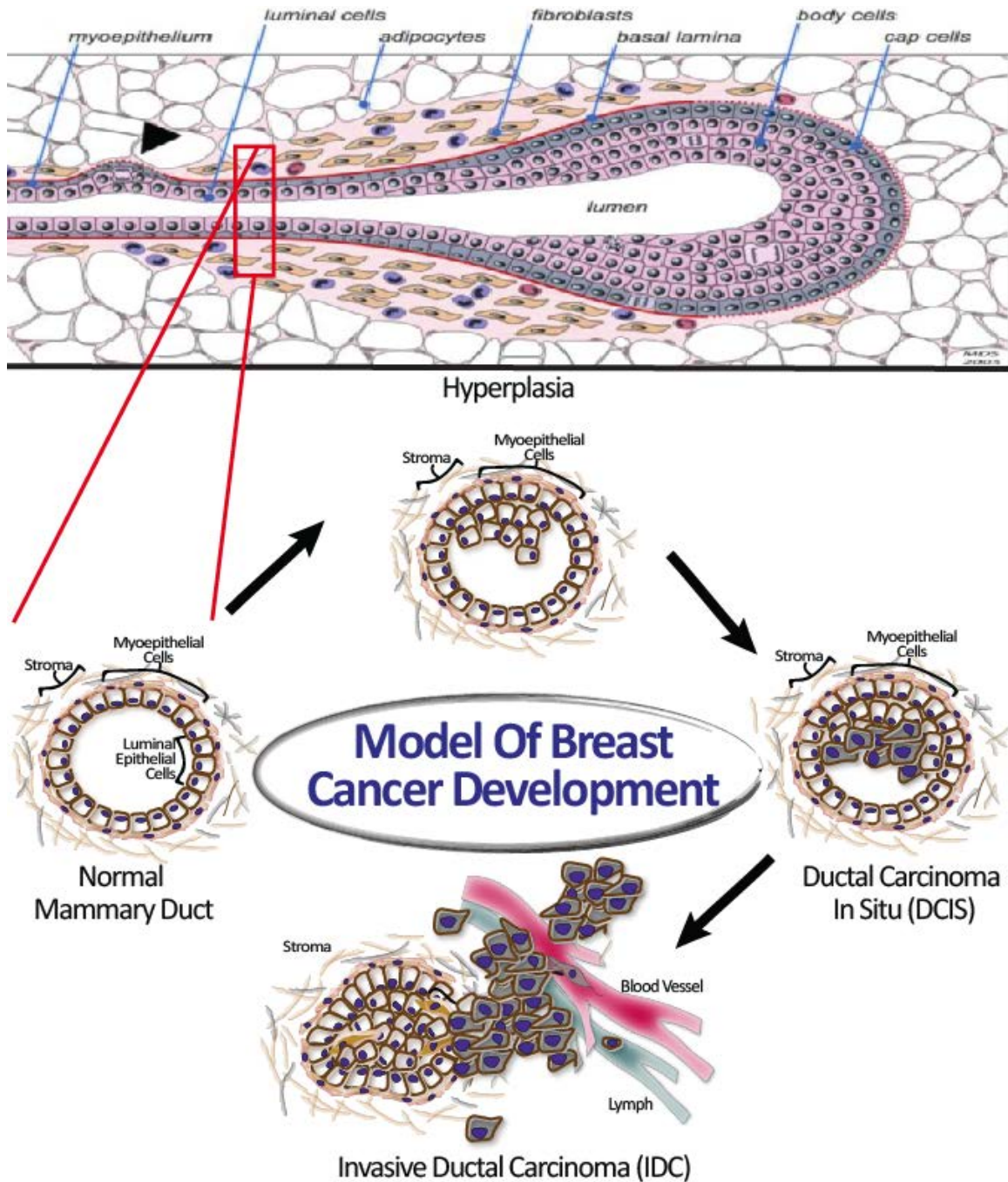


Figure 1-3 Progression of Invasive Ductal Carcinoma in the Breast.

Representation of a labeled duct and stromal tissue with different cells indicated (above). A closer examination of a selected cross-section of a duct undergoing cancer progression is presented (below). Featured are two layers of epithelial cells and changes that occur to the duct through this progression. Epithelial cells lining the mammary ducts begin to grow and divide inappropriately and begin to fill the duct (hyperplasia). As these cells undergo deregulated growth, they acquire mutations that drive further loss of ductal morphology and increased cell growth into the lumen of the duct (DCIS). Eventually, these cells could break through into the stroma and are diagnosed as invasive ductal carcinoma. Figure adapted from (Sternlicht, 2006) and (Adler et al., 2013c).

1.2. Serum Factors and Their Roles in Epithelial Cell Growth

Breast cancer can arise from changes in the epithelial cells that line the ducts. Within the breast tissue, these epithelial cells react to changes in their microenvironment, which can modify their rates of cell division and growth. These microenvironmental conditions are influenced by cell-cell contact with neighboring cells and various juxtacrine, autocrine, or paracrine factors that come into contact with the cell (Castor, 1972). In many cases these factors are packaged and released from one cell and then distributed through the bloodstream or extracellular fluids to the targeted cell. Within blood, serum contains many factors important for cell division and proliferation (Rutherford and Ross, 1976). These factors are easily distributed via the bloodstream and extracellular fluids, throughout tissues accessing cells where they may act via interactions with membrane receptors on the cell surface. In turn, these factors act to initiate changes within the cell. Specifically, a subset of factors has been identified to influence cell growth and apoptosis in mammary epithelial cells and is demonstrated to impact cancers.

An example of a secreted polypeptide factor that promotes cell growth is the epidermal growth factor (EGF), which can activate a number of intracellular signaling pathways. EGF, upon binding to a growth factor receptor, causes that receptor to dimerize with another growth factor receptor. These dimerized receptors undergo auto-phosphorylation and activation, which leads to a cascade of pro-growth intracellular signaling pathways (Ushiro and Cohen, 1980; Wells, 1999) (Figure 1-4).

EGF-dependent signaling plays a major role in the ductal development of breast (Tonelli and Sorof, 1980), and are deregulated in cancer development. Several of the receptors that bind the EGF ligand are overexpressed in many types of breast cancers. Further, inhibition of epithelial cell proliferation can be achieved via specific drug inhibition of the EGF receptors in human DCIS xenograph models (Bundred et al., 2001; Chan et al., 2001; Muthuswamy et al., 1994;

Ullrich and Schlessinger, 1990; Wells, 1999). Thus, EGF plays a key role in the induction of growth in mammary epithelial cells.

Mitogenic lipids in the mammary microenvironment also play major roles in promoting cellular growth. The family of lysophospholipids, which have similar functions as the polypeptide growth factors, are produced in a variety of cell types; however, 90 % are produced from platelets (Xie et al., 2002). They are active when bound to protein albumin in human serum at concentrations ranging from 0.5-5 μM (Baker et al., 2001; Sano et al., 2002; Yatomi et al., 2000). Upon reaching a targeted epithelial cell, they bind highly specific membrane-bound receptors that are coupled to G-proteins (commonly known as G-protein coupled receptors, GPCRs). Initiation of different GPCRs leads to the activation or inhibition of a variety of biochemical pathways. Two bioactive lysophospholipids, lysophosphatidic acid (LPA) and sphingosine 1-phosphate (S1P) induce signaling through specific GPCRs to promote cellular proliferation and suppression of apoptosis. This, in turn, has implications on cellular differentiation and survival in many cell types (Ishii et al., 2004) (Figure 1-4). LPA is important in wound healing, cell growth, actin stress fiber formation, and regenerating tissue (Moolenaar, 2000). Importantly, LPA has a role in breast development and is upregulated in cancers, being able to induce breast cancer cells to initiate cellular growth, migration, and promote metastasis to bone (Du et al., 2010; Yuh, 2011). Additionally, LPA levels are elevated in the plasma of ovarian cancer patients (Xu et al., 1995b) and correlate with cell proliferation in breast cells (Yuh, 2011).

S1P acts similar to LPA, but works through its own set of specific GPCRs. Both are able to activate many growth and survival pathways like those involving mitogen-activated protein kinase and phosphoinositide 3-kinase (Ishii et al., 2004). Recent examination of the Hippo signaling pathway, important in the regulation of growth control and organ size, was found to be highly inhibited by LPA, S1P, and EGF (Fan et al., 2013; Miller et al., 2012; Yu et al., 2012). However, the exact mechanisms whereby the components of serum regulate Hippo signaling are still poorly understood.

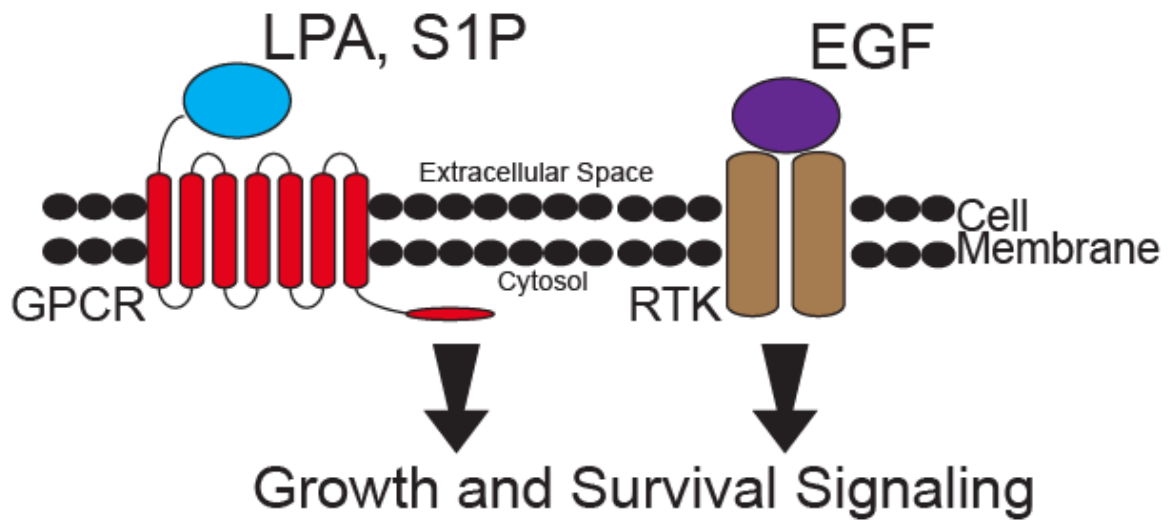


Figure 1-4 Brief Overview of Serum Factors LPA, S1P, and EGF Signaling Pathways.

Growth signaling in mammary epithelial cells is initiated in response to microenvironmental factors found in the serum including the lysophospholipids LPA and S1P, and the protein EGF. LPA and S1P bind to specific receptors coupled to G-proteins (GPCR), which upon activation induce cell growth and survival pathways. EGF binds to receptor tyrosine kinases (RTK), to induce their dimerization and activation of many cell growth and survival pathways. Figure adapted from an unpublished figure by Brandon Lane.

1.3. Hippo Signaling and Its Role in Epithelial Cell Growth

Over the past decade, the Hippo tumor suppressor pathway has been identified as a preeminent signaling network in the control of organ size, stem cells, and cancer (Harvey et al., 2013; Pan, 2007; Zhao et al., 2011b). Many of the Hippo pathway components were originally discovered in *Drosophila melanogaster* via genetic mosaic screens (Harvey et al., 2003; Jia et al., 2003; Justice et al., 1995; Pantalacci et al., 2003; Udan et al., 2003; Wu et al., 2003; Xu et al., 1995a). Recent studies have identified mammalian homologues of the Hippo pathway that can functionally rescue their *Drosophila* mutants *in vivo*, suggesting functional conservation of the Hippo pathway across metazoans (Huang et al., 2005; Lai et al., 2005; Wu et al., 2003). The Hippo pathway functions to negatively regulate the transcriptional co-activators Yes-associated protein (YAP) and its functional homologue transcriptional co-activator with PDZ-binding motif (TAZ) (Kanai et al., 2000; Yagi et al., 1999). Upon entry into the nucleus, YAP and TAZ act as potent co-activators of transcriptional programs involved in organ size control, cell proliferation, and apoptosis. This is through their ability to co-activate many different transcription factors, including the RUNX, p73, and TEA-domain containing (TEAD) (Strano et al., 2001; Vassilev et al., 2001; Vitolo et al., 2007) (Figure 1-5). Specifically, the TEAD transcription factors are well described in transcribing a subset of the CCN family of matricellular proteins, whose name is derived from the first three members, cysteine-rich angiogenic inducer 61 (Cyr61 or CCN1); connective tissue growth factor (CTGF or CCN2); nephroblastoma overexpressed (NOV or CCN3). CTGF and Cyr61 are transcribed by activated TEAD via YAP and TAZ, which regulate pathways involved in cell proliferation and survival, but their effects tend to be cell specific (Dupont et al., 2011; Lai et al., 2011; Zhao et al., 2008b). Likely, other CCN family members are also targets of YAP and TAZ, but the evidence to date on these members are not as strong. CTGF and Cyr61, interact with several extracellular matrix proteins and integrins leading to increased survival and cell proliferation (Chen and Lau, 2009; Hoshijima et al., 2006; Lin et al., 2004). In

breast cancer, Cyr61 and CTGF are associated with poor prognosis, tumorigenesis, resistance to anti-cancer drugs, and metastasis (Hu et al., 2008; Kang et al., 2003; Lai et al., 2011; Xie et al., 2001).

Given the high association of the genes that are induced by YAP and TAZ with breast cancer, it reasons that YAP and TAZ should promote breast cancer as well. Consistently, YAP and TAZ are classified as potent oncogenes (Overholtzer et al., 2006; Zender et al., 2006), whose inhibition is considered a prime target for cell growth inhibition and prevention of tumorigenesis (Kango-Singh and Singh, 2009; Zhao et al., 2008a). Thus, the understanding of YAP and TAZ activity in cancer epithelial cells may yield how cancer potently activates and manipulates cell growth signaling. Consistent with their involvement in breast cancer, the general induction of YAP is linked to migration and tumorigenesis in normal mammary epithelial cells (Overholtzer et al., 2006). Further, recent work on TAZ revealed its requirement for sustaining breast cancer stem cell populations (Cordenonsi et al., 2011).

YAP and TAZ activity are inhibited by formation of cell-cell contacts and serum deprivation. These changes in the cellular microenvironment inhibit YAP and TAZ by spawning activation of the Hippo signaling pathway (Dong et al., 2007). Canonical Hippo signaling entails the activation of two sets of related protein kinases (Figure 1-5). Protein kinases, in general, catalyze the transfer of a phosphoryl group from the γ -phosphate of adenosine triphosphate (ATP) to the hydroxyl group of a serine, threonine, or tyrosine residue on the substrate protein (Endicott et al., 2012). Within the Hippo pathway, the mammalian Ste20-like protein kinases 1 and 2 (MST1/2) (Avruch et al., 2012), catalyze the phosphorylation and activation of the large tumor suppressor protein kinases 1 and 2 (LATS1/2) (Chan et al., 2005). LATS1/2, in turn, catalyze the phosphorylation of YAP and TAZ at multiple residues, including residues serine-127 on YAP and serine-89 on TAZ (Hao et al., 2008). Upon phosphorylation, these sites bind 14-3-3 proteins, which in turn, sequester YAP and TAZ in the cytosol (Kanai et al., 2000; Zhao et al., 2007). This is typical of 14-3-3 proteins, which bind phosphorylated serine and threonine residues in

hundreds of proteins to alter their function (Bridges and Moorhead, 2005; Jin et al., 2004). It was suggested that the phosphorylation of YAP and TAZ also targets them for ubiquitination by the ubiquitin ligase SCF-(β)-TRCP that is reported to lead to the degradation of TAZ via the 26S Proteasome (Liu et al., 2010; Zhao et al., 2010). However, there is no direct evidence linking ubiquitination of YAP by SCF-(β)-TRCP with its degradation. Therefore, the exact mechanism for the degradation of YAP in response to Hippo signaling remains unclear. This will be the topic of this thesis.

YAP and TAZ are also inactivated by the prevention of actin stress fiber formation (Dupont et al., 2011; Sansores-Garcia et al., 2011). Conversely, the stiffening of the extracellular matrix and stress fiber formation activates YAP and TAZ, which in turn, further increase matrix stiffening, via increased CCN transcription and integrin signaling (Calvo et al., 2013). This sets up a self-reinforcing activation loop to activate growth. While LATS inhibits this process, its exact role is unknown (Wada et al., 2011). It is possible that LATS works indirectly to influence the activity of YAP, as very recent work indicates that the mechanical forces are the predominant determinant of YAP nuclear activity (Aragona et al., 2013). Overall, YAP activity is heavily impacted by actin dynamics.

YAP and TAZ contain several distinct regions that orchestrate their function in cells (Figure 1-6). The first region is a C-terminal Post synaptic density protein/Drosophila disc large/Zonula occludens-1 protein (PDZ) binding motif that associates with several proteins that are integrated in cellular membranes (Kanai et al., 2000). Additionally, YAP binds Zona Occluden 2 (ZO-2) via its PDZ binding motif, which can direct YAP into the nucleus (Oka et al., 2010). N-terminal to the PDZ binding motif is the transactivation domain of YAP and TAZ, which is important for the co-activation of the p73 and RUNX transcription factors via YAP and TAZ (Yagi et al., 1999). Depending on the splice forms, 1 or 2 WW domains lie roughly in the middle of both YAP and TAZ. The WW domains consist of 30-40 amino acids each that are

named for two conserved tryptophans (WW) (Sudol et al., 1995). These WW domains bind many proteins involved in cell growth regulation including the LATS1/2 protein kinases (Hao et al., 2008; Zhao et al., 2011a). Finally, the N-terminal TEAD binding domain allows YAP and TAZ to associate with TEAD transcription factors that promote the transcriptional co-activation of TEAD-dependent genes and growth signaling (Li et al., 2010).

Recent work on Hippo signaling in mammals has focused on the upstream activation of Hippo protein kinases. Compared to *Drosophila*, these events are still largely unknown, due to the increased complexity found in mammals involving numerous adapter proteins and redundant kinases.

Recently, serum factors were found to promote growth via inhibition of Hippo protein kinases. Specifically, LPA, SIP, and EGF were uncovered as factors in serum that inhibit Hippo signaling via loss of LATS1/2 activity (Fan et al., 2013; Yu et al., 2012) or indirectly via the dephosphorylation of YAP (Cai and Xu, 2013). Together, these factors all promote YAP nuclear activity. However, it is unclear how LATS1/2 is inhibited in response to serum levels.

Cell-cell contacts are a primary means to inhibit cell growth (Castor, 1972). As it turns out, cell-cell contacts activate Hippo signaling to inhibit YAP and TAZ activities through multiple proposed mechanisms (Dong et al., 2007; Hao et al., 2008; Lei et al., 2008; Oka et al., 2008; Zhao et al., 2007). For instance, in *Drosophila*, protocadherins atypical Fat and Dachshous, as well as other complexes, including the Expanded-Merlin-Kibra pathway activate Hippo signaling (Matakatsu and Blair, 2004). However, studies in mammals suggest that neither Fat, Dachshous, nor the Expanded axis are major contributors to Hippo activation, as many of these *Drosophila* proteins are not even present in the same form in mammals (Bossuyt et al., 2013) (Figure 1-7). For example, mammalian protein Expanded lacks a C-terminal region found in its counterpart from *Drosophila* and other arthropods. Thus, in mammals, unique candidates likely play major roles in relaying cell-cell contact inhibition through the Hippo pathway. Recently, components of cell polarity complexes were demonstrated to activate Hippo signaling in response

to cell-cell contacts via formation of cell polarity (Chan et al., 2011; Schlegelmilch et al., 2011; Silvis et al., 2011; Wada et al., 2011; Wang et al., 2011; Yi et al., 2011; Zhao et al., 2011a; Zhao et al., 2012). Generally, epithelial cells utilize cell polarity protein complexes to maintain structure and prevent cell division and growth signaling. These complexes contain proteins that surround the contacts between cells and are involved in cell-cell attachment and intracellular signaling, linking contact between cells and growth inhibition via control of proteins like YAP and TAZ (Genevet and Tapon, 2011; Ota and Sasaki, 2008; Zhao et al., 2007). Closer examination of these protein complexes revealed a family of adapter proteins currently being investigated as a replacement pathway for Fat and Dachshous in mammals. These are identified as a group of tight junction-associated proteins, called Angiomotins (Bossuyt et al., 2013; Wells et al., 2006). Importantly, recent studies suggest the Angiomotins are major components of the Hippo signaling pathway (Chan et al., 2011; Wang et al., 2011; Zhao et al., 2011a). Therefore, it is important to understand the roles of the Angiomotins in the context of Hippo signaling, as these proteins could shed light on how the core Hippo signaling components are regulated.

Co-Transcriptionally Active YAP and TAZ

Nucleus



Hippo Signaling Suppresses YAP and TAZ Activity

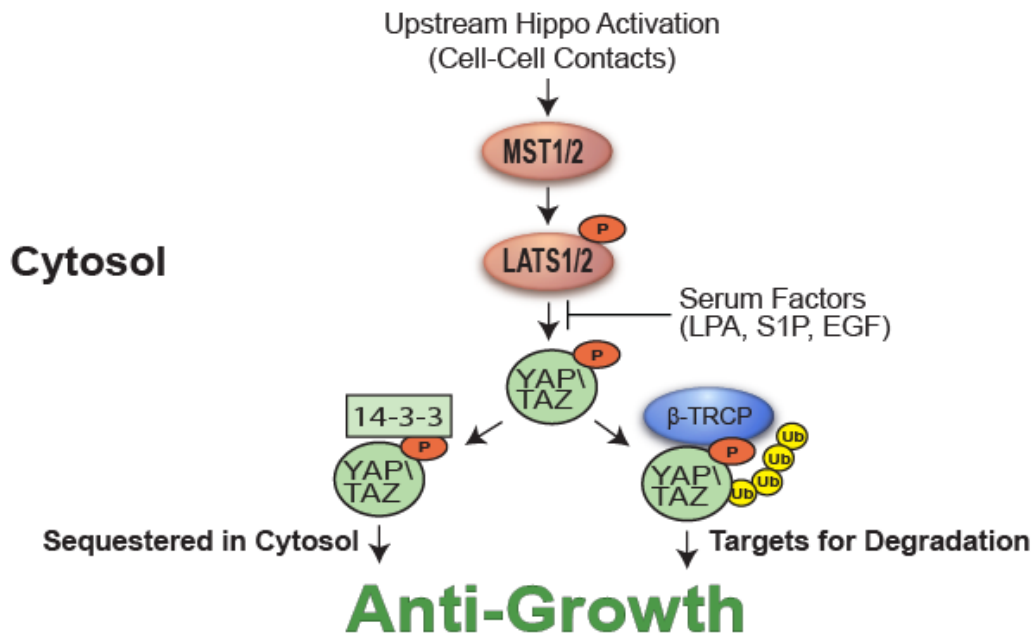


Figure 1-5 Overview of Hippo Signaling in Mammals.

YAP and TAZ proteins enter the nucleus and co-activate transcription factors, such as TEAD that promote the transcription of pro-growth and survival genes, including CTGF (above). Hippo pathway activation (below) initiates with the activation of MST1/2 protein kinases and consequent phosphorylation of LATS1/2 protein kinases. As a consequence, LATS1/2 is activated, resulting in phosphorylation of YAP and TAZ at multiple residues. Phosphorylation of YAP and TAZ signals inactivation through their binding 14-3-3, which sequesters YAP and TAZ in the cytosol, as well as targeting these transcriptional co-activators for ubiquitination, via the protein ubiquitin ligase SCF-(β)-TRCP (β -TRCP), and degradation. Prevention of YAP and TAZ nuclear activities suppresses cell growth and survival. Interestingly, the serum factors LPA, S1P, and EGF can inhibit LATS1/2 phosphorylation of YAP and TAZ, and thus inhibit Hippo signaling. Figure adapted from an unpublished figure by Clark Wells.

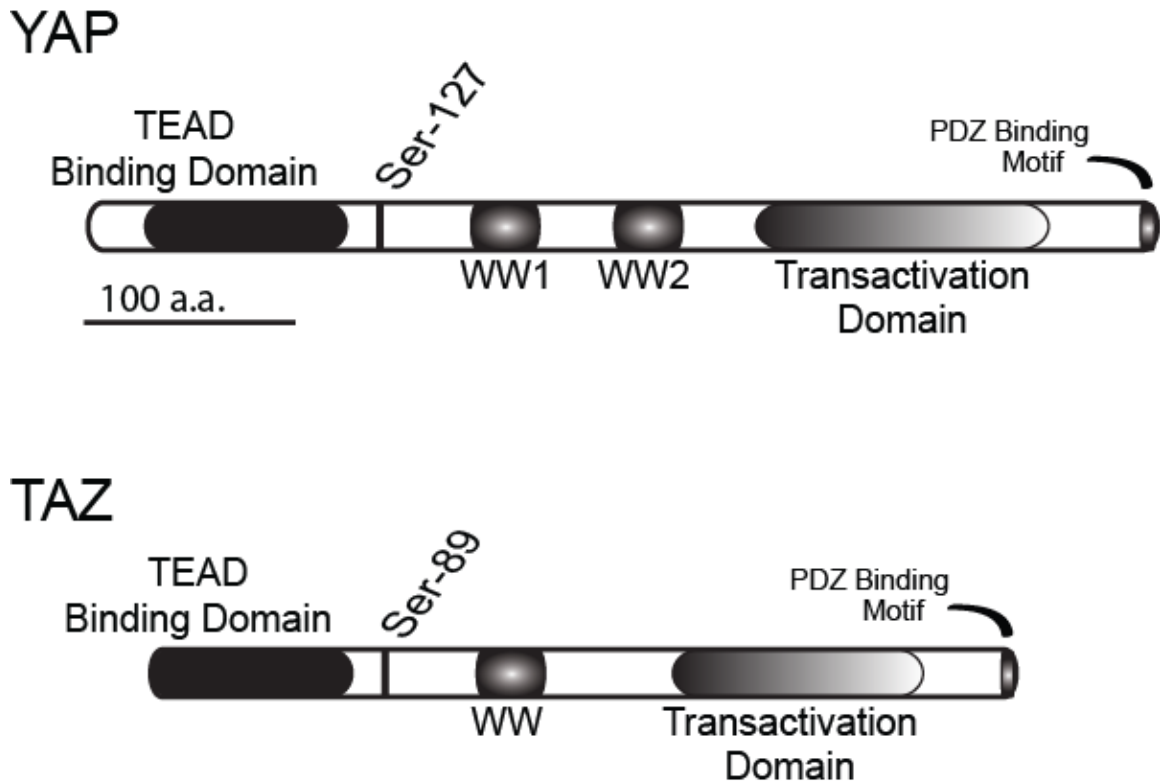
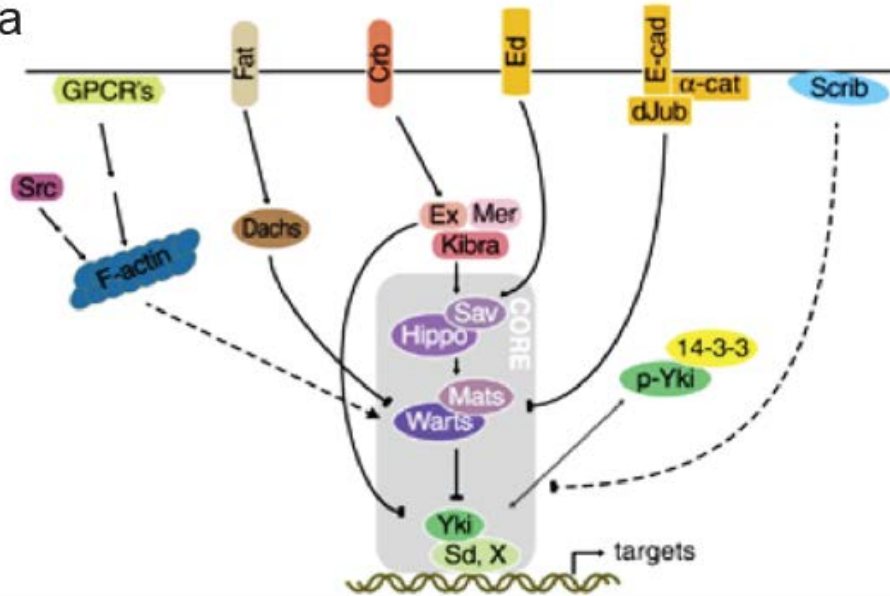


Figure 1-6 The Functional Regions of the Transcriptional Co-activators YAP and TAZ.

This is a schematic of the domain architecture of mammalian YAP and TAZ. Each protein contains a PDZ binding motif on their C-terminus. This motif interacts with different PDZ domain containing proteins, like ZO-2. They also contain transactivation domains that elevate the activity of transcription factors. Further, WW domains in the center of these proteins allow for key functional interactions with proteins that regulate their activity, like LATS1/2 and Angiomotin family members (section 1.4). Importantly, both of these proteins are phosphorylated at multiple residues by LATS. LATS phosphorylation sites, serine-127 (YAP) and serine-89 (TAZ), are highlighted in this schematic. Finally, each contains a TEAD binding domain on their N-terminus, which directly interacts with the TEAD transcription factors.

Drosophila



Mammals

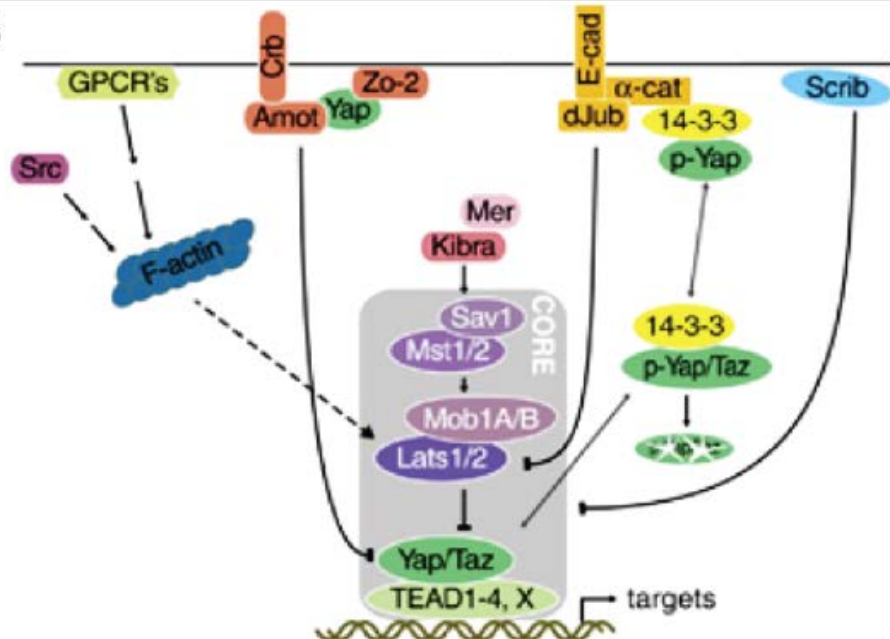


Figure 1-7 Comparison of Upstream Effectors of Canonical Hippo Signaling in *Drosophila* Versus Mammals.

While the core Hippo pathway components in mammals and *Drosophila melanogaster* are similar, the upstream regulation is quite different. For example in *Drosophila*, atypical cadherins Fat and Dachshous (Dachs), Echinoid (Ed), and the Expanded (Ex)-Merlin (Mer)-Kibra complex play critical roles in regulating Hippo signaling. However, in mammals many alternative pathways have evolved to control Hippo signaling. For example, the Angiomotin (Amot) protein family links polarity proteins, including Crumbs (Crb), to the regulation of Hippo signaling. Figure adapted from (Bossuyt et al., 2013).

1.4. The Angiomotins and Their Roles in Epithelial Cell Growth and Hippo Signaling

The Angiomotin family of adapter proteins coordinates the core signaling pathways that regulate cell shape and growth control (Aase et al., 2007; Paramasivam et al., 2011; Wells et al., 2006; Zhao et al., 2011a). These proteins play pivotal roles in cell polarity and growth control by binding Hippo signaling and polarity proteins. Three separate genes, paralogs in humans, *Angiomotin (AMOT)*, *Angiomotin-like 1 (AMOTL1)*, and *Angiomotin-like 2 (AMOTL2)* encode proteins that can be grouped by sequence homology and analogous domain topology (Bratt et al., 2002) (Figure 1-8). Each Angiomotin protein contains a C-terminal PDZ binding motif, important for anchoring it to polarity proteins composing the Partition defective (Par) and Crumb (Crb) polarity protein complexes. These complexes control the organization of the apical cortex of epithelial cells, helping to mediate intercellular signaling and associated gene transcription (Assémat et al., 2008). Importantly, Angiomotin is present at the tight junctions near cell-cell contacts and regulates cell polarity via binding and modifying the localization of the Par and Crb polarity protein complexes (Wells et al., 2006).

N-terminal to the PDZ binding motif, the Angiomotins all contain an Amot coiled-coil homology (ACCH) domain, which is important for their ability to associate with lipids in the membrane of cells. The ACCH domain drives Angiomotin association with the membrane and helps Angiomotin influence changes in cellular polarity (Heller et al., 2010). Further, the ACCH domain is required for the Angiomotin family members to homo- and hetero-dimerize (Ernkvist et al., 2008; Gagné et al., 2009; Moreau et al., 2005; Patrie, 2005). These dimerization events allow for multiple Angiomotins to be in the same complex spatially and temporally; however, the functions of the individual pairs of homo- and hetero-dimers remain to be identified.

N-terminal to the ACCH domain, each Angiomotin contains a set of conserved proline and tyrosine-rich (P-Y) motifs. These P-Y motifs bind WW domains of a variety of proteins (Sudol et al., 1995). In fact, P-Y motifs in the Angiomotin proteins bind a variety of WW domain

containing proteins involved in growth signaling, including YAP and TAZ (Adler et al., 2013a; Wang et al., 2012; Wang et al., 2011; Zhao et al., 2011a).

Two less well characterized regions of the Angiomotins are the residues that mediate binding to actin and LATS. These regions are both predicted to lie in the N-terminus of the protein in a region containing the P-Y motifs, as previously described (Paramasivam et al., 2011). Although the precise locations and mechanisms are vague, the functional relevance is highly visible. For example, the ability of the Angiomotins to bind actin allows them to modify the architecture of filamentous actin in several cell types (Ernkvist et al., 2006; Gagné et al., 2009). Also, the Angiomotin family members activate the protein kinase activity of LATS2, via direct binding, leading to increased phosphorylation of YAP by LATS2 (Paramasivam et al., 2011). However, exactly how the Angiomotins are able to accomplish actin reorganization and the activation of LATS remains unknown. Therefore, this thesis further examined the relationships between the Angiomotins and LATS activity and their impact on actin fiber formation, as these are likely important aspects of the functions of the Angiomotins.

Angiomotin was first identified in 2001 as an 80-kDa isoform (Amot80) in endothelial cells (Trojanovsky et al., 2001). In mammary epithelial cells, Amot80 induces the loss of organization of apical junctions and stimulates cellular proliferation (Ranahan et al., 2011; Sugihara-Mizuno et al., 2007; Wells et al., 2006; Yi et al., 2011). This may explain why high levels of *AMOT* transcript strongly correlate with increased breast tumor grade as well as poor patient survival (Jiang et al., 2006). Angiomotin, therefore, was considered likely to be an oncogene. However in 2005, an alternative longer splice isoform of Angiomotin, the 130-kDa isoform of Angiomotin (Amot130) was identified, which was subsequently shown to inhibit migration and cell growth (Bratt et al., 2005; Ernkvist et al., 2006; Ernkvist et al., 2008). Thus, the *AMOT* gene encodes a transcript that is spliced to produce a long protein (Amot130) and a shorter version (Amot80) that have opposing functions. Mechanisms by which Amot130 could present such a different phenotype was largely unanswered (Roudier et al., 2009) until 2011,

when Amot130 along with the two other Angiotensin family members, Angiotensin-like 1 (AmotL1) and Angiotensin-like 2 (AmotL2), were demonstrated to directly bind the transcriptional co-activators, YAP and TAZ. YAP and TAZ bind Angiotensins via their WW domains that recognize P-Y motifs within the long forms of Angiotensins (Chan et al., 2011; Wang et al., 2011; Zhao et al., 2011a). Interestingly, Amot80 lacks these N-terminal P-Y motifs, and no evidence exists that it directly binds YAP and TAZ. Importantly, Amot130, AmotL1, or AmotL2 prevents YAP nuclear localization and they inhibit cell proliferation in mammary epithelial cells (Chan et al., 2011). Various mechanisms for how Angiotensins inhibit YAP nuclear activity, both dependent and independent of YAP phosphorylation by LATS1/2 have been proposed (Chan et al., 2011; Leung and Zernicka-Goetz, 2013; Zhao et al., 2011a) (Figure 1-9). Thus, further research into the mechanisms of YAP inhibition by the Angiotensins could lead to insight into their roles as tumor suppressor proteins and involvement in Hippo signaling.

This thesis work found that the Neuronal-precursor-cell-expressed developmentally down-regulated protein 4 (Nedd4) family of ubiquitin ligases bind and regulate Angiotensin proteins via their P-Y motifs. The interactions identified an important family of proteins whose involvement in growth control and Hippo signaling is now being appreciated (Skouloudaki and Walz, 2012; Wang et al., 2012).

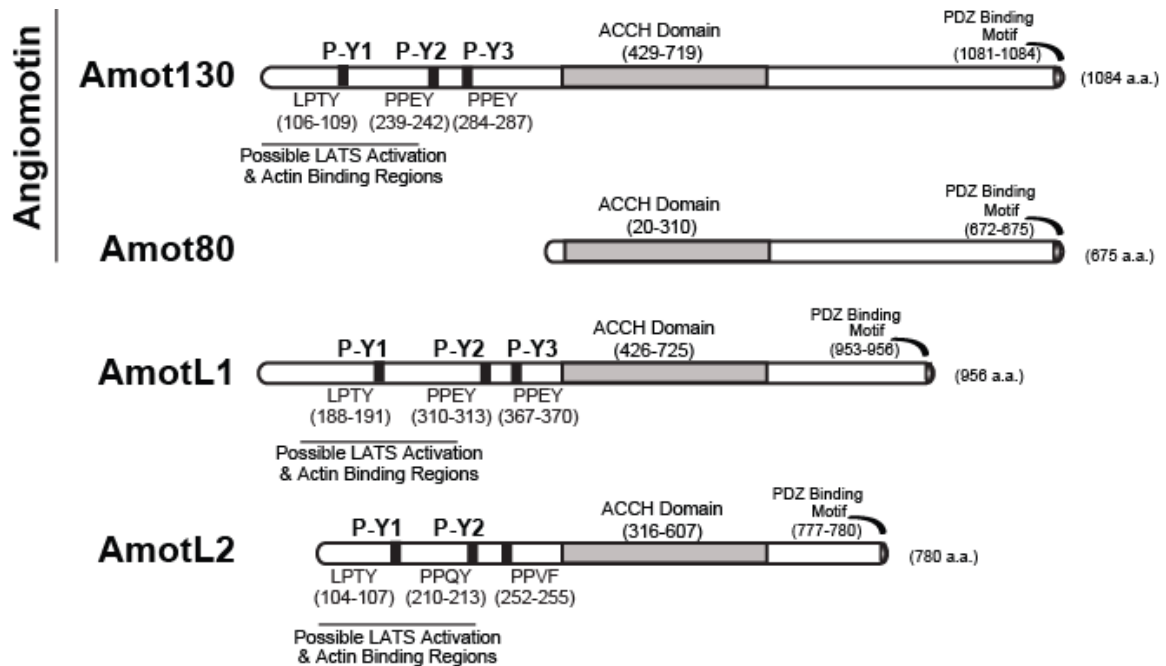


Figure 1-8 A Schematic Diagram of the Angiomotin Family.

The Angiomotin family of adapter proteins consists of three genes *Angiomotin (AMOT)*, *Angiomotin-like 1 (AMOTL1)*, and *Angiomotin-like 2 (AMOTL2)* transcribing the four proteins presented. The gene *AMOT* has two protein isoforms, the 130-kDa isoform of Angiomotin (Amot130) and the 80-kDa isoform of Angiomotin (Amot80). *AMOTL1* and *AMOTL2*, both have one protein form each in Angiomotin-like 1 (AmotL1) and Angiomotin-like 2 (AmotL2). These proteins share architecture. Each member has a PDZ binding motif that allows for interactions with polarity proteins containing PDZ domains. In the heart of all these proteins lies an ACCH domain, which is a coil-coiled domain that allows for homo- and hetero-dimerization of the Angiomotins and also interactions with membrane lipids. The long forms of the Angiomotins contain 2-3 P-Y motifs in their N-termini that allow them to bind proteins containing WW domains, such as YAP and TAZ. Finally, less well documented regions in Angiomotin proteins promote LATS activation and binding to actin in their N-termini. Relative amino acid residues for each domain/motif are provided in parentheses below the protein diagrams.

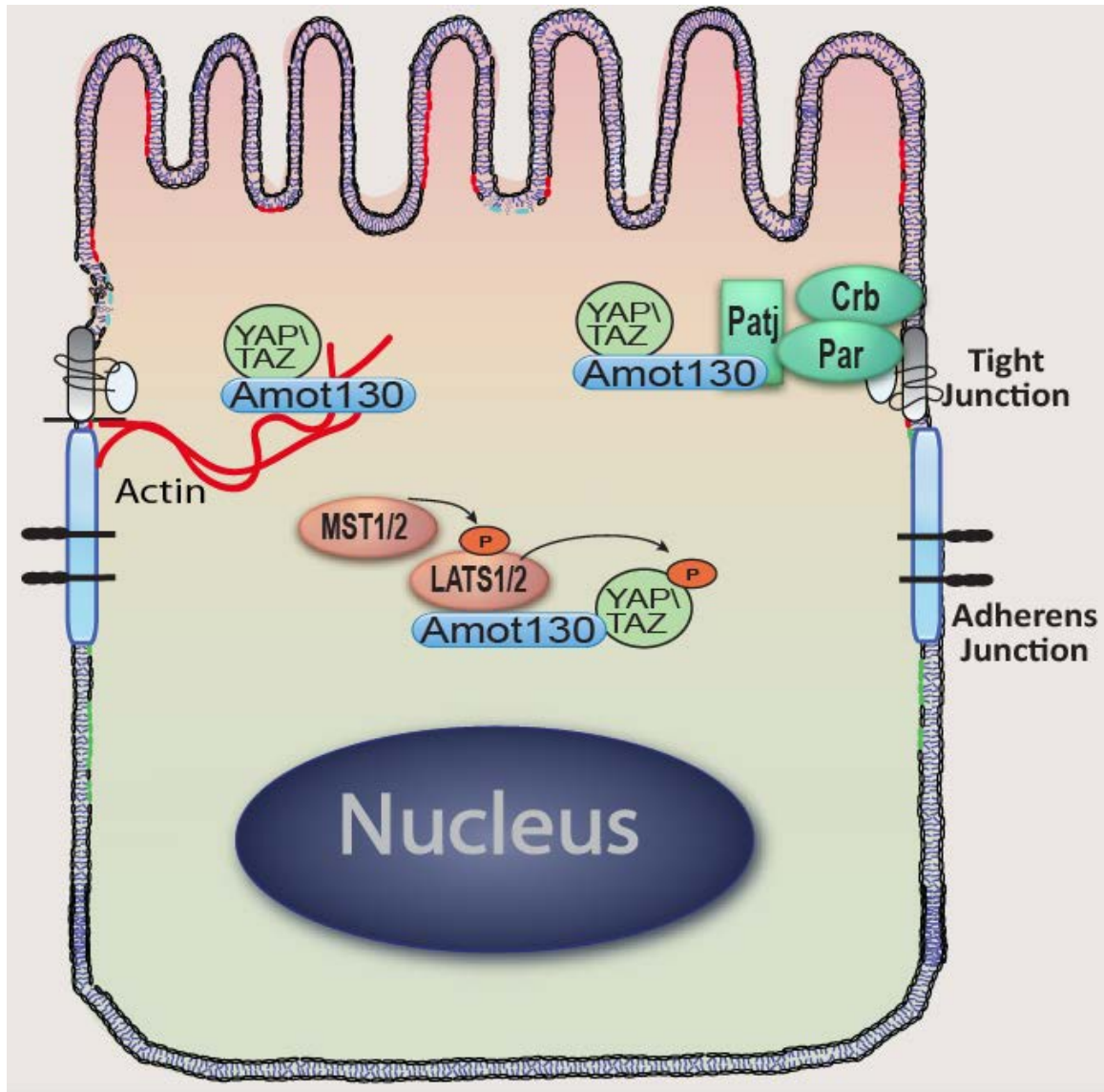


Figure 1-9 The Role of Angiomotin in the Inhibition of YAP and TAZ Nuclear Activity.

Amot130 inhibits YAP and TAZ nuclear activity by multiple mechanisms. First, Amot130 localizes YAP/TAZ to cell contacts, which is in part promoted by association with polarity proteins of the Crb and Par polarity complexes, possibly via the interaction of Amot130 with PALS1-associated tight junction protein (Patj). Secondly, Amot130 can also localize YAP/TAZ to filamentous actin and prevent their nuclear localization. Finally, Amot130 can increase the amount of phosphorylated YAP/TAZ, via Amot130 interaction with and activation of LATS protein kinases. Overall, Amot130 interacts with YAP and TAZ and prevents their translocation into the nucleus. This prevents YAP and TAZ from initiating transcription of pro-growth genes. The locations and size representations in this diagram are relative and not to scale. Figure modified from an unpublished figure by Clark Wells.

1.5. The Nedd4 Ubiquitin Ligases and Their Roles in Epithelial Cell Growth

The attachment of ubiquitin moieties to target proteins is an important signal for a variety of cellular processes (Glickman and Ciechanover, 2002). Covalent attachment occurs first with the activation of a small ubiquitin protein. Activated ubiquitin requires energy from ATP hydrolysis to allow the ubiquitin activating enzyme (E1) to form a thiol-ester bond with ubiquitin (Pickart, 2001). This ubiquitin is then transferred and covalently attaches to an ubiquitin conjugating enzyme (E2). Typically, the E2 will bind to a specific ubiquitin ligase (E3) and transfer the ubiquitin directly to the bound targeted substrate. The ubiquitin binds to the substrate through an isopeptide bond between the C-terminal glycine residue of ubiquitin and the ϵ -amino group of a lysine residue on the substrate protein (Figure 1-10). However, in the case of some E3 ligases, like the homologous to the E6-AP carboxyl-terminus (HECT) family, the E2 transfers the ubiquitin to a specific cysteine residue within the E3 before linking it to the already bound targeted substrate (Glickman and Ciechanover, 2002).

The Nedd4 family proteins are examples of HECT E3 ubiquitin ligases that utilize themselves as an intermediate in the process of covalently attaching an ubiquitin moiety to a targeted substrate. Nedd4-like family proteins are encoded in eukaryotes that are grouped by their common architecture. *Saccharomyces cerevisiae* encode a single protein, Rsp5, which regulates varied cellular pathways involved in cell growth and cell shape (Rotin et al., 2000). Humans encode nine known Nedd4 family ligases that regulate many diverse cellular signaling including targeting for degradation many proteins like those involved in transforming growth factor beta and EGF signaling pathways (Chen and Matesic, 2007; Ingham et al., 2004). Because of their involvement in the degradation of tumor suppressive proteins, many of the Nedd4 ligases are labeled as proto-oncogenes.

Nedd4 proteins rely on three important moieties for their function (Figure 1-11). First, they contain in their C-terminus, a catalytic HECT domain (Huibregtse et al., 1993a, b). A

cysteine in HECT domains transfers the ubiquitin moiety from an ubiquitin-conjugated E2 to the target substrate (Scheffner et al., 1995). This reaction is part of a thiol-ester cascade resulting in ubiquitination of a target protein. The reaction can add a single ubiquitin moiety, termed *monoubiquitination*, or it can serially add multiple ubiquitin moieties to form a polymer, termed *polyubiquitination*. Monoubiquitination is recognized by subcellular trafficking machineries for substrate internalization via endocytosis and recycling pathways (Hicke and Riezman, 1996; Marchese and Benovic, 2001; Roth and Davis, 1996). There are different types of polyubiquitination that vary in the lysine residue from which the new ubiquitin forms an isopeptide bond. Self-conjugation of ubiquitin occurs commonly at lysine-29, -48, or -63 on ubiquitin. Ubiquitination at lysine-48 almost exclusively targets substrates for degradation via the 26S Proteasome (Thrower et al., 2000). Ubiquitination at lysine-29 and lysine-63 present different outcomes for the target based upon signaling context, localization, and specificity of the E3 ligase (Bonifacino and Traub, 2003; Hicke, 2001; Soetens et al., 2001).

Nedd4 proteins also contain a C2 domain in their N-terminus that promotes direct interactions with phospholipids and proteins at the cellular membrane. The C2 domain therefore promotes interactions with substrates that localize at membranes (Nalefski and Falke, 1996; Plant et al., 1997). The C2 domain was originally identified in Ca^{2+} -dependent isoforms of protein kinase C (Knopf et al., 1986). Beyond changes in localization, the C2 domain in some Nedd4 proteins is inhibitory to the catalytic activity of the enzyme. In some cases, this inhibition can be released upon Ca^{2+} -dependent binding to the C2 domain (Wang et al., 2010).

Nedd4 proteins also contain 2-4 WW domains, similar to those seen in YAP and TAZ (section 1.3). These WW domains provide the E3 ligase with substrate specificity, by binding substrates with P-Y motifs (Chen and Sudol, 1995; Macias et al., 2002). The activity and function of Nedd4 proteins are altered or enhanced based upon their interactions with these proteins. For example, the Nedd4 ligase, Nedd4-2, is able to bind to and ubiquitinate the epithelial sodium

channel protein via its P-Y motif, leading to its degradation and thus reduce sodium transport across cell membranes.

Nedd4 ligases ubiquitinate and thereby regulate proteins in a variety of cellular pathways. Generally, Nedd4 ligases are found to function as proto-oncogenes in many different types of cancers including breast cancer (Chen et al., 2009; Wang et al., 2007; Yeung et al., 2013). However, the Nedd4 ligase Atrophin-1 interacting protein 4 (AIP4), also known as Itch, is one of only three Nedd4 ligases that is not known to be altered, overexpressed, or amplified in cancer cells (Chen and Matesic, 2007). Therefore, the precise role of AIP4 in growth control is of significant interest. There is also evidence that AIP4 increases cell survival by degrading various proteins involved in apoptosis (Azakir et al., 2010; Rossi et al., 2005). Initially, AIP4 was examined in immune response pathways, as inactivation of AIP4 in mice results in a variety of inflammatory conditions due to an altered immune response (Hustad et al., 1995; Perry et al., 1998). Direct evidence of AIP4 in pro-growth signaling was first identified in studies that showed that AIP4 polyubiquitinated and led to the degradation of the protein kinase, LATS1, via the 26S Proteasome. Expression of AIP4 increased cellular growth and tumorigenicity in mammary epithelial cells (Ho et al., 2011; Salah et al., 2011; Yeung et al., 2013). Further analysis of how AIP4 influences Hippo signaling and cell proliferation is therefore important to clarify its role in growth control regulation in mammary cells, and is examined in this thesis.

The lack of specificity of HECT domains is compensated by the ability of Nedd4 proteins to be directed to specific subcellular regions and substrates by binding to adapter proteins. Thus, depending on the adapter protein which interacts with the Nedd4 ligase, Nedd4 proteins can have dramatically different substrates and cellular effects. Further, the Nedd4 ligase AIP4 exists normally in an inhibited conformation that prevents AIP4 from ubiquitinating its substrates (Scialpi et al., 2008). The scaffold protein Spartin contains one P-Y motif that binds AIP4 and activates it, allowing for its self-ubiquitination. Self-ubiquitination is therefore a sign of increased ligase activity of AIP4. Binding of AIP4 to Spartin also brings AIP4 to lipid droplets allowing

AIP4 to ubiquitinate its substrate adipophilin (Hooper et al., 2010). Another adapter protein Nedd4 family-interacting protein 2 (NDFIP2) has three P-Y motifs, which bind to AIP4 and localize to the membrane, where active AIP4 ubiquitinates endophilin (Mund and Pelham, 2009). Both adapter proteins activate AIP4 through relieving its auto-inhibited conformation through the WW domain binding the adapter instead of the HECT domain (Figure 1-12). In both cases, the adapter protein was also essential for bringing the ligase into a specific region with the targeted substrate. Recently, the Angiotensin II type 1 receptor (AT1R) was also found to bind Nedd4 family proteins (Adler et al., 2013a; Skouloudaki and Walz, 2012; Wang et al., 2012). Therefore, the relationship between the Nedd4 ubiquitin ligases and the Angiotensin II type 1 receptor adapter proteins is considered of great interest and is examined in this thesis.

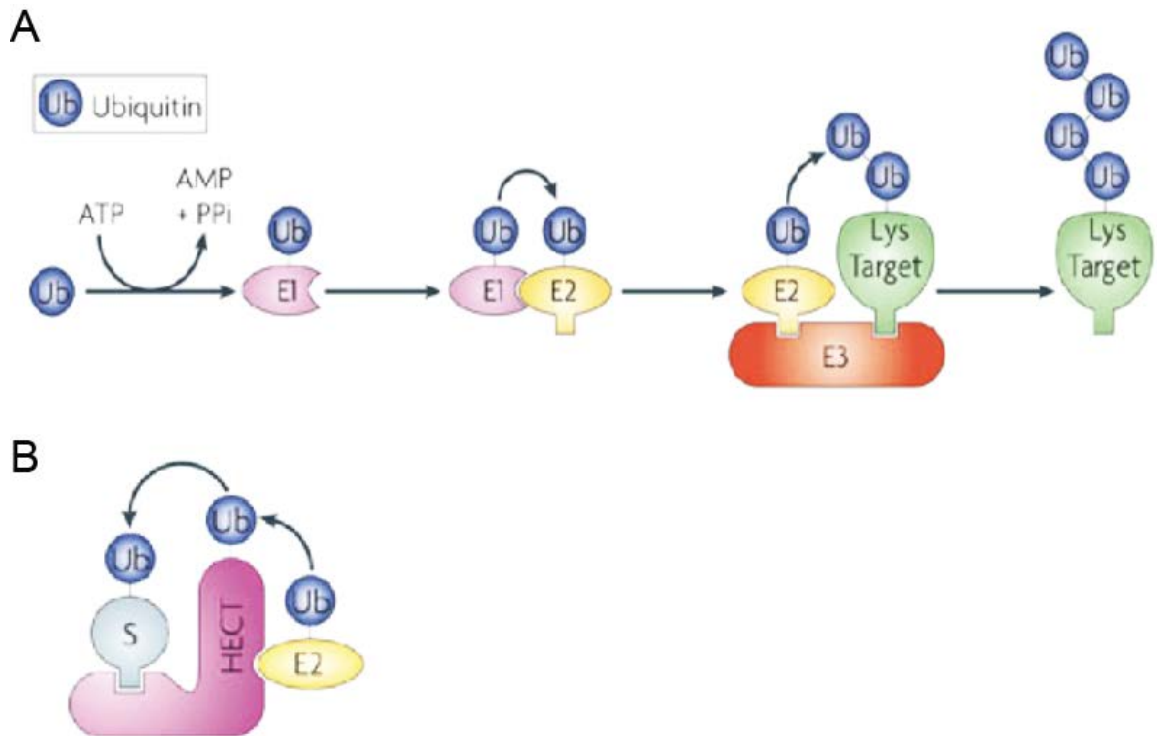


Figure 1-10 Overview of the Process of Ubiquitination of a Target Protein.

(A) Ubiquitination of a target protein begins with the activation of an ubiquitin moiety and subsequent covalent attachment to an ubiquitin activating enzyme (E1), using one molecule of ATP. The ubiquitin is then transferred and covalently attached to an ubiquitin conjugating enzyme (E2). Typically the E2 then binds to the ubiquitin ligase (E3). The ubiquitin is then transferred from the E2 to the targeted substrate via a covalent bond to a lysine residue (Lys). (B) Some E3 ubiquitin ligases function differently than presented in A. In this example, as seen with HECT domain ubiquitin ligases, the E2 binds to the E3, but instead of a direct transfer of the ubiquitin to the targeted substrate, the HECT domain is used as an intermediate via covalent attachment of the ubiquitin to a specific cysteine residue prior to its transfer to the targeted lysine on the substrate protein. Figure adapted from (Rotin and Kumar, 2009).

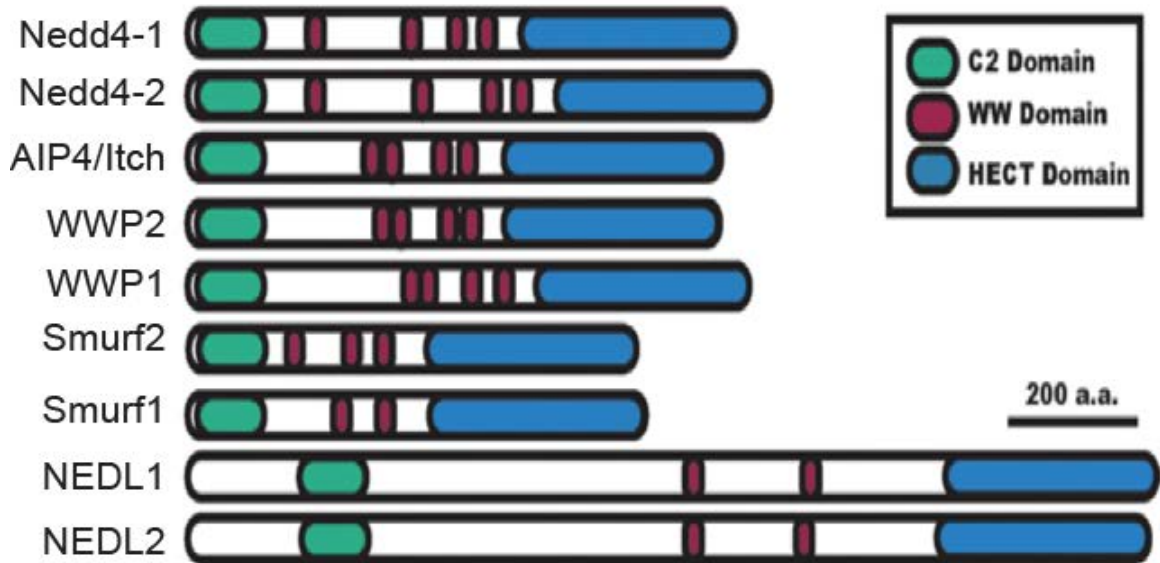


Figure 1-11 Conserved Domains of the Nedd4 Family of Ubiquitin Ligases in Humans.

Nedd4 ubiquitin ligases share three characterized domain regions that are important for their functions in cells. The HECT domain (blue) is the catalytic core of the protein and contains a required cysteine for the transfer of an ubiquitin moiety to the targeted substrate. Secondly, each contains 2-4 WW domains (red) that interact with P-Y motifs in other proteins. These WW domains help bring specificity to the ligase, via direct interactions with substrates or adapter proteins containing P-Y motifs. They also serve to inactivate the HECT domain when not bound to adapter proteins. Finally, in the N-terminus, a C2 domain (green) allows for phospholipid and protein binding at the cell membrane and brings specificity for substrates localized in these regions. Figure adapted from (Ingham et al., 2004).

Active Conformation



Inactive Conformation

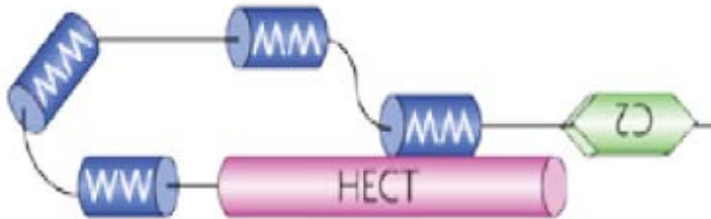


Figure 1-12 Adapter Proteins Increase the Activity of Nedd4 Ubiquitin Ligases.

Nedd4 ubiquitin ligases have active and inactive conformations. Typically, Nedd4 ligases remain in an inactive form until needed. There are many ways to form this inhibited conformation. One way pictured (below) is through the WW domains, which can directly interact with the HECT domain, preventing it from functioning. The C2 domain can also inhibit the HECT domain in a similar manner. However, upon binding of an adapter protein like the one pictured here (N4BP1) (above) the conformation of the protein opens up allowing the HECT domain to perform its catalytic function of transferring the ubiquitin moiety to the targeted substrate. Therefore, these adapter proteins can alter the function of the ligases. Figure adapted from (Rotin and Kumar, 2009).

1.6. Cell Lines and Model Systems Used in This Study

The cell growth control pathways involved in mammary tumorigenesis were analyzed in a panel of cell lines. Mammary tumors are influenced by a variety of hormones and growth factors that have differing cancerous potentials (de Waard, 1969; Russo J, 1992). Importantly, examination of mammary epithelial cell growth regulation requires establishment of cell lines that are able to reflect tumor types from which they were derived (Kao et al., 2009; Neve et al., 2006). To this end, both tumorigenic and non-tumorigenic mammary epithelial cells were utilized to create a more accurate picture of influences on growth control across mammary epithelia. Cancer cell lines chosen were representative of a range of tumor types. These are examined below and include receptor status examining estrogen receptor (ER), progesterone receptor (PR), and human epidermal growth factor receptor 2 (HER2) as diagnostic markers for tumor type. The status of these receptors helps differentiate tumor type and may provide clues about specific growth signaling pathways in one tumor type versus another (Neve et al., 2006). Further, different cell lines had different signaling properties that enabled particular experimental approaches.

MDA-MB-468 cells were used to represent a basal A, triple negative (ER-, PR-, HER2-) metastatic adenocarcinoma tumor type, lacking hormone (ER- and PR-) dependence and HER2 overexpression (HER2-) (Cailleau et al., 1978). These cells were originally obtained from a pleural effusion of a 51-year old African American woman. These cells typically show high endogenous protein levels of Angiotensin II and moderate levels of AIP4 and YAP.

MCF7 cells represent a luminal, hormone receptor positive (ER+ and PR+) lacking HER2 overexpression (HER2-) IDC tumor type (Soule et al., 1973). These cells were obtained from a pleural effusion of a 69-year old Caucasian woman. The MCF7 cells were used especially in imaging experiments due to their high adhesiveness and flatness. This cancer cell model has very little endogenous Angiotensin II and YAP protein levels, but maintains moderate AIP4 protein levels.

BT-474 cells represent a luminal, hormone receptor positive (ER+, PR+), and HER2 overexpression (HER2+) IDC tumor type (Lasfargues et al., 1978). These cells were obtained from a primary breast tumor of a 60-year old Caucasian woman. This cancer cell line model has relatively high protein levels of Amot130 compared to Amot80.

MCF10A cells represent non-tumorigenic mammary epithelia. These cells were obtained from a reduction mammoplasty of a primary breast of a 36-year old Caucasian woman, which spontaneously immortalized (Soule et al., 1990). Interestingly, these cells share the same receptor status as MDA-MB-468 cells (ER-, PR-, HER2-) and other basal-like lineages (Neve et al., 2006), but do not form tumors in nude mice. Therefore, these cells have been classified as a model to study normal mammary gland function (Debnath and Brugge, 2005).

Experiments requiring high levels of endogenous proteins (Angiomotin and AIP4) or for co-immunoprecipitation experiments utilized the Human Embryonic Kidney (HEK) 293T cells. HEK 293T cells are genetically modified HEK 293 cells that contain the SV40 T-antigen (DuBridge et al., 1987). These cells excel at lentivirus production, gene expression, and protein production. Parental HEK 293 cells, were derived from embryonic kidney cells transformed with fragments of adenovirus type 5 DNA (Graham et al., 1977).

Because two-dimensional growth of mammalian cells on plastic lacks microenvironmental cues and responses (Barcellos-Hoff et al., 1989; Bissell et al., 1982; Xu et al., 2009), a three-dimensional system was employed. This utilized a laminin-rich extracellular matrix (lrECM), termed *Matrigel*TM (Petersen et al., 1992). This system allows for formation of more physiologically relevant microenvironments (Debnath and Brugge, 2005; Debnath et al., 2003; Kenny et al., 2007). For example, MCF10A cells, grown in the presence of lrECM, form polarized growth arrested structures called acini (Muthuswamy et al., 2001) (Figure 1-13). These acini more accurately represent a normal ductal environment according to genetic expression profiles (Kenny et al., 2007). Further, examination of cancer cell lines in this environment allows

for differentiation between cancer types, which present themselves differently in lrECM, depending upon the cancer tumor types from which they were derived (Kenny et al., 2007).

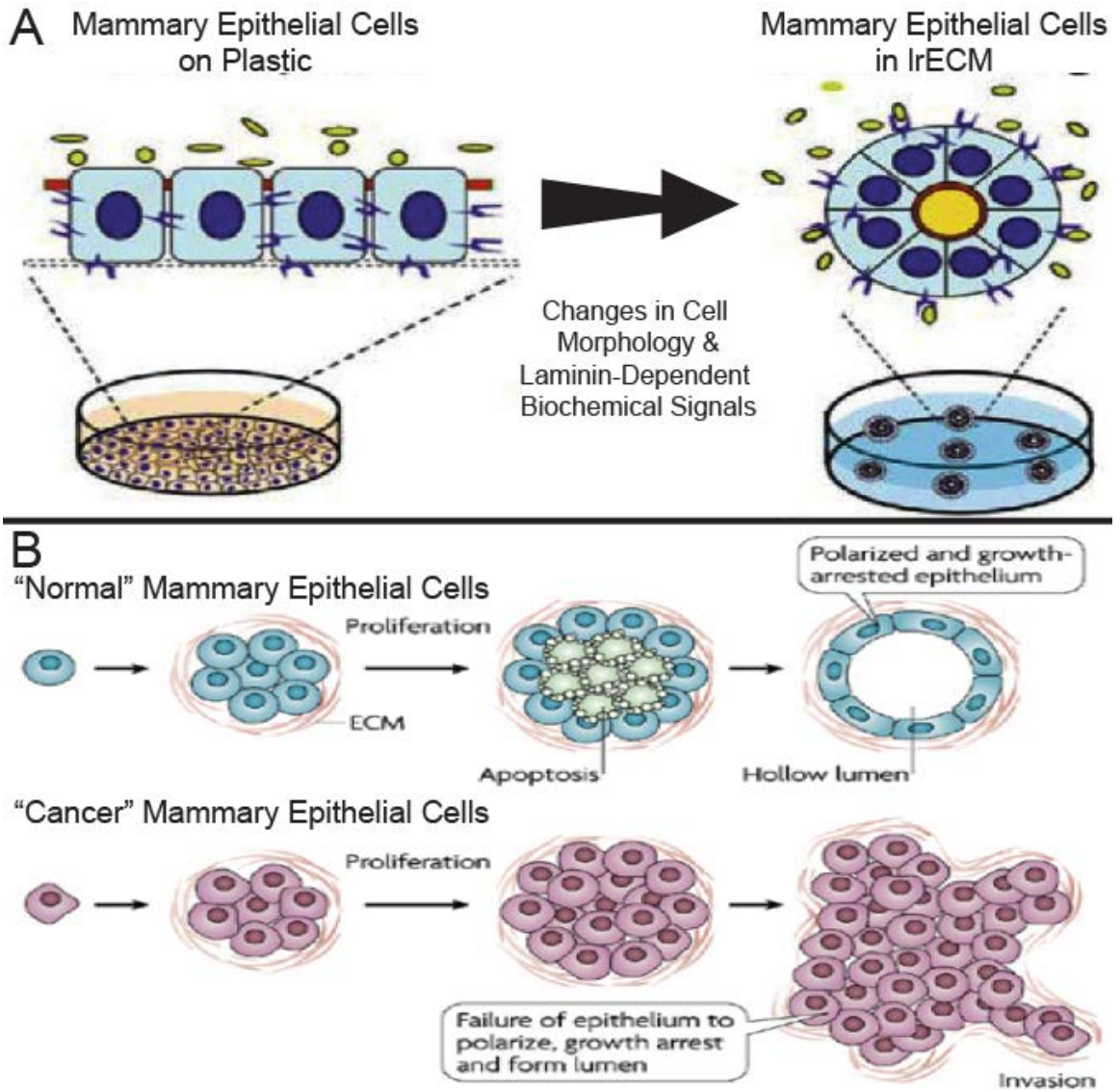


Figure 1-13 Growth Conditions of Mammary Epithelial Cells.

(A) Illustration of mammary epithelial cells grown on two-dimensional plastic dishes or in a laminin-rich extracellular matrix (IrECM). Normal mammary epithelial cells plated on plastic grow into a monolayer, until contact-mediated inhibition shuts down their growth (left). When normal mammary epithelial cells are grown in IrECM (right), cells form a hollow sphere termed *acini*, which display functionally and genetically similar characteristics as mammary ductal epithelia *in vivo*. Acini have dramatically different morphologies and are sensitive to some biochemical signaling not seen when cells are grown on plastic. (B) The growth of normal and cancerous mammary epithelial cells appears different in IrECM. In normal cells, they undergo a quick proliferation phase, followed by a period of apoptosis of luminal cells resulting in luminal clearing and polarized acini (top). Cancer cells grown in IrECM display tumor-like properties and many times can grow into a tumor-like mass of cells, well after the polarized acini have stopped proliferating. Figure adapted from (Xu et al., 2009) and (Vargo-Gogola and Rosen, 2007).

1.7. Rationale and Central Focus

The overarching goal of this dissertation is to describe the signaling mechanisms that relate microenvironmental cues such as serum loss to the control of cell growth. Epithelial cells respond to factors in their surrounding microenvironment to modulate their rates of cellular division and proliferation (Hussein and Hassan, 2006; Rutherford and Ross, 1976). Some factors in serum, including LPA, S1P, and EGF, activate specific receptors that then initiate complex signaling that promotes cell proliferation and survival (Ishii et al., 2004; Wells, 1999). Recent studies find such signaling includes the Hippo pathway, a major mechanism for controlling cell growth, organ size, and tumorigenesis. LPA, S1P, and EGF accomplish this by inducing the activity of the transcriptional co-activators YAP and TAZ (Fan et al., 2013; Miller et al., 2012; Yu et al., 2012). However, very little is known about how epithelial cells, in the absence of these factors keep YAP and TAZ inhibited. In cell culture, epithelial cells are typically grown in medium containing 10 % Fetal Bovine Serum (FBS) (v/v), which contains high levels of LPA and S1P. Upon depriving cells of FBS, YAP phosphorylation increases and its ability to activate transcription is blocked (Miller et al., 2012). How this occurs remains unknown.

Recent work implicates the Angiotensins in Hippo signaling, by directly binding and sequestering YAP out of the nucleus (Chan et al., 2011; Wang et al., 2011; Zhao et al., 2011a). Further, Angiotensins activate LATS1/2 protein kinases leading to increased phosphorylation of YAP (Paramasivam et al., 2011). However, there are no reported links between serum factors and the regulation of Angiotensins. It is hypothesized that serum factors play an important role in YAP activity through modulation of the functions of Angiotensins.

Further, the Nedd4 ubiquitin ligase, AIP4 binds to and polyubiquitinates LATS1, leading to LATS1 degradation (Salah et al., 2011). Recently, AIP4 was demonstrated to bind Angiotensins, although the functional outcome of this interaction is unclear (Wang et al., 2012)

Based upon the above observations, there is a gap in the understanding about the function of factors in the microenvironment that influence the growth of epithelial cells through Hippo

signaling. While significant advances have been made in our understanding of this pathway, the role of the Angiotensins and Nedd4 ligases, like AIP4, in this process remains unknown.

The central focus of this dissertation is the discovery of a major mechanism for growth inhibition in response to serum deprivation. The central focus was tested by examining: 1) The phosphorylation of the long isoform of Angiotensin, Amot130, and its effects on growth in mammary epithelial cells. 2) The fundamental role of Amot130-AIP4 complex formation and its effects in mammary cancer epithelial cells. 3) The effects of both serum deprivation and Amot130-AIP4 complex formation on downstream YAP activity in mammary cancer epithelial cells. Here, serum deprivation is found to activate the Hippo protein kinase, LATS1, which phosphorylates Amot130. Phosphorylation of Amot130 promotes the stability of Amot130 via formation of a complex with AIP4. The Amot130-AIP4 complex is further found to promote the degradation of YAP. Together, these events help explain how serum deprivation activates Hippo-dependent pathways to prevent cellular proliferation and growth in mammary epithelial cells.

CHAPTER 2. MATERIALS AND METHODS

Some text in this chapter was originally published in The Journal of Biological Chemistry and the Proceedings of the National Academy of Sciences USA. Adler et al. Amot130 Adapts Atrophin-1 Interacting Protein 4 to Inhibit Yes-Associated Protein Signaling and Cell Growth. *Journal of Biological Chemistry*. 2013; Vol: 288, 25: 15181-15193. © the American Society for Biochemistry and Molecular Biology. Adler et al. Serum deprivation inhibits the transcriptional co-activator YAP and cell growth via phosphorylation of the 130-kDa isoform of Angiotensin II type 1 receptor by the LATS1/2 protein kinases. *Proceedings of the National Academy of Sciences*. 2013; Vol: 110, 43: 17368-17373. © Proceedings of the National Academy of Sciences USA.

2.1. Methods of Cell Culture

Cells in two dimensions were cultured at 37 °C with 5 % CO₂ (v/v) and defrosted and passaged as follows. Cells were rapidly defrosted from -80 °C in a 37 °C water bath. Then cells were collected by centrifugation for 1.5 minutes at 0.4 x g at room temperature. Medium was aspirated from the cell pellet, and the cells were resuspended with fresh medium into a 10 cm² plate. During the next day and continuing as needed, cells were washed with warm phosphate-buffered saline (PBS). Cells were coated with a solution of 2.5 g/L trypsin (Sigma) combined with 5 mM EDTA (Sigma), rocked back and forth gently, and placed in the 37 °C incubator until the cells no longer adhered to the plastic. The released cells were then collected in an equal volume of medium, as that used to trypsinize cells. Cells were transferred to a conical vial and centrifuged at 0.4 x g for 1.5 minutes at room temperature. The resulting cell pellets were resuspended in medium before further dilutions or cell counting, transferred to the appropriate size plate, and placed back in the incubator.

MDA-MB-468, MCF7, and HEK 293T cells were cultured in Dulbecco's Modified Eagle Medium (DMEM) with 10 % FBS (v/v) (10 % serum). BT-474 cells were cultured in Roswell Park Memorial Institute (RPMI) medium with 10 % FBS. MCF10A cells were cultured in equal parts Hams-F12/DMEM supplemented with 50 µg/mL Bovine Pituitary Extract (Hammond, 1078-NZ), 0.5 µg/mL hydrocortisone, 5 µg/mL human insulin, 10 ng/mL EGF, and 100 ng/mL cholera toxin. MCF10A cells were placed onto laminin-rich extracellular matrix (lrECM) (MatrigelTM, 7.5 mg/mL or greater protein, BD Bioscience) in MCF10A medium as described above except lacking only EGF. The cultured cells were incubated overnight and then replaced after 16 hours with medium supplemented with 5 ng/mL EGF. All cell lines were cultured with 1 % (v/v) penicillin/streptomycin. MDA-MB-468, MCF7, and BT-474 cell lines were gifts from Harikrishna Nakshatri, Linda Malkas, and Brittney Shea-Herbert, respectively. MCF10A and HEK 293T cells were purchased from American Type Culture Collection (ATCC).

Cells were treated with cycloheximide (CHX) (Sigma, C7698) at 200 $\mu\text{g}/\text{mL}$ as previously reported (Pervin et al., 2011), and treated with MG-132 (Calbiochem, 474790) at 25 μM , as indicated. Cells were treated with Opti-MEM (Gibco, ref. # 31985-070) for all serum starvation studies, for times indicated.

2.2. Stable Cell Line Generation Using Lentivirus

The following method was used to generate stably expressed proteins or short hairpin RNA (shRNA). At the first day, HEK 293T cells were seeded at 4 million cells into a 10 cm^2 dish, before noon. Transient transfection of HEK 293T cells was carried out the next day about 32 hours after plating. The target DNA construct (protein or shRNA) required the following: 1 mL Opti-MEM, 6 μg pCMV-VSVG, 5 μg psRSV-Rev, 10 μg pMDLg-RRE, 20 μg target DNA construct, and 25 μL polyethylenimine (PEI) (2 $\mu\text{g}/\text{mL}$). Transient transfections utilizing PEI were carried out as described below (section 2.3). The cells at the time of transfection should be about 75 % confluent. If less, reduce the PEI to 20 μL . The following morning, about 16 hours after transfection, the medium was aspirated and replaced with 7 mL of fresh medium. At that same time, target cell lines were plated for infection in cell line specific medium. For example, 400,000 cells were split into a 6 cm^2 dish per condition for the infection of 1-2 target DNA constructs. The following day about 24 hours after medium change, viral medium was removed from the HEK 293T cells, and then passed through a 0.45 μm filter before 10 μL polybrene (5 mg/mL) was added per plate of viral medium. This viral medium was stored at 4 $^{\circ}\text{C}$ for up to two weeks. If a second round of viral harvesting was desired, 7 mL of fresh medium was added to viral producing HEK 293T cells. Finally, harvested viral medium was added to target cell lines (which had at least 24 hours to adhere) and allowed to infect for at least 4-6 hours prior to being replaced with appropriate cell line specific medium. Target cells were harvested between 24 and 72 hours as indicated.

2.3. Method of Transient Transfection

Transient transfection of cells was accomplished as follows. Cells were plated based on assay requirements. Typically, cells were allowed about 24 hours to adhere to the culture dishes, reaching about 80 % confluent, prior to transfection. The desired construct(s) or shRNA was added to a plastic falcon tube containing 1 mL of Opti-MEM. While vortexing at medium speed, a slightly lower volume of 2 µg/mL PEI (Sigma) was added dropwise to the Opti-MEM/DNA solution compared to the amount of DNA added (i.e. 4 µL PEI for 5 µg DNA). This mixture was allowed to incubate for 5 minutes at room temperature before addition to the cells. Transfection mixture was added to the sides of the plate of cells already covered in the appropriate medium from the previous cell split.

2.4. Plasmids, Antibodies, and Lysis Buffers

Plasmids: Full length Amot130, AmotL1, AmotL2, Nedd4 ligases, MST2, and YAP2 were subcloned by PCR from Kazusa and IMAGE complimentary DNAs (cDNAs) into Creator based acceptor vectors (Colwill et al., 2006) for mammalian expression with the N-terminal tags 2X-Myc, 3X-Flag-, monomeric(m) mCitirine- (referred to as YFP), mCerulean- (referred to as CFP), and mCherry-. Previously described vectors include Myc-tagged AIP4, Myc-tagged AIP4 (C830A) (Ingham et al., 2005), HA-tagged Ubiquitin (Guo et al., 2006), and pRL-TK-Renilla (Promega, E2241) (Ranahan et al., 2011). Vectors acquired from Addgene: Flag-tagged YAP2 (19045), Flag-tagged LATS1 (18971), HA-tagged Lys-0 (K0) Ubiquitin (17603) (Lim et al., 2005), pCMV-VSVG (8454), psRSV-Rev (12253), pMDLg-RRE (12251), and shRNA control pLKO.1 (1864). The three P-Y motifs LPTY (P-Y1), PPEY (P-Y2), and PPEY (P-Y3) as well as serine-175 in Amot130 were mutated by the Stratagene QuikChange™ site directed mutagenesis to encode LPTF (P-Y1F), PPEF (P-Y2F), PPEF (P-Y3F), and serine-175 mutated to alanine

(S175A) as single mutations. The P-Y mutants were subsequently used as templates for the double mutations. The lysine-481 in Amot130 was mutated to an arginine (K481R) and was ordered as a synthesized gene fragment from Eurofins MWG Operon and cloned into pBluescript II SK(+). The cDNA encoding Amot130 (K481R) mutant was sub-cloned by restriction enzymes into the vectors described in the Appendix. All mutants cloned are also outlined in the Appendix. The cDNA segments encoding the WW domains of AIP4 and YAP2 were amplified by PCR and cloned into PGEX-KG for glutathione s-transferase (GST) pull-down analysis. Plasmids used in this thesis that were given as gifts and described previously include: His-tagged Ubiquitin wild-type, (K48R), and (K63R) (Hua Lu) (Lo et al., 2012), 5XGal4-luc and Gal4-TEAD4 (Lawrence Quilliam) (Nguyen et al., 2012). Full descriptions of each cloning strategy for each cDNA used and all sets of sense and anti-sense oligonucleotide primers are found in the Appendix.

Antibodies for immunoblot and dilutions: Amot 1:1000, AmotL1 1:5000, HA (12CA5) 1:1000, Myc (9E10) 1:1000, as described in (Ranahan et al., 2011). Purchased antibodies include: Flag (Sigma, F3165) 1:10000, Flag (Sigma, F7425) 1:1000, Myc (Cell Signaling, 2272S) 1:1000, YFP/GFP (Invitrogen, A6455) 1:1000, AIP4 (BD Biosciences, 611198) 1:1000, AIP4 (Santa Cruz, G-11 sc-28367) 1:200, GAPDH (Millipore, MAB374) 1:5000, LATS1 (Bethyl, A300,-477A) 1:1000, pS909 LATS1 (Cell Signaling, 9157S) 1:1000, YAP (Abnova, H00010413-MO1) 1:1000, pS127 YAP (Cell Signaling, 4911S) 1:1000, TAZ (BD Biosciences, 560235) 1:1000, His (Abnova, MAB1274) 1:1000, Caveolin1 (BD Biosciences, 610407) 1:1000, snRNP70 (Santa Cruz, C-18 sc-9571) 1:1000, and Thiophosphate Ester (Abcam, 92570) 1:5000. Antibodies for immunoprecipitation and amount used per reaction: AIP4 (Santa Cruz, G-11 sc-28367) 4 µg, YFP/GFP (Invitrogen, A6455) 2 µg, Amot (Heller et al., 2010) 2 µg, or Flag (Sigma, F3165) 2 µg.

Lysis buffers: Cells on plastic and lrECM were lysed in radioimmunoprecipitation assay (RIPA) buffer (50 mM Tris pH 8.0, 2 mM EDTA, 10 % Triton-100, 150 mM NaCl, 0.1 % SDS) containing 1 mM NaVO₄, 2 mM β-glycerol phosphate, and protease inhibitor cocktail (Sigma)

unless otherwise noted. For immunoprecipitation reactions, cells on plastic were lysed in phospholipase C (PLC) lysis buffer (50 mM HEPES pH 7.5, 150 mM NaCl, 10 % Glycerol, 1 % Triton X-100, 1.5 mM MgCl₂, and 1 mM EGTA) containing protease inhibitor cocktail (Sigma). The volume of lysis buffer used was variable between assays.

2.5. Method of Immunoblot and Western Analysis

Proteins were resolved and analysis of protein completed via a sodium dodecyl sulfate polyacrylamide gel electrophoresis (SDS-PAGE) combined with a western blot analysis method that follows. First, cells were placed on ice and medium was aspirated off the cells. Cells were washed twice with cold PBS. Lysis buffer, described in section 2.4, was added directly to cells on plates. For HEK 293T cells, plates were scraped immediately and mixture was transferred to 1.5 mL tubes. For all other cell lines, cells were left to incubate with the lysis buffer on the plates for 5 minutes, then were scraped and transferred to 1.5 mL tubes. Cells in lysis buffer were pipetted several times to ensure disruption of aggregates, then transferred to ice and incubated for 10 minutes before a 10 minute centrifugation at 17,949 x g at 4 °C. The supernatant was saved and used as clarified lysates. Bicinchoninic acid (BCA) (Bio-Rad) assay was used to determine the protein concentrations of clarified lysates. Normalized protein concentrations from lysates were boiled in SDS-PAGE sample buffer and loaded onto 6, 8, or 10 % polyacrylamide gels, depending upon size of proteins of interest. For example, the Angiotensins are best visualized with an 8 % polyacrylamide gel. Gels were run at 80 Volts for 15 minutes, then 140 Volts for about 45 minutes. Proteins were then transferred to Protran BA85 nitrocellulose membranes (GE Healthcare Life Sciences) via Genie-Blotter (Idea-Scientific) for 1.5 hours at 12 Volts. Membranes were briefly washed with ultrapure water. Then, membranes were blocked in a 5 % low-fat milk solution for 30 minutes on an orbital shaker at room temperature. Membranes were washed 3 X in TBS with 0.075 % (v/v) Tween20 (Sigma) (TBST) for 5 minutes using an orbital

shaker at room temperature. Then, membranes were transferred to sealed hybridization bags and incubated with 4 mL TBST and diluted primary antibody, as described in section 2.4, on a nutator for 1 hour at 4 °C. Then, membranes were washed 3 X in TBST for 5 minutes on an orbital shaker at room temperature. Membranes were then incubated with goat anti-rabbit Dylight 680 (Thermo-Scientific) conjugated secondary and/or goat anti-mouse Dylight 800 (Thermo-Scientific) conjugated secondary or a donkey anti-goat Dylight 800 (Licor Odyssey) conjugated secondary at a 1:20000 dilution in TBST for 30 minutes, on an orbital shaker at room temperature, in the dark. Membranes were washed 3 X in TBST for 5 minutes on an orbital shaker at room temperature in the dark before being imaged on LiCor Odyssey scanner and quantified with ImageJ (Rasband, 2011).

2.6. Immunoprecipitation Procedure

Immunoprecipitation of proteins from cell lysates with a Flag (Sigma, F3165) or YFP/GFP (Invitrogen, A6455) antibodies was achieved as follows. Cells were grown on a 10 cm² plate and harvested in 1 mL PLC lysis buffer, as described in section 2.4. After the centrifugation step described for cell harvesting of protein, as described in section 2.5, 100 µL of lysate from tube was removed and saved on ice as lysate. To the remaining volume, 2 µg of the desired antibody was added to the 1.5 mL tube containing the immunoprecipitation (IP) reaction. The IP reaction was allowed to rock for 1-2 hours on a nutator at 4 °C. IP reactions were then centrifuged at 956 x g for 2 minutes at 4 °C. To the tube, 20 µL of diluted protein G sepharose, using a cut pipette tip, was added to each IP reaction. The IP reaction rotated on a nutator at 4 °C for 1 hour. IP reactions were then centrifuged at 956 x g for 2 minutes at 4 °C. The supernatant was removed and discarded. The bead pellet was then washed 3 X with PLC lysis buffer, without protease inhibitors for 5 minutes each at 4 °C and then centrifuged at 956 x g for 2 minutes at 4 °C following each wash. At end of the last centrifugation, the supernatant was removed, and 60 µL

of 2X-concentrated SDS-PAGE sample buffer was added to each tube. At the same time, 20 μ L of 1X SDS-PAGE sample buffer was added to the lysates that were saved. Both lysates and IP reactions were boiled for 5 minutes at 100 $^{\circ}$ C. The IP reactions were centrifuged at 956 x g for 2 minutes at room temperature. Then roughly 60 μ L of IP reaction mixture was removed and added to a new 1.5 mL tube, which was centrifuged again at 956 x g for 2 minutes at room temperature. Finally, 15 μ L of the IP reactions and lysates were added to an appropriate SDS-PAGE gel and analyzed, as described in section 2.5.

Immunoprecipitation of proteins from cell lysates with Amot (Heller et al., 2010) or AIP4 (Santa Cruz, G-11 sc-28367) antibodies were achieved as follows. Following protocol outlined above, prior to incubation with primary antibody, IP reaction was pre-incubated with 20 μ L diluted protein A sepharose and allowed to rock on nutator for 30 minutes at 4 $^{\circ}$ C. Then tubes were centrifuged at 956 x g for 2 minutes at 4 $^{\circ}$ C. The supernatant was saved and transferred to a new tube. Remaining steps are the same as outlined above. Exceptions include the utilization 4 μ g of the AIP4 antibody for the IP and utilizing protein A sepharose instead of protein G sepharose for the 1 hour incubation to bind the primary antibodies.

2.7. Glutathione S-Transferase Pull-Down Procedure

Analyses of GST-fused proteins binding to endogenous proteins from cellular lysates were accomplished as follows. HEK 293T cells were grown in a 10 cm² plate and were lysed, as described in section 2.5, with 500 μ L PLC lysis buffer. From this clarified lysate, 100 μ L was saved as a control. In a separate 1.5 mL tube, 20 μ L glutathione-sepharose beads were added using a cut tip on a pipette. Beads were washed with cold PBS twice and centrifuged at 956 x g for 2 minutes at 4 $^{\circ}$ C. Further, these beads were then incubated with 500 μ mol GST-fused protein for 30 minutes on nutator at 4 $^{\circ}$ C. Finally, beads were centrifuged at 956 x g for 2 minutes at 4 $^{\circ}$ C and washed 3 X in cold PBS. The immobilized GST-fused protein on glutathione-sepharose was

incubated in its 1.5 mL tube to a final concentration of 2 µg/µL, with the remaining HEK 293T cell lysate to a total volume of 500 µL for 2 hours at 4 °C on nutator with constant mixing. Immobilized protein complexes were washed 3 X with PLC lysis buffer with centrifugation steps of 956 x g for 2 minutes at 4 °C. The bound protein was eluted with 2X-concentrated SDS-PAGE loading buffer, and analyzed as described in section 2.5.

2.8. RNA Interference and Short Hairpin RNA Information

Transient knockdown of proteins utilized 20 nM small interference RNA (siRNA) AIP4 ON-TARGETplus SMARTpool (L-007196-00-0005, Dharmacon), 20 nM siRNA LATS1 siGenome SMARTpool (M-003865, Dharmacon), or 20 nM control ON-TARGETplus (#1 D-001810-01-20, Dharmacon) and the DharmaFECT transfection protocol using the DharmaFECT Duo transfection reagent (# T-2010-01, Dharmacon).

For stable silencing, shRNA plasmid Angiotensin II (Sigma, cat. # TRCN0000162009), shRNA plasmid AIP4 (Sigma, cat. # TRCN0000002087) (Salah et al., 2011), or shRNA plasmid LATS1 (Sigma, cat. # TRCN0000001777) (Nguyen et al., 2012) sequences in pLKO.1 or a scramble shRNA control pLKO.1 (1864, Addgene) were transfected into HEK 293T cells with packaging vectors (pCMV-VSVG, psRSV-Rev, pMDLg-RRE) by PEI method, as described in sections 2.2 and 2.3. All plasmids have been previously described or validated. Cells silenced for Angiotensin II were harvested 24 hours after infection. All other silencing experiments were harvested 48 hours after infection. The shRNA sequences are provided in the Appendix.

2.9. RNA Extraction, cDNA Synthesis, and Quantitative Real Time PCR

RNA for quantitative real time polymerase chain reaction (qRT-PCR) was extracted by the following method. Stably infected cells were plated onto 6 cm² plate. When ready for harvest,

media was aspirated and cells were washed with 1 mL cold PBS. Then 1 mL Tri-Reagent LS (Sigma) was added directly to cells. This mixture was transferred to a 1.5 mL tube and incubated at room temperature for 5 minutes. Then 200 μ L of chloroform was added, followed by inverting the tube to mix for 15 seconds. This mixture was allowed to incubate at room temperature for 5 minutes. Tube was centrifuged at 4 °C for 10 minutes at 17,949 x g. Importantly, all remaining steps were performed on ice, unless otherwise noted. The upper aqueous phase containing RNA was transferred to new 1.5 mL tube. The other two layers, interphase (DNA, white) and organic phase (proteins, lipids, pink), were discarded. To the upper aqueous phase, 500 μ L cold isopropanol was added to precipitate the RNA. The tube was inverted to mix for 15 seconds and allowed to incubate on ice for 5 minutes. The sample was centrifuged at 4 °C for 10 minutes at 17,949 x g. Supernatant was removed completely from tube and discarded, being careful not to lose the pellet. The RNA pellet was washed with 1 mL cold 70 % ethanol. The sample was centrifuged at 10,621 x g at 4 °C for 5 minutes, and then ethanol was removed completely and discarded. The RNA pellet dried for 7 minutes with tube open before resuspension in 20-50 μ L diethylpyrocarbonate (DEPC)-treated water. Finally, the NanoDrop spectrophotometer (Nanodrop Technologies) was used to determine RNA concentration.

Utilizing the RNA generated above, generation of cDNA was accomplished as follows. First, 2-5 μ g RNA were added to 2 μ L Oligo dT (Invitrogen) and 4 μ L dNTP Mix (10 mM) (Invitrogen). The total volume was raised to 24 μ L with DEPC-treated water in a 1.5 mL tube. Mixture was incubated for 5 minutes at 65 °C. Mixture was quickly placed on ice followed by rapid centrifugation. Then 9.5 μ L DEPC-treated water, 0.5 μ L RNase Out (Invitrogen), 4 μ L 10X reverse transcriptase buffer MuLV (New England Biolabs), and 2 μ L of an in-house reverse transcriptase (RT) was added to a tube. Tube was gently mixed with a pipette tip then incubated at 50 °C for 45 minutes. This followed with incubation at 85 °C of the tube for 5 minutes to inactivate the RT. The sample was placed on ice and followed with a quick centrifugation. The sample was then incubated with 0.4 μ L RNase Cocktail (Ambion, cat. #AM2286) for 30 minutes

at 37 °C. Samples were then placed on ice, followed with a quick centrifugation, and then stored at 4 °C for up to one week until ready for real time PCR. Longer term storage was at -20 °C.

The cDNA made from above steps was then used for qRT-PCR as follows. Realplex2 epGradient mastercycler (Eppendorf) with 2X SensiMix SYBR No-ROX Mastermix (BioLine) was utilized per manufacturer's instructions for all qRT-PCR reactions. cDNA was diluted to 400 ng/mL in DEPC-treated water. Each reaction was 20 µL, and contained 3 µL DEPC-treated water, 1 µL sense primer (2.5 µM), 1 µL anti-sense primer (2.5 µM), 10 µL 2X SYBR Mastermix, and 5 µL cDNA template. Oligonucleotide primers used for qRT-PCR are described in the Appendix. All values were normalized to GAPDH, which was run alongside the genes of interest.

2.10. Three-Dimensional Growth Assay Procedure

Three-dimensional growth assays for MCF10A and MDA-MB-468 cells was completed by the following method to be used for stereomicroscopic imaging and immunoblot. Four hours prior to seeding, 1 mL aliquots of lrECM were placed on ice. Once depolymerization of lrECM was complete, cells were trypsinized, as described in section 2.1. Then 200 µL of lrECM was spread per 35 mm² dish. Dishes were transferred to the tissue culture incubator and allowed to incubate for 10 minutes. Each 35 mm² dish received 300,000 MCF10A cells or 200,000 MDA-MB-468 cells. MCF10A cells were resuspended in MCF10A medium, as described in section 2.1, lacking only EGF, overnight then replaced after 16 hours with medium supplemented with 5 ng/mL EGF. MDA-MB-468 cells were resuspended in DMEM with 10 % FBS (v/v). MCF10A medium was replaced every four days as needed. Stereoscope images were taken at times indicated. MDA-MB-468 cell stereoscopic images taken at 10X magnification in lrECM were analyzed for total pixel intensity per field of view because of the complex structures they formed in lrECM. MCF10A acini stereoscopic images taken at 4X magnification in lrECM were

analyzed for cross-sectional area/acini because of the fairly uniform spheres they formed in IrECM. MCF10A acini were also imaged with 10X magnification for high resolution images.

Proteins were extracted from MCF10A acini grown on 35 mm² dishes at time of imaging for immunoblot with the following protocol. Plates were placed on ice and medium was aspirated, and acini were washed with 500 µL cold PBS. Then acini were lysed by addition of 100 µL RIPA with inhibitors, as described in section 2.4. Acini were scraped into slurry and transferred to a 1.5 mL tube. Solution was passed 3 X through a 27-gauge needle into a 10 mL syringe, then transferred to ice for 10 minutes. Tubes were centrifuged at 4 °C for 15 minutes at 20,817 x g. Supernatant was removed and transferred to new tube. Subsequent steps are described in section 2.6.

2.11. TEAD Reporter Assay

Cells were transiently transfected 24 hours after passaging, as described in section 2.3, with 0.02 µg TK-Renilla as a transfection control, 0.05 µg 5XGal4-luc, and 0.4 µg Gal4-TEAD4, in addition to the indicated plasmid vectors (0.63 µg Flag-tagged YAP2 along with 0.63 µg YFP-tagged Amot130 or YFP-tagged Control Vector). Luciferase was allowed to accumulate for 16 hours before cell lysis in passive lysis buffer per manufacturer's instructions (Promega). Samples were processed per manufacturer's instructions for Dual-Luciferase Reporter Assay System (Promega, TM040). A dual luminometer (BioSystems) was used to analyze all samples. Data is presented as average ratios of Firefly luciferase counts over control Renilla luciferase counts.

2.12. Cell Accumulation Assay

Cellular accumulation was assayed after plating 10,000 MDA-MB-468 cells in 12-well plates in 10 % serum (v/v) or in Opti-MEM (Gibco, ref. # 31985-070), for serum starved

conditions. Cells were trypsinized at the indicated times, as described in section 2.1. Cells were counted with a hemocytometer. Data represents the mean of three experiments.

2.13. Cell Proliferation Assay

Measurement of cellular proliferation was carried out per manufacturer's instructions for the CellTiter96® Non-Radioactive Cell Proliferation Assay (Promega, G4000). Measurements were made three days after plating 5,000 MDA-MB-468 cells stably expressing indicated proteins into 100 µL total volume of 10 % serum (v/v) in a 96-well chamber. Data represents the mean of four experiments.

2.14. Method of Nuclear Fractionation

In order to isolate the nuclear fraction of cells for immunoblot analysis, the method that follows was used. MDA-MB-468 cells were harvested 24 hours after plating 5 million cells onto a 10 cm² dish. Cells were removed from the incubator and the medium was aspirated. Cells were washed 2 X with cold PBS. Cells were lysed using 500 µL Nuclear Fractionation Buffer (10 mM HEPES (pH 7.9), 1.5 mM MgCl₂, 10 mM KCl, and 0.05 % IGEPAL (octylphenoxyethoxyethanol), supplemented with inhibitors, as described in section 2.4. Cells were immediately scraped into a 1.5 mL tube and incubated on ice for 10 minutes. Cells were centrifuged at 956 x g for 10 minutes at 4 °C. Then the supernatant was removed and saved as the cytosolic fraction. Pellet was gently washed 3 X in 1 mL Nuclear Fractionation Buffer, and each wash followed with centrifugation at 956 x g for 1 minute at 4 °C. Pellet was then resuspended in 80 µL RIPA lysis buffer with inhibitors, as in section 2.4, and passaged 40 times with a P-200 pipette. Mixture was incubated on ice for 10 minutes before centrifugation at 20,817

x g for 10 minutes at 4 °C. The supernatant was saved and labeled as the nuclear fraction. The protein concentrations of both the cytosolic and nuclear fractions were determined with BCA assay, and then analyzed with SDS-PAGE and western blot, as described in section 2.5.

2.15. Method of Membrane Fractionation

Membranes were isolated with less than 1 mL PLC buffer as described in section 2.4, but lacking detergent. Cells were lysed in a 1 mL glass dounce with 20 strokes of the pestle, and added to a 1.5 mL tube and then centrifuge at 1,000 x g for 3 minutes at 4 °C. The supernatant was added to a TLA 120.2 rotor (Beckman, SN 0641484) and spun at 175,000 x g for 30 minutes at 4 °C. The supernatant was saved as the cytosolic fraction. Then the pellet was washed in PLC detergent-free buffer and spun again at 175,000 x g for 10 minutes at 4 °C. Then the pellet was resuspended in 80 µL PLC detergent-free buffer with a 20-gauge needle. The mixture was spun at 20,000 x g for 10 minutes at 4 °C and supernatant was saved as the membrane fraction. These fractions were analyzed for protein concentrations of both the cytosolic and membrane fractions. Immunoprecipitation reactions were carried out, as described in section 2.6, with detergent-free PLC lysis buffer.

2.16. *In Vitro* SPOTS Phosphorylation Assay Procedure

15-residue peptides were synthesized using the standard SPOT method onto β-alanine derivatized cellulose membranes via a MultiPep synthesizer (Intavis AG, Cologne, Germany) and subjected to a kinase phosphorylation assay in the presence of 25 mM MOPS pH 7.2, 25 mM MgCl₂, 5 mM EGTA, 2 mM EDTA, 0.2 mg/mL BSA, 1 mM DTT, 12.5 mM β-glycerol phosphate, 50 µM cold ATP, 12 µCi/mL [γ -³²P] ATP, and 0.8 µg/mL (7 nM) of GST-LATS2 (SignalChem, L02-11G). The peptide blots were blocked with 0.5 % BSA in PBS pH 7.4 as well

as 1 mM ATP in PBS for 30 minutes each followed by PBS washes. The reactions were incubated for overnight at room temperature, terminated with three washes (100 mM sodium phosphate pH 7.0, 1 M NaCl, 10 mM EDTA) and dried; the extent of radioactive phosphate incorporation was quantified using a Fujifilm phosphoimager and expressed as photostimulated luminescence density (PSL/mm²). 15-residue peptides used for assay: Amot130 Ser-175: QGHVRSLSERLMQMS, Amot130 control (S175A): QGHVRSLSLAERLMQMS, AmotL1 Ser-262: QGHVRSLSERIMQLS, AmotL1 control (S262A): QGHVRSLSLAERIMQLS, AmotL2 Ser-159: HGHVRSLSERLLQLS, AmotL2 control (S159A): HGHVRSLSLAERLLQLS, and YAP Ser-127: PQHVRAHSSPASLQL.

2.17. *In Vitro* Kinase Assay Procedure

The immunoprecipitated Flag-tagged Amot130, Amot130 (S175A) or control vector was incubated with 1.5 μ M serine/threonine protein phosphatase 1 (PP1) α (His-tag purified) for 4 hours at 4 °C in the presence of 50 mM HEPES pH 7.4, 100 mM NaCl, 1 mM MnCl₂, 0.01 % Brij-35, 2.5 mM DTT, 2X-concentrated Calbiochem Protease Inhibitor Cocktail Set V. The samples were then washed 3 X with 25 mM MOPS pH 7.2, 25 mM MgCl₂, 5 mM EGTA, 2 mM EDTA, 0.2 mg/mL BSA and then subjected to a kinase assay in the presence of 25 mM MOPS pH 7.2, 25 mM MgCl₂, 5 mM EGTA, 2 mM EDTA, 0.2 mg/mL BSA, 1 mM DTT, 12.5 mM β -glycerol phosphate, 2X-concentrated Calbiochem Protease Inhibitor Cocktail Set V, 2X-concentrated Calbiochem Phosphatase Inhibitor Cocktail Set I, and 50 μ M ATP- γ -S tetralithium salt (Tocris Bioscience, 4080). The substrates were incubated with either purified GST-LATS2 kinase (0.8 μ g/mL) (SignalChem, L02-11G) or immunoprecipitated Flag-tagged LATS1 kinase (activated via co-expression with MST2 in HEK 293T cells), as described in section 2.6, overnight at 4 °C, terminated with the addition of 50 mM EDTA. The samples were then alkylated via the addition of 2.5 mM p-nitrobenzyl mesylate/5 % DMSO (v/v) (Abcam,

ab128910), incubated for 1 hour at room temperature, and analyzed by SDS-PAGE and western blot, as described in section 2.5.

2.18. Immunofluorescence and Stereomicroscopy

Confocal images were acquired using structured light via an Apotome on a Zeiss Axio ObserverZ1 and processed and analyzed with Zeiss Zen. Stereo images were acquired using a Nikon SMZ1500 microscope. Immunofluorescence was performed as previously described (Heller et al., 2010) with the YAP (Abnova, H00010413-MO1) antibody at a 1:500 dilution. Secondary antibodies included Alexa 546 (Invitrogen) at a dilution of 1:500. Endogenous actin was imaged with Phalloidin-594 Conjugate (Santa Cruz, sc-363795). Nuclei were stained with Hoechst. All labels including primary and secondary antibodies were diluted in blocking buffer solution of (PBS/5 % BSA/1 % Saponin). The three fluorescent signals (green, red and blue) were excited with the Zeiss epifluorescent YFP, DsRed, and DAPI filter sets.

Three-dimensional acini images were obtained from 5,000 MCF10A cells plated onto IrECM, as described in section 2.10, but onto collagen coated filters. After 14 days, the slides were methanol fixed at the indicated times, as previously described (Ranahan et al., 2011).

2.19. Statistical Analysis

Immunoblot (pixel intensities), real time, cell proliferation, cell accumulation, total cross-sectional area/acini, and pixel integrated intensity/field data are presented as the means \pm standard deviation (S. D.). P-values showing differences were calculated by an unpaired two-tailed *t*-test and for showing no differences by a one-tailed *t*-test.

**CHAPTER 3. THE LONG ISOFORM OF ANGIOMOTIN IS PHOSPHORYLATED BY
THE LATS1 AND LATS2 PROTEIN KINASES AND INHIBITS GROWTH IN
MAMMARY EPITHELIAL CELLS**

Some text in this chapter was originally published in Proceedings of the National Academy of Sciences USA. Adler et al. Serum deprivation inhibits the transcriptional co-activator YAP and cell growth via phosphorylation of the 130-kDa isoform of Angiotensin II type 1 receptor (AT1R) by the LATS1/2 protein kinases. *Proceedings of the National Academy of Sciences*. 2013; Vol: 110, 43: 17368-17373. © Proceedings of the National Academy of Sciences USA.

3.1. Introduction

Cells deprived of serum have inhibited proliferation (Pardee, 1974). Many pathways have been implicated in this inhibition of growth via serum starvation, including those that inhibit cell division and control cell cycle checkpoints (Khammanit et al., 2008; Welsh et al., 2001).

Recently, components of the Hippo signaling pathway were found to be regulated by serum factors including LPA, S1P, and EGF (Fan et al., 2013; Miller et al., 2012; Yu et al., 2012). For instance, these serum factors negatively regulate LATS to promote pro-growth signaling in epithelial cells. However, it was unclear how, under steady state conditions, LATS activity was inhibited.

The LATS protein, as its name implies, is a potent tumor suppressor protein. It is a serine/threonine protein kinase shown originally to phosphorylate multiple substrates involved in cell proliferation and survival pathways in *Drosophila* (Xu et al., 1995a). There are two mammalian homologs (LATS1 and LATS2) (Tao et al., 1999; Yabuta et al., 2000) that play critical roles in phosphorylation of substrates involved in cytokinesis, actin polymerization, and cell-cycle checkpoints (Chiyoda et al., 2012; Li et al., 2003; Visser-Grieve et al., 2011; Yang et al., 2004). Mice with inactivated LATS1 develop soft-tissue sarcomas and other tumors, highlighting its tumor suppressive functions (St John, 1999). Reasonably, new substrates of LATS will likely regulate cell division and growth control to transmit LATS tumor suppressive functions in cells.

In this thesis, serum starvation is shown to activate the LATS1 protein kinase. Further, active LATS1 and LATS2 protein kinases are found to directly phosphorylate the Ser-175 residue in the N-terminus of the long isoform of Angiomotin (Amot130). While Amot130 is known to be inhibitory to YAP via its ability to promote LATS activity, little is known about a direct mechanism for how Amot130 may relay Hippo signaling for growth inhibition (Paramasivam et al., 2011; Zhao et al., 2011a). Here, phosphorylation of Amot130 at Ser-175 is shown to be

critical for Amot130 to inhibit cellular growth in mammary epithelial cells. This indicates a novel kinase-substrate pairing between LATS and Amot130 that likely is part of an inhibitory mechanism leading to cellular growth arrest.

3.2. Results

3.2.1. Serum Deprivation and LATS1 Protein Impact the Protein Levels of Amot130

The serum factors EGF, S1P, and LPA activate YAP through GPCR and receptor tyrosine kinase (RTK) initiated signaling. Here, the converse process, of starving cells of serum is shown to induce Hippo signaling and YAP inhibition in breast cancer and non-transformed model cell lines. This delineates a mechanism for how cells lacking these factors actively inhibit their growth. Initially, the effects of serum starvation over time in MDA-MB-468 breast cancer cells were measured on the Hippo pathway proteins LATS1, YAP, and TAZ. The phosphorylation of LATS1 at Ser-909, a surrogate measure of activity, increased by 24 hours, while the levels of YAP and TAZ declined (Figure 3-1), as previously reported (Miller et al., 2012). Additionally, the relative levels of two Angiotensins (Amot130 and AmotL1) were examined during this timecourse. Interestingly, the levels of Amot130 increased between 24-30 hours, unlike levels of AmotL1, which were unchanged. Thus, serum starvation specifically increases Amot130 steady state protein levels. This increase in steady state protein levels in response to serum starvation was found to be significant in all lines tested including MDA-MB-468, HEK 293T, and BT-474 cells (Figure 3-2A-C), which all show relatively high basal protein levels of Amot130. In a study by William Ranahan, the dramatic reduction in Amot130 steady state protein levels upon reintroduction of medium with 10 % serum highlights that there is a tight regulation of Amot130 protein stability (Adler et al., 2013b). Importantly, this is the first demonstration that an Angiotensin is influenced by factors in serum.

The temporal concordance between LATS1 activation and increased steady state protein levels of Amot130 at 24 hours suggests that LATS1 activity may contribute to the stability of Amot130. Consistently, Amot130 protein (Figure 3-3A) was reduced in HEK 293T cells silenced for LATS1 by siRNA expression compared with control cells. Further, LATS1 stable silencing with shRNA demonstrated a significant reduction in Amot130 protein steady state levels in HEK 293T cells (Figure 3-3B), but not *AMOT* mRNA levels (Figure 3-3C). Overall, serum starvation leads to an increase in Amot130 steady state protein levels in cells. Further, this increase in Amot130 steady state protein levels appears to correlate with LATS1 activity. Understanding the possible connections between Amot130 and LATS1 will be examined in the next section.

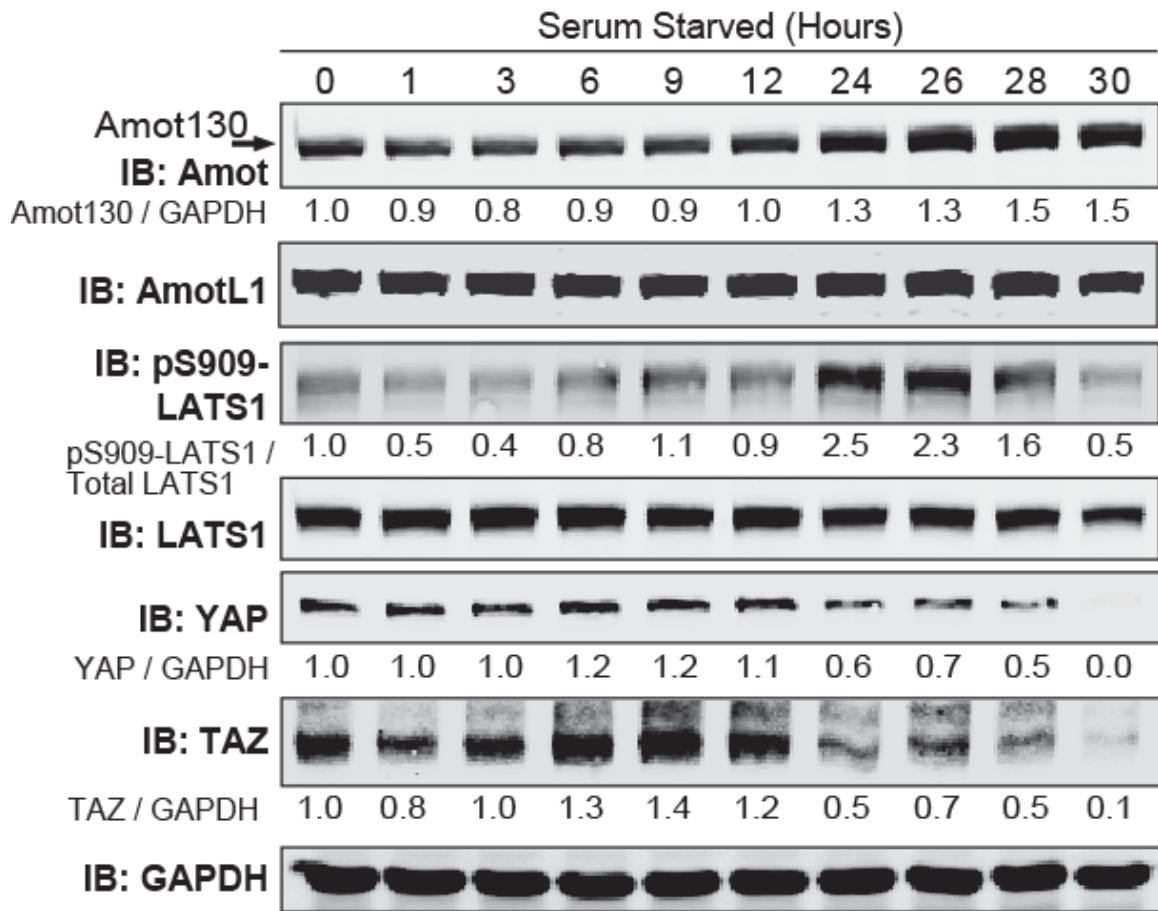


Figure 3-1 Correlation of Amot130 Protein and Hippo Signaling Components Under Serum Starvation Conditions.

The levels of endogenous proteins at the indicated times after initiation of serum starvation were measured by immunoblot from lysates of MDA-MB-468 cells. Pixel intensities of endogenous proteins normalized to GAPDH and the ratios of phosphorylated LATS1 at Ser-909 (pS909) to total LATS1 are provided. Figure adapted from (Adler et al., 2013b).

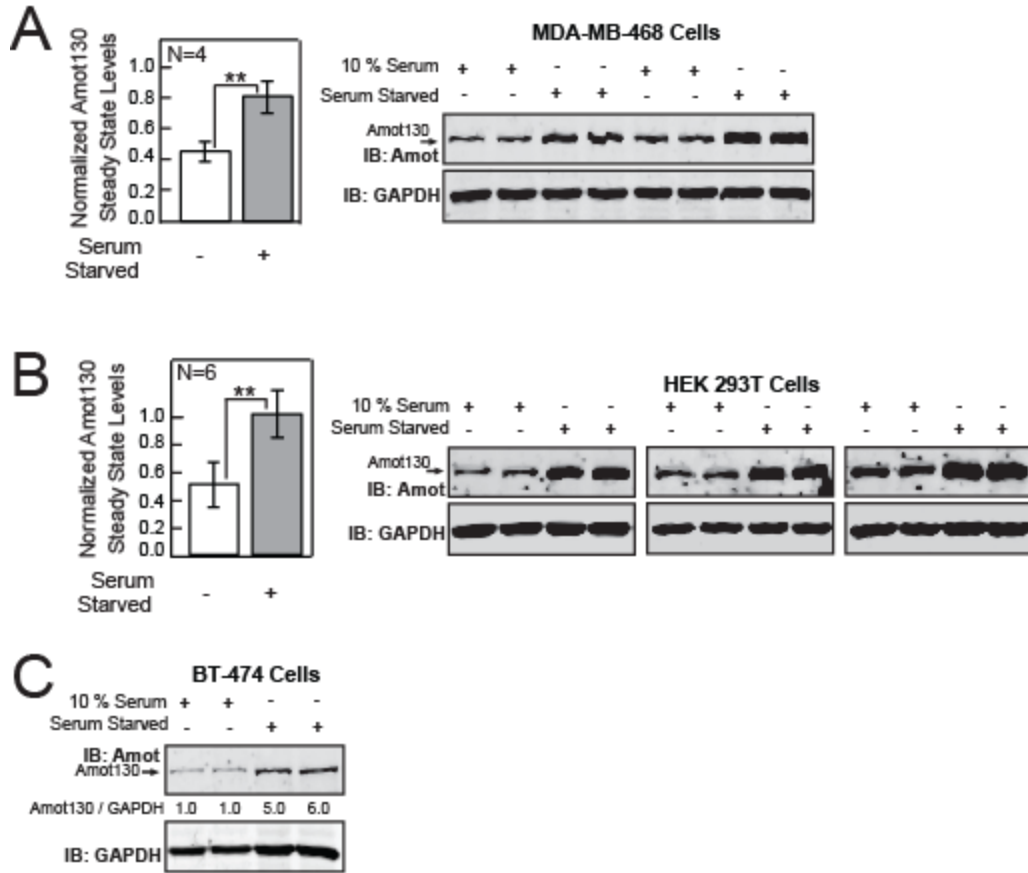


Figure 3-2 Serum Starvation Conditions Increase Amot130 Steady State Protein Levels.

(A-B) Graphs (left) of the mean ratios of endogenous Amot130 over GAPDH from PLC lysates of (A) MDA-MB-468 or (B) HEK 293T cells grown in DMEM with 10 % serum or serum starved for 24 or 16 hours, respectively, for 4 or 6 separate experiments. Immunoblots used to calculate ratios are presented (right). (C) BT-474 cells were treated and harvested as in B and the ratios of endogenous Amot130 over GAPDH are presented below top panel for two separate experiments. Error bars represent \pm S. D. p-values: ** < 0.005. Figure adapted from (Adler et al., 2013b).

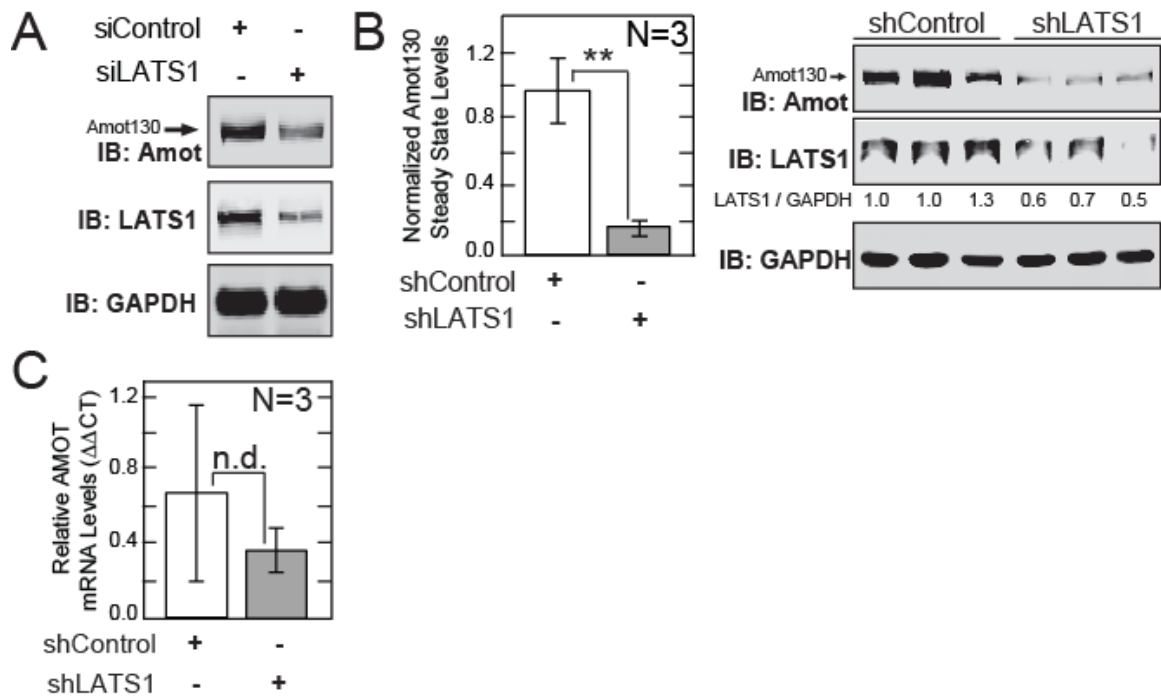


Figure 3-3 Loss of LATS1 Protein Decreases Amot130 Steady State Protein Levels.

(A) Immunoblot analysis of the levels of endogenous Amot130, LATS1, and GAPDH in lysates from HEK 293T cells expressing LATS1 or control siRNA. (B) A graph of the mean ratio of endogenous Amot130 over GAPDH from three experiments ($n = 3$) detected by immunoblot from lysates prepared from HEK 293T cells stably expressing control or LATS1 shRNA. Immunoblots used to calculate Amot130 ratios are presented, with ratios of LATS1 normalized to GAPDH below middle panel (right). (C) Real time quantitative PCR measurements of *AMOT* mRNA from three separate experiments with each performed in technical triplicate ($n = 3$) from paired cells cultured identically and at the same time as in B. Error bars represent \pm S. D. p-values: ** < 0.005; n.d. no statistical difference. Figure adapted from (Adler et al., 2013b).

3.2.2. Amot130 is Phosphorylated by LATS1 and LATS2 at Serine Residue 175

Because of the observed correlated changes in the levels of steady state Amot130 protein in response to LATS1 activity, connections between the Angiomotins and LATS1/2 protein kinases were examined. In doing so, a consensus LATS phosphorylation motif (HVRSLS) in Amot130 (Ser-175), AmotL1 (Ser-262), and AmotL2 (Ser-159) (Figure 3-4A) was predicted via protein sequence analysis. LATS2 catalyzed phosphorylation of these motifs was measured using an array of 15-residue peptides encompassing each motif, control peptides with an alanine at the predicted site of phosphorylation, and the Ser-127 motif in YAP, as a positive control (Figure 3-4B). Peptides were synthesized as individual immobilized spots on a membrane. A purified fragment of active LATS2 phosphorylated the Amot130 motif similarly to the YAP motif, which were both significantly higher than the Amot130 control peptide. AmotL1 motif peptides were also phosphorylated to significantly higher levels than the control peptide. The AmotL2 motif and control peptides were phosphorylated to a similarly low level. It is possible that the serine outside of the LATS consensus site in the control peptides may explain their basal levels of phosphorylation. Further, it is unclear why AmotL2, containing a very similar motif as Amot130 and AmotL1 would not show increased phosphorylation over the control peptide. Closer examination of the Angiomotin peptides reveal the sequences surrounding these motifs are more similar between Amot130 and AmotL1 compared with AmotL2. Alternatively, this peptide may have synthesized poorly.

To confirm a kinase-substrate connection between LATS and Amot130, the phosphorylation of Flag-tagged wild-type Amot130 and the mutant Amot130 with an alanine substituted for serine-175 (S175A) by purified LATS2 and immunoprecipitated Flag-tagged LATS1 was measured in an *in vitro* kinase assay. The purified LATS2 was constitutively active, while Flag-tagged LATS1 was activated in HEK 293T cells by co-transfection with MST2. Immunoprecipitated Amot130 samples were pre-incubated with the protein phosphatase PP1 α

and then assayed for phosphorylation via incorporation of ATP- γ -S by either LATS1 or LATS2, as previously described (Allen et al., 2007). Wild-type Amot130 was phosphorylated 10-fold more than Amot130 (S175A) by LATS2 and over 2-fold more by activated LATS1 (Figure 3-4C). Together, this directly demonstrates that Amot130 is phosphorylated by LATS1 and LATS2 at Ser-175.

The 14-3-3 family of proteins binds specifically to phosphorylated serine residues (Muslin et al., 1996), including phosphorylated Ser-127 in YAP (Zhao et al., 2007). Based upon the similarity between the consensus motifs of Ser-127 in YAP and Ser-175 in Amot130 (Figure 3-4A), the ability of LATS1 to induce 14-3-3 binding to Amot130 was defined. The co-immunoprecipitation of YFP-tagged Amot130 with Flag-tagged 14-3-3 γ was found to be induced in cells expressing MST2 and LATS1, but not from HEK 293T cells expressing either protein kinase in isolation or control vector (Figure 3-5A). Importantly, the LATS1 protein kinase in low confluent HEK 293T cells was relatively inactive, unless it was co-expressed with its upstream protein kinase, MST2 (Figure 3-5B). Together, this demonstrates that active LATS1 protein kinase induces Amot130 to bind 14-3-3 γ . Because 14-3-3 γ failed to bind Amot130 (S175A) under these conditions of high LATS1 activity (Figure 3-5C), the binding of 14-3-3 γ to Ser-175 in Amot130 indicates Amot130 phosphorylation *in vivo*. These results raise many questions about the possible role of 14-3-3 in Amot130 function. While no evidence exists about a connection between 14-3-3 binding and Amot130 function, many studies show that 14-3-3 inhibits cell signaling by blocking interactions with effector proteins and promoting cytosolic sequestration (Bridges and Moorhead, 2005). Studies exploring the impact of 14-3-3 interacting with Amot130 in response to LATS phosphorylation at this residue will potentially explain how this promotes Amot130 to transduce LATS1/2 signaling.

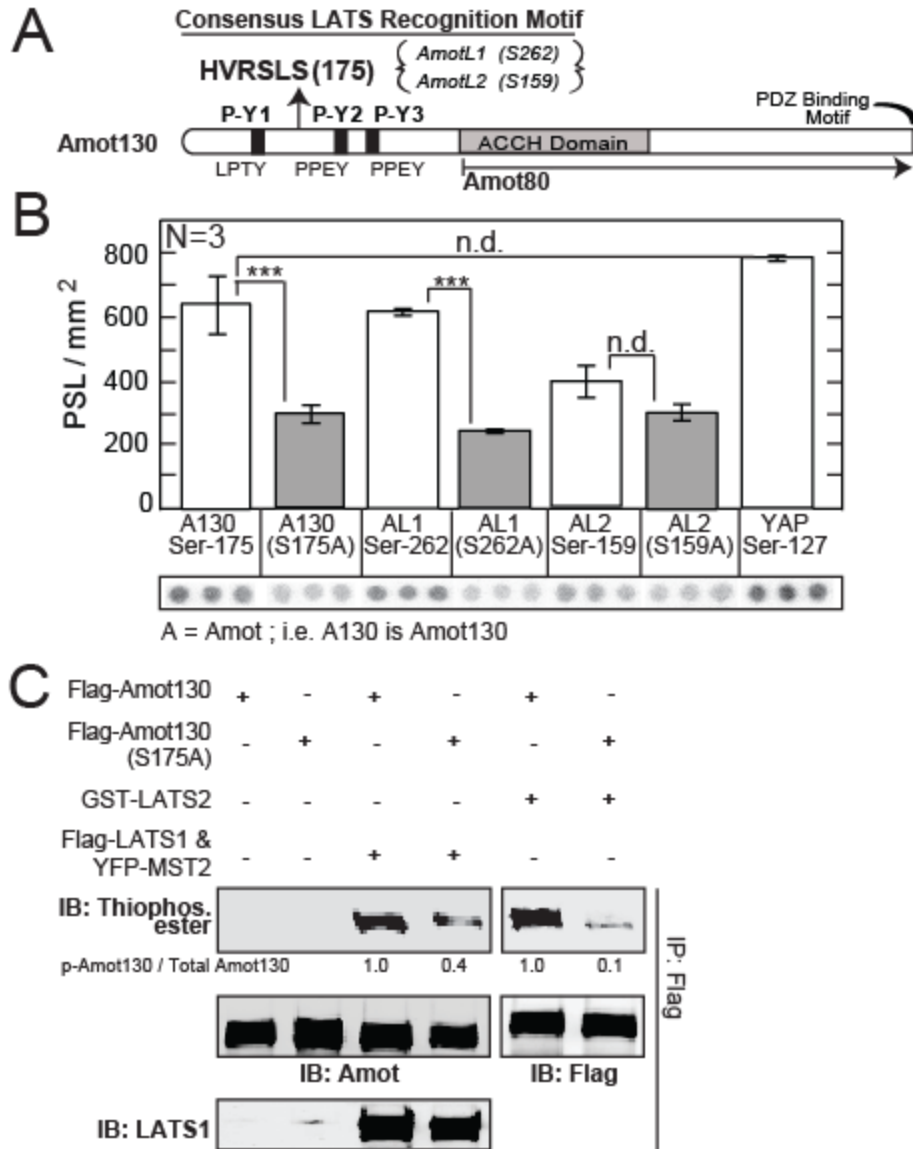


Figure 3-4 LATS1 and LATS2 Phosphorylate Amot130 at Serine-175.

(A) Schematic of the predicted LATS phosphorylation motifs in Amot130, AmotL1, and AmotL2. (B) Graph of the means incorporation of ³²P-phosphate from three independent experiments (n = 3) into the indicated immobilized 15-residue peptides by purified active LATS2. Values represent photostimulated luminescence density (PSL/mm²). Spots are re-arranged from their orientation on original membrane for matching clarity. A = Amot. (C) Immunoblot detecting the ATP-γ-S incorporated into immunoprecipitated Flag-tagged wild-type Amot130 or Amot130 (S175A) by purified LATS2 or immunoprecipitated Flag-tagged LATS1, using an antibody against thiophosphate esters (Thiophos. ester) (top panel) and the ratio of phosphorylated Amot130 to total Amot130 (below), Flag-tagged Amot130 with antibodies against Amot or Flag (middle panel) or LATS1 (bottom panel). Parts B-C were in collaboration with Derrick Johnson. Error bars represent ± S. D. p-values: *** < 0.005; n.d. no statistical difference. Figure adapted from (Adler et al., 2013b).

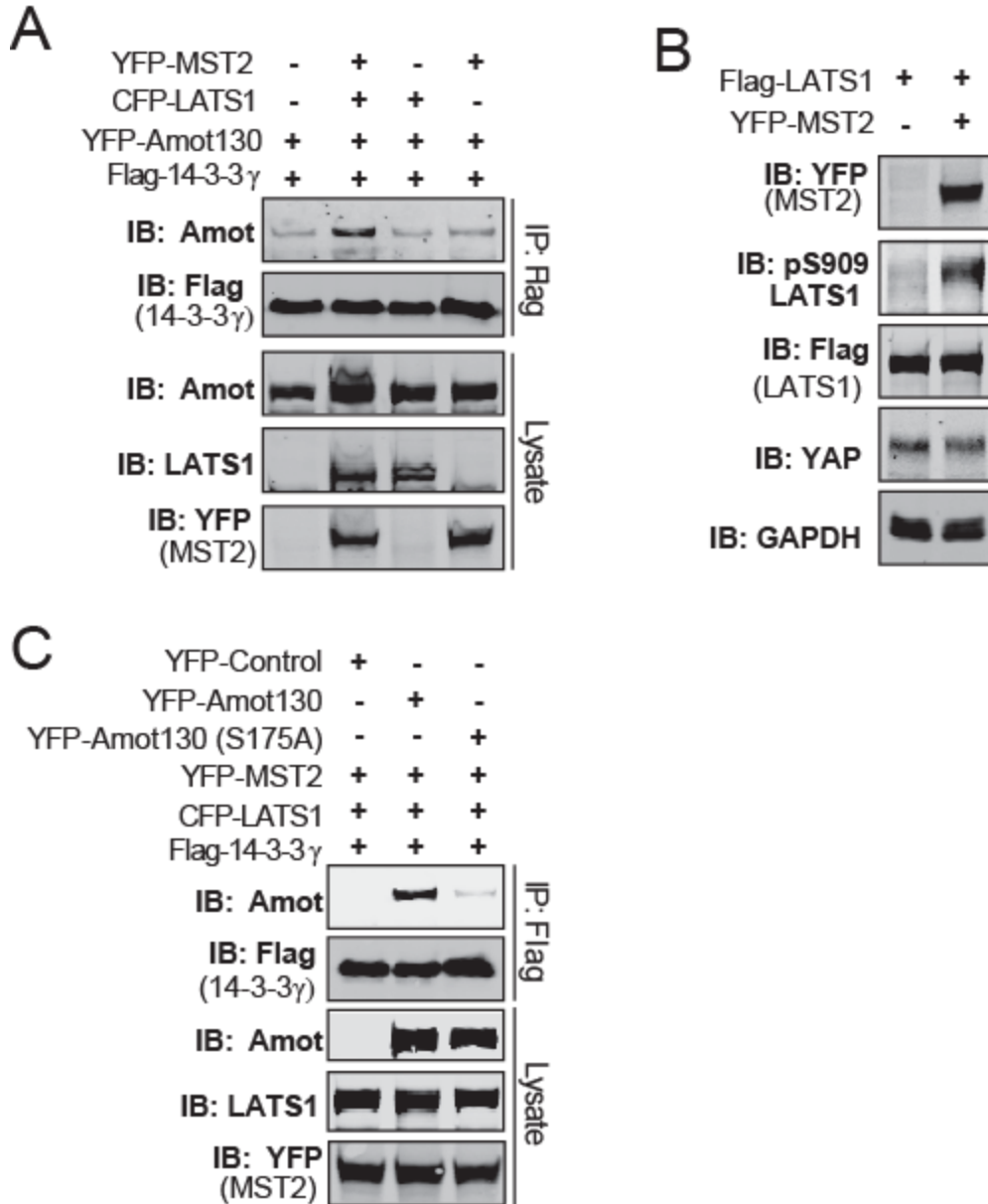


Figure 3-5 LATS1 Phosphorylation of Amot130 at Serine-175 Promotes Binding of the 14-3-3 γ Protein.

(A) Immunoblot of the levels of YFP-tagged wild-type Amot130 in an anti-Flag (14-3-3 γ) immunoprecipitation and the indicated proteins in lysates from HEK 293T cells transfected as indicated. (B) Immunoblot of phosphorylation of Flag-tagged LATS1 at Ser-909 (pS909) as well as YFP-tagged MST2, total Flag-tagged LATS1, endogenous YAP and GAPDH from lysates of HEK 293T cells transfected as indicated. (C) Immunoblot of the levels of YFP-tagged wild-type Amot130 or Amot130 (S175A) in anti-Flag (14-3-3 γ) immunoprecipitations and the indicated proteins in lysates from HEK 293T cells transfected as indicated. Figure adapted from (Adler et al., 2013b).

3.2.3. The Mutant Amot130 (S175A) Lacks the Ability of Wild-type Amot130 to Inhibit the Growth of Breast Cancer Cells and Mammary Acini

Hippo signaling has long been associated with a tumor suppressive role in mediating growth inhibition in response to cell-cell contacts. Therefore, the impact on the ability of Amot130 to be phosphorylated by LATS on cellular growth in breast cancer cells was examined. To measure the effects of expression of wild-type Amot130 and Amot130 (S175A) on contact inhibition, the rate of growth of MDA-MB-468 cells, in tissue culture, in serum free medium or medium containing 10 % serum that stably expressed either protein or a control vector over 4 days was measured by cell counting (Figure 3-6A-C). Cells were stably infected with proteins as indicated (Figure 3-6A) and then 10,000 of these cells were plated into 12-well dishes and allowed to grow. Cells were trypsinized and counted each day. Cells expressing wild-type Amot130 grew at significantly slower rates in the presence or absence of serum, while cells expressing Amot130 (S175A) grew similarly to cells expressing a control vector. Growth of cells was also analyzed using a Promega CellTiter 96® Non-Radioactive Cell Proliferation Assay (Figure 3-6D). The results demonstrated that the wild-type Amot130 had lower rates of proliferation than either the Amot130 (S175A) or control vector. Further, stable expressing cells containing wild-type Amot130, Amot130 (S175A), or a control vector were placed onto laminin-rich extracellular matrix (lrECM) for analysis of their growth as three-dimensional colonies. Cancer cells on lrECM grew as colonies. Cells expressing wild-type Amot130 formed colonies that were about three-fold smaller after four days versus colonies formed by cells expressing Amot130 (S175A) or control vector (Figure 3-6E-G). Thus, in a cancer cell line with defective growth control, the ability of Amot130 to be phosphorylated at Ser-175 was essential for it to induce cell growth arrest.

The growth and differentiation of the non-transformed MCF10A cells into hollow acini in lrECM is highly sensitive to Hippo signaling. Because of the kinase-substrate connection between LATS and Amot130, the effects of expression of wild-type Amot130 and Amot130 (S175A) on

the ability of Hippo-sensitive cells to form acini were therefore compared. After one day of growth, the sizes of cell clusters were nearly identical between all conditions (Adler et al., 2013b). However, MCF10A cells expressing wild-type Amot130 formed significantly smaller clusters that stopped growing by day 4 (Figure 3-7A-D). Conversely, cells expressing Amot130 (S175A) displayed a loss of growth inhibition, where colonies were significantly larger at days 4 and 8 versus those expressing a control vector (Figure 3-7A-D). Furthermore, unlike control cells, which formed hollow acini by day 14, cells expressing Amot130 (S175A) formed solid tumor-like structures (Figure 3-7E). These structures failed to clear their lumen, and resembled cancer-like colonies in IrECM, as presented in chapter 1. Taken together, phosphorylation of Ser-175 is pivotal for Amot130 to inhibit cellular growth in mammary epithelial cancer cells and to inhibit acini development.

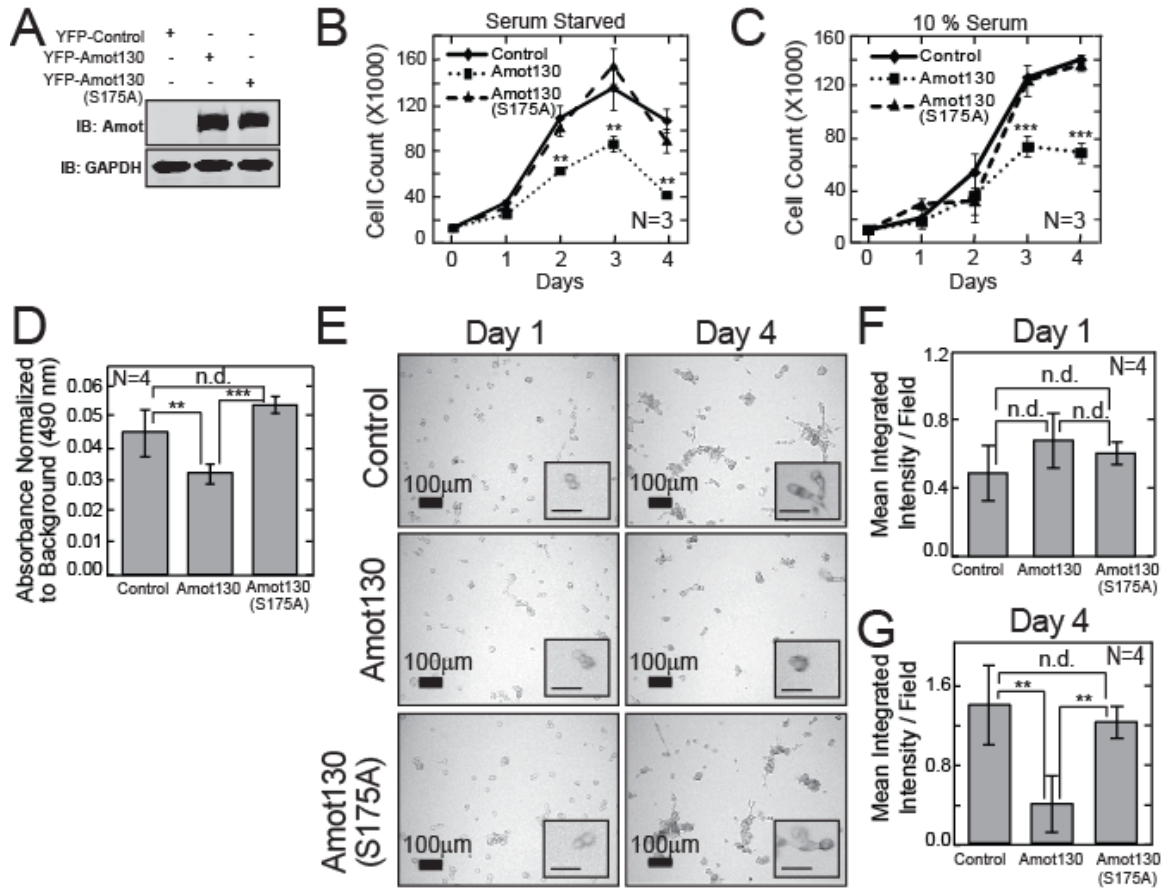


Figure 3-6 Ability of Amot130 to be Phosphorylated at Serine-175 is Essential for Amot130 to Inhibit the Growth of Cancer Cells.

(A) The protein levels of YFP-tagged Amot130 and GAPDH in MDA-MB-468 cells transfected with YFP-tagged wild-type Amot130, Amot130 (S175A), or control vector. (B-C) Cells from A, stably expressing (◆) YFP-tagged control vector, (■) YFP-tagged Amot130, or (▲) YFP-tagged Amot130 (S175A) were grown in (B) serum starved or (C) 10 % serum medium. In both B and C, cells were grown for the indicated days and counted. Average cell counts were derived from three separate experiments (n = 3). (D) Cells from A, were analyzed with a cell proliferation assay for four independent experiments (n = 4) with average absorbance values obtained at 490 nm per assay instructions. (E-G) MDA-MB-468 cells stably expressing YFP-tagged Amot130, Amot130 (S175A), or control vector, as in A, were seeded onto IrECM and imaged after one and four days. (E) Representative brightfield stereo images and (F-G) plots of the mean pixel integrated intensity values/field from four experiments (n = 4) at (F) day 1 and (G) day 4 are presented. Error bars represent \pm S. D. p-values: *** < 0.001; ** < 0.05; n.d. no statistical difference. Unlabeled scale bars represent 50 μ m. Figure adapted from (Adler et al., 2013b).

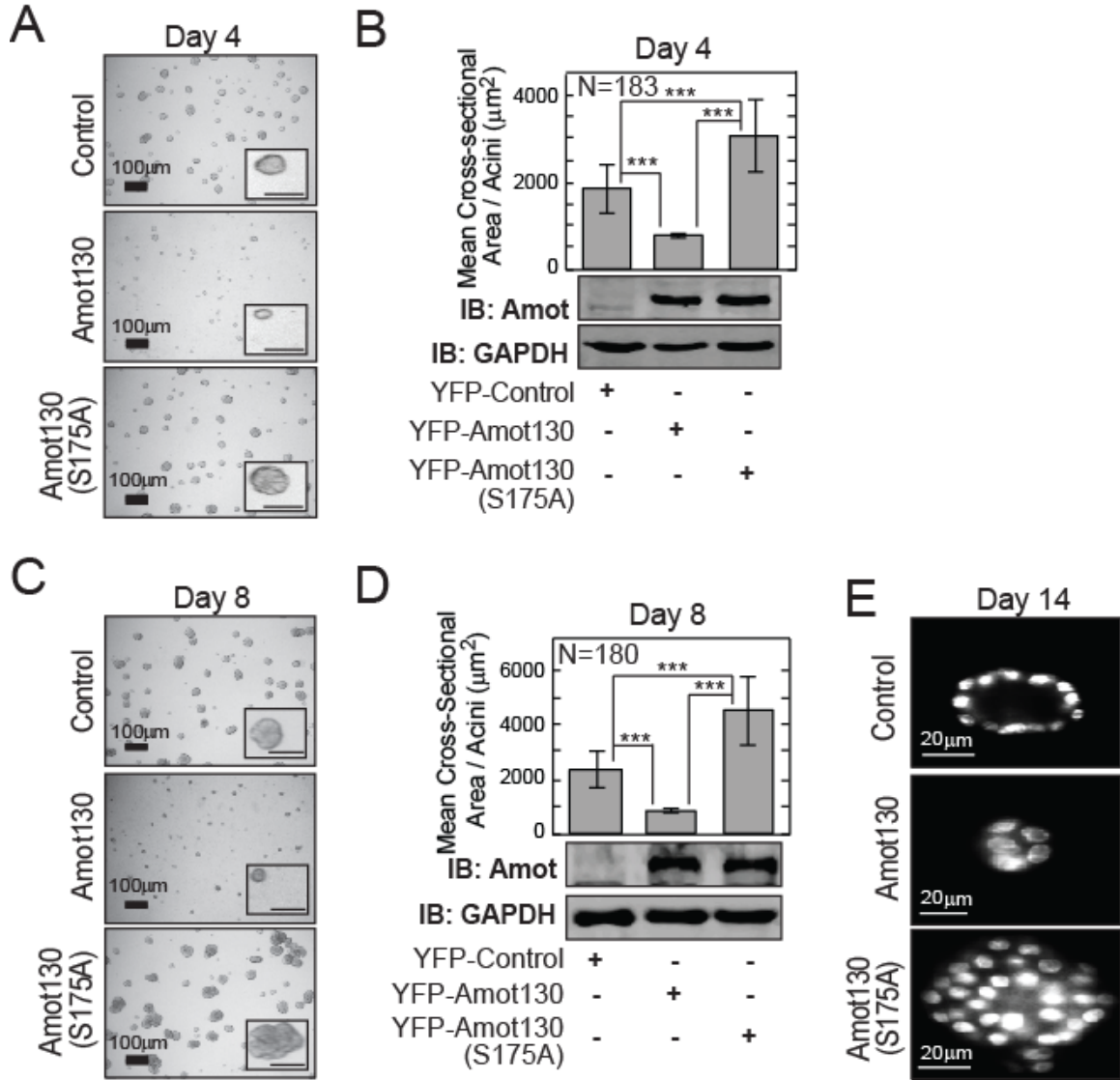


Figure 3-7 Ability of Amot130 to be Phosphorylated at Serine-175 is Essential for Amot130 to Regulate the Growth of Mammary Acini.

(A-E) MCF10A cells stably expressing YFP-tagged wild-type Amot130, Amot130 (S175A), or control vector were seeded onto IrECM and grown for 14 days. (A) Brightfield representative stereo images of colonies at day 4 and (B) plots of the mean cross-sectional area/acini (μm^2) from three experiments each with 61 acini ($n = 183$) at day 4 are graphed. Below plot is an immunoblot measuring YFP-tagged Amot130 or Amot130 (S175A) and GAPDH from cells extracted from IrECM at day 4. (C-D) Brightfield representative stereo images of colonies and plots from three experiments each with 60 acini ($n = 180$) at day 8 as in A and B. (E) Confocal fluorescence images of representative acini stained with Hoechst for nuclei at day 14 of growth. Figure in collaboration with William Ranahan. Error bars represent \pm S. D. p-values: *** $< 1 \times 10^{-40}$. Unlabeled scale bars represent 50 μm . Figure adapted from (Adler et al., 2013b).

3.3. Discussion

3.3.1. A Novel Substrate for LATS1/2 in Hippo Signaling

Several lines of evidence point to LATS1/2 protein kinases as major controllers of cell growth. LATS1/2 protein kinases lead to the phosphorylation of many substrates, including those involved in cell growth control, both inside and outside the Hippo pathway. Understanding the important roles of LATS1/2 protein kinases in inhibiting cellular growth is therefore tied to understanding their substrates. Importantly, this study identifies a novel substrate of LATS1/2 protein kinases in Amot130.

Within the Hippo pathway, serum starvation promotes YAP protein phosphorylation at Ser-127 and decreases YAP steady state levels (Miller et al., 2012). This is thought to be largely due to increased LATS1/2 activity. Here, we show a correlation between prolonged serum starvation and LATS1 phosphorylation at Ser-909, an indicator of its activity. These events temporally correlated with the decreased steady state levels of YAP and TAZ. Decreases in YAP and TAZ protein steady state levels could be due in part to the reported role of LATS1/2 mediated degradation of YAP and TAZ via recruitment of SCF-(β)-TRCP, as previously predicted (Zhao et al., 2010). However, this study indicates that Amot130 is also an important determinate of the output of Hippo signaling. The temporal correlation of an increase in Amot130 steady state protein levels with LATS1 activity and YAP/TAZ reduction indicates a possible connection between Amot130 and the Hippo proteins kinases LATS1/2. Further, the reported role of Angiomotins binding to and activating the LATS2 protein kinase further connects Amot130 with LATS (Paramasivam et al., 2011). Here, Amot130 is shown to be phosphorylated by LATS1/2 at Ser-175. Because LATS1/2 protein kinases are inhibitory to YAP function and pro-growth signaling, it was important to examine how this phosphorylation site on Amot130 would impact growth in mammary epithelial cells. Importantly, the mutation of the serine-175 to an alanine (S175A) prevented the growth inhibition seen by wild-type Amot130. This difference in

growth control potentially indicates the LATS1/2 protein kinases are playing a major role in the inhibitory actions of Amot130. The possible mechanisms of action are examined in the next couple of chapters.

3.3.2. Proposed Mechanism of Amot130 Inhibition of Mammary Epithelial Cell Growth in Response to LATS1/2 Activity

Upon prolonged serum deprivation, MDA-MB-468 breast cancer cells show an activation of the tumor suppressor protein LATS1 (Figure 3-8). Active LATS1/2 protein kinases were able to directly phosphorylate Amot130. This phosphorylation at Ser-175 appears to play an important role in the ability of Amot130 to inhibit cellular growth in cancer cells and to differentiate mammary acini, as mutation of this serine to alanine (S175A), prevented its ability to alter growth. Interestingly, the mutant Amot130 (S175A) actually significantly increased the area of MCF10A acini, which are reported to have active Hippo signaling (Debnath et al., 2003; Kenny et al., 2007; Zhao, 2012). Thus, Amot130 could present itself as a transmitter of upstream Hippo signaling via LATS phosphorylation. Exactly how this proposed regulation of growth occurs downstream of Amot130 phosphorylation by LATS will be examined in the next two chapters.

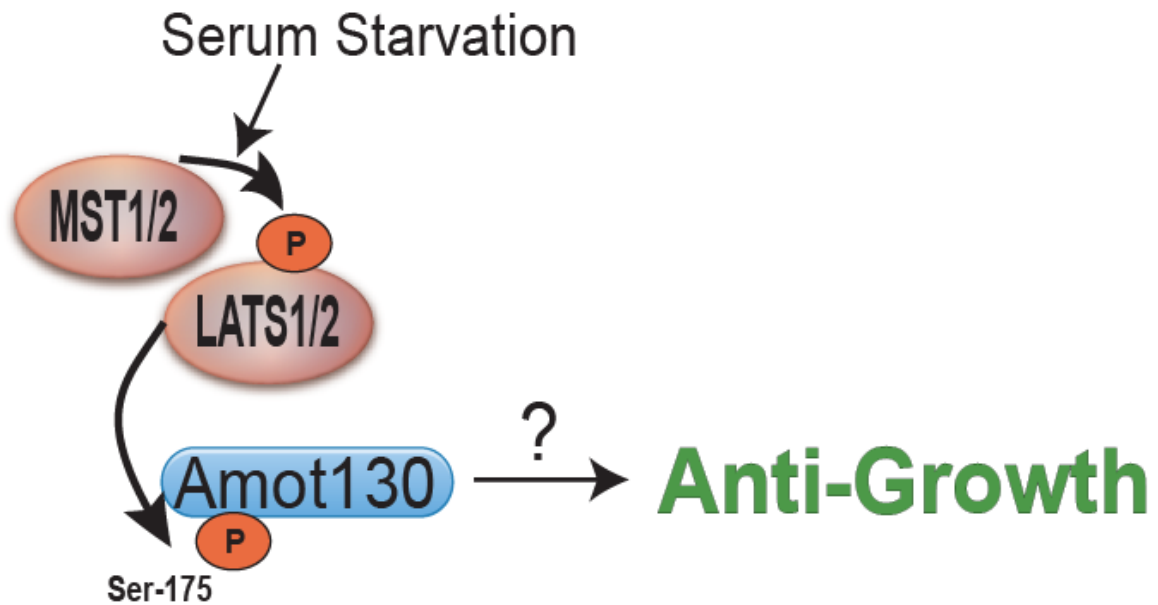


Figure 3-8 Working Model for Serum Starvation Inhibition of Cell Growth.

Amot130 presents itself as a major contributor to the anti-growth phenotype in mammary epithelial cells. Here, LATS1 is activated in breast cancer cells upon serum starvation. Active LATS1 phosphorylates Amot130 *in vitro* and *in vivo*. This phosphorylation site (Ser-175) is critical for growth inhibition, as mutation of this serine to alanine prevents the ability of Amot130 to inhibit cellular growth in cancer cells. Further, this growth inhibition by Amot130 in normal mammary epithelia, that are Hippo sensitive, has a reverse effect when the phosphorylation site is mutated. Thus, it appears that this phosphorylation event is essential for the ability of Amot130 to transduce Hippo signaling to inhibit cellular growth. However, major questions exist about how Amot130 is able to transduce Hippo signaling. Further, the correlation of increased Amot130 steady state protein levels with serum starvation and LATS activity remains to be examined.

**CHAPTER 4. SERUM DEPRIVATION AND LATS1 PROTEIN KINASE ACTIVITY
LEAD TO INCREASED STEADY STATE PROTEIN LEVELS OF THE LONG
ISOFORM OF ANGIOMOTIN VIA THE NEDD4 UBIQUITIN LIGASE AIP4**

Some text in this chapter was originally published in The Journal of Biological Chemistry and the Proceedings of the National Academy of Sciences USA. Adler et al. Amot130 Adapts Atrophin-1 Interacting Protein 4 to Inhibit Yes-Associated Protein Signaling and Cell Growth. *Journal of Biological Chemistry*. 2013; Vol: 288, 25: 15181-15193. © the American Society for Biochemistry and Molecular Biology. Adler et al. Serum deprivation inhibits the transcriptional co-activator YAP and cell growth via phosphorylation of the 130-kDa isoform of Angiomotin by the LATS1/2 protein kinases. *Proceedings of the National Academy of Sciences*. 2013; Vol: 110, 43: 17368-17373. © Proceedings of the National Academy of Sciences USA.

4.1. Introduction

Atrophin-1 Interacting Protein 4 (AIP4), also known as Itch, is a member of the Nedd4 ubiquitin ligases. The effects of ubiquitination on a targeted protein can vary, in some cases it signals for cellular relocalization or degradation. AIP4 binds different substrates and adapter proteins via its WW domains to confer specificity for its catalytic HECT domain. The identification of novel substrates of AIP4 likely will lead to new regulators of growth signaling, as have many of the Nedd4 ligases. Recently, mass spectrometry screens identified Nedd4 ubiquitin ligases interacting with the adapter Angiomotin proteins (Ingham et al., 2005; Wang et al., 2011). Additionally, several of the Nedd4 ubiquitin ligases were able to directly interact with Angiomotins (Wang et al., 2012); however, the functional consequences of these interactions are unknown. Further, while evidence exists for other Nedd4 family members in the degradation of Angiomotins, less is known about the regulation via AIP4.

Here, Amot130 is discovered to be a substrate for AIP4. The interaction is mediated through direct interactions between the WW domains of AIP4 and two specific P-Y motifs of Amot130. The interaction leads to the ubiquitination of Amot130 at Lys-481 and potentially other unidentified sites. Ablation of this ubiquitination site, or silencing of AIP4, leads to decreased protein stability of Amot130, likely via a relocalization of Amot130 off of cell-cell contacts. Importantly, serum starvation and active LATS1 expression increased the interaction of Amot130 with AIP4. Further, active LATS1 promoted the ubiquitination of Amot130 by AIP4. Because Amot130 phosphorylation at Ser-175 is critical for the stability of Amot130, AIP4 activity is identified as a primary mechanism to increase Amot130 steady state protein levels in response to serum starvation and phosphorylation of Amot130 by LATS.

4.2. Results

4.2.1. Amot130 Directly Binds AIP4

Consistent with other reports that Angiotensins bind Nedd4 ubiquitin ligases (Wang et al., 2012), Amot130 co-precipitated with many Nedd4 family members in HEK 293T cells (Figure 4-1). Interestingly, the different Nedd4 ligases had diverse abilities to interact with Amot130. In many cases, the relative binding varied depending on the cellular environment (i.e. cellular confluence). However, the consistent high level of AIP4 binding versus six other members, over many experiments, indicates that AIP4 is a preferred binding partner of Amot130. This was confirmed with endogenous Amot130 co-immunoprecipitation with AIP4 from lysates of HEK 293T cells (Figure 4-2A). The enhanced levels of Amot130 immunoprecipitated with AIP4 in cells treated with MG-132, a drug preventing protein degradation via the proteasome, suggests that the Amot130-AIP4 complex is somehow regulated by the proteasome.

Because AIP4 has four WW domains and Amot130 encodes three P-Y motifs, the relative abilities of the WW domains of AIP4 to bind Amot130 were determined (Figure 4-2B). Initially, immunoprecipitation of fragments of AIP4 indicate that only the absence of functional WW domains reduces binding to endogenous Amot130 (Adler et al., 2013a). Further, pull-downs using the purified GST-tagged WW domains of AIP4 and of YAP, a known binding partner of the P-Y motifs of Amot130 (Zhao et al., 2011a), indicate that the WW1 and WW2 domains of AIP4 precipitate endogenous Amot130 from HEK 293T lysates predominantly versus the WW3 or WW4 domains (Figure 4-2C). This matches the reported specificity of another Nedd4 family member, Nedd4-2, with AmotL1 (Skouloudaki and Walz, 2012). Thus, AIP4 may utilize a combination of multiple WW domains to mediate a stronger interaction with Amot130, like other Angiotensin family members.

While three P-Y motifs within Amot130 are reported to mediate their binding to Nedd4-1 (Wang et al., 2012), their relative importance for binding to AIP4 is undetermined. Consistent

with AIP4 binding to the P-Y motifs in Amot130, Amot80 was unable to co-immunoprecipitate AIP4 (Figure 4-2D). Further, both the P-Y2 (P-Y2F) and P-Y3 (P-Y3F) mutants of Amot130, which contained a phenylalanine residue in the place of the conserved tyrosine residue, showed substantially reduced immunoprecipitation with AIP4 (Figure 4-2E). However, unlike Nedd4-1 (Wang et al., 2012), but like Nedd4-2 (Skouloudaki and Walz, 2012), AIP4 showed no reduction in binding to the P-Y1 (P-Y1F) mutant of Amot130. Taken together, the WW1 and WW2 domains of AIP4 most likely bind the P-Y2 and P-Y3 motifs of Amot130 (Figure 4-2F). Similar to other proteins containing multiple WW domains and P-Y motifs, it is likely that two WW domains of AIP4 bind to two P-Y motifs of Amot130 for a higher affinity interaction within the cell.

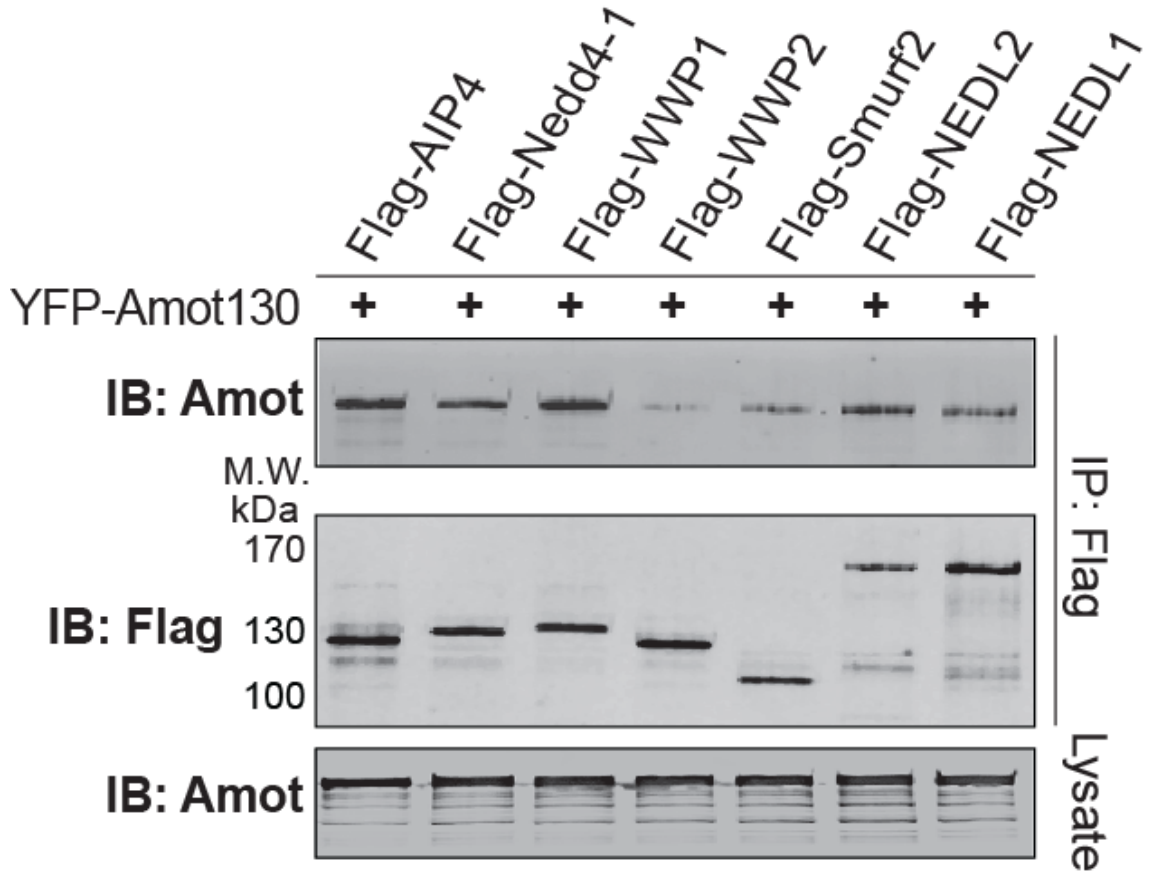


Figure 4-1 Nedd4 Family of Ubiquitin Ligases Differentially Bind Amot130.

The relative levels of YFP-tagged Amot130 that co-immunoprecipitate with seven different Flag-tagged Nedd4 family members were detected by immunoblot from lysates and immunoprecipitations with an anti-Flag antibody prepared from HEK 293T cells. The relative molecular weights (M.W.) of the Flag-tagged Nedd4 family members (in kDa) based upon a protein marker are indicated to left of middle panel. Figure adapted from (Adler et al., 2013a).

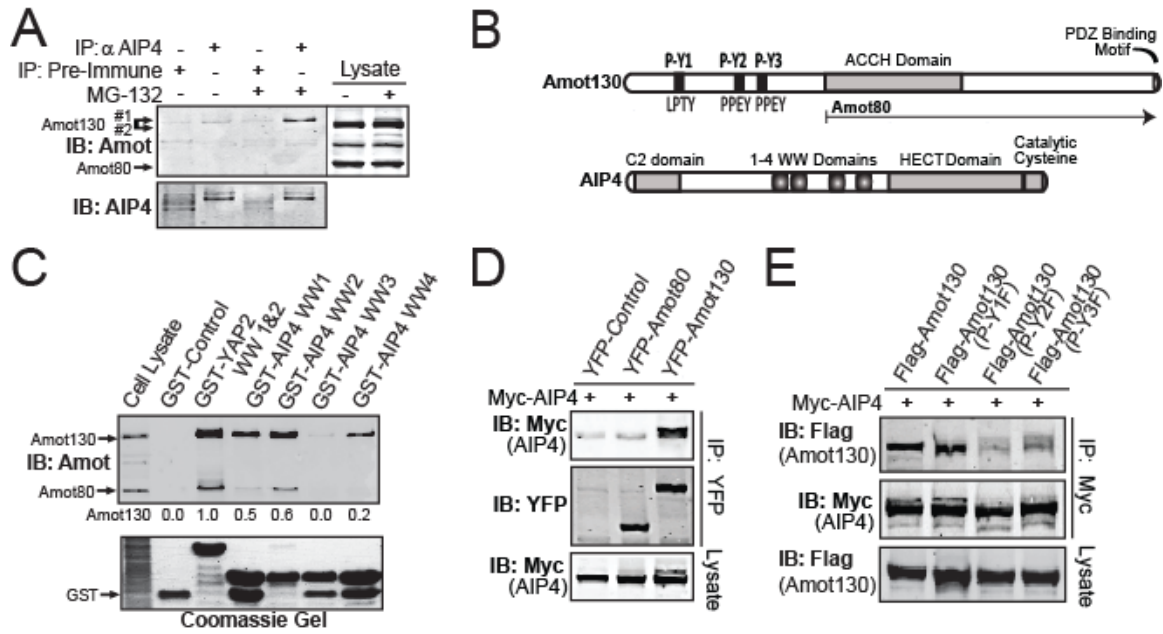


Figure 4-2 WW Domains of AIP4 Directly Bind Amot130 Specific P-Y Motifs.

(A) The relative endogenous levels of Amot130, Amot80, and AIP4 in an immunoprecipitation with an anti-AIP4 antibody from lysates of HEK 293T cells pre-incubated with (+) 25 μ M MG-132 or (-) vehicle DMSO for 2 hours were measured by immunoblot. (B) A schematic representation of Amot130 and AIP4 protein architecture including the P-Y1, 2, and 3 motifs in Amot130. Amot80 is represented to indicate the lack of the N-terminal P-Y motifs in this protein. (C) An immunoblot showing the relative levels of endogenous Amot130 and Amot80 precipitated from HEK 293T cells by purified GST-tagged WW domains of YAP and AIP4. Below top panel are the ratios of pixel intensities of bound Amot130 over GST-tagged input. (D) The relative levels of Myc-tagged AIP4 that co-immunoprecipitate with YFP-tagged Amot80 or Amot130 from HEK 293T cells were detected by immunoblot. (E) An immunoblot showing the relative levels of Myc-tagged AIP4 that co-immunoprecipitate with Flag-tagged wild-type Amot130 or the (P-Y1F) (Y109F), (P-Y2F) (Y242F), or (P-Y3F) (Y287F) mutants of Amot130. Part E performed by Brigitte Heller. Figure adapted from (Adler et al., 2013a).

4.2.2. Serum Starvation and LATS1 Activity Enhances the Association of AIP4 with Amot130

Due to low serum levels and LATS1 activity enhancing Amot130 protein levels (section 3.2.1), it was hypothesized that serum starvation and LATS1 activity could promote the Amot130-AIP4 complex formation. To examine this possibility, HEK 293T cells were infected with lentiviral shRNA targeting LATS1 or an unrelated control shRNA. Infected cells were placed in 10 % serum or serum starved conditions for 24 hours prior to harvest. While Myc-tagged AIP4 co-immunoprecipitated with Amot130 to a greater extent from lysates prepared from serum starved cells versus cells grown in 10 % serum (Figure 4-3A), this association was undetectable in cells partially silenced for LATS1 regardless of serum conditions. Thus, the formation of the Amot130-AIP4 complex is increased upon serum starvation and is dependent on LATS1 protein levels within these cells.

To further examine if LATS phosphorylation of Amot130 plays a role in the Amot130-AIP4 complex formation, the mutant Amot130 with an alanine substituted for the serine-175 (S175A) was used to examine its ability to bind AIP4. The co-precipitation of AIP4 with wild-type Amot130 but not Amot130 (S175A) was enhanced from lysates from cells expressing both MST2 and LATS1 (Figure 4-3B). The phosphorylation by active LATS1 on Amot130 thus appears to be important for AIP4 binding. The induction of the Amot130-AIP4 complex is likely via direct binding, as LATS1 did not induced AIP4 to bind the domain interaction mutant Amot130 (P-Y1,2,3F) that encodes phenylalanine at tyrosine residues in all three P-Y motifs (Figure 4-3C). Together, the Amot130-AIP4 complex association is enhanced by serum starvation. Further, this association requires active LATS1 and might yield an important function of LATS and serum levels on Amot130. The outcome of this Amot130-AIP4 complex on Amot130 protein will be addressed in the next section.

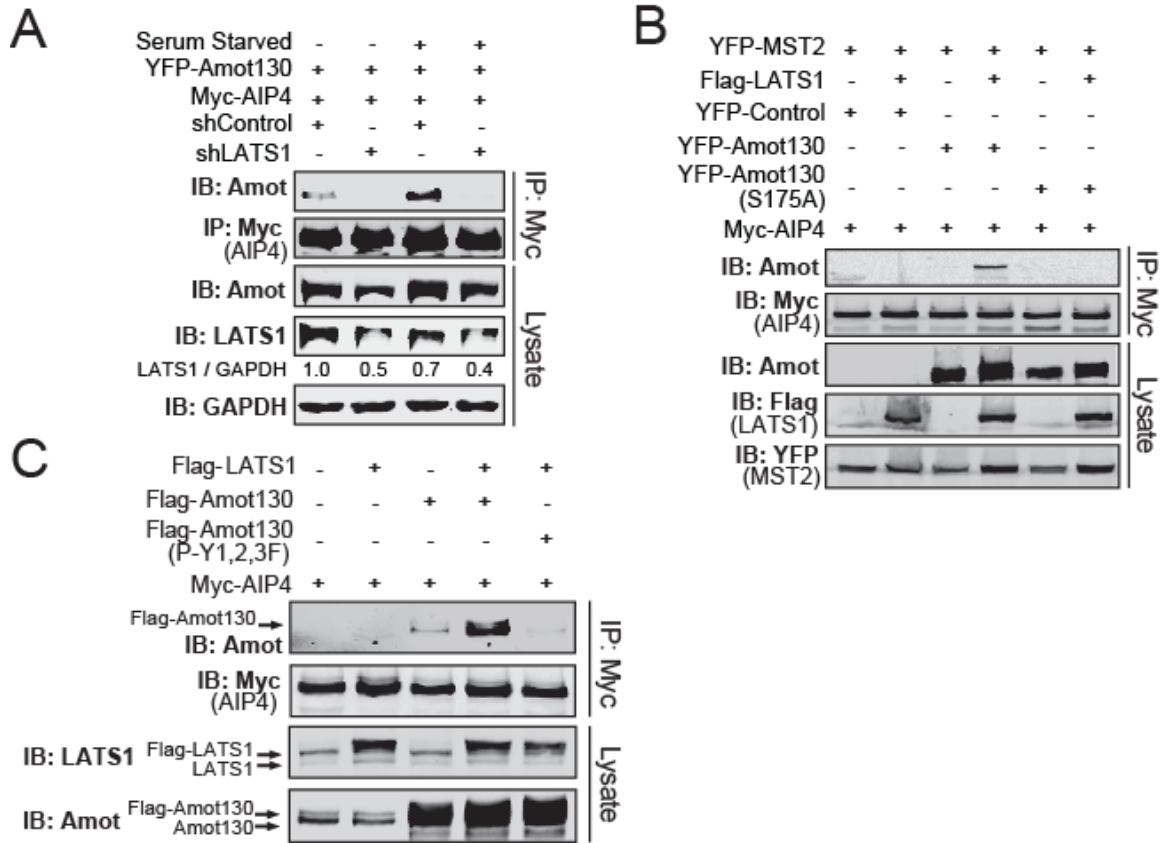


Figure 4-3 Amot130 Binding to AIP4 is Enhanced by Serum Starvation and Requires LATS1 Activity.

(A) An immunoblot of YFP-tagged Amot130 in immunoprecipitates of Myc-tagged AIP4 as well as the total levels of indicated proteins in lysates from HEK 293T cells that were co-infected with the indicated combinations of shRNA and tagged proteins and then grown with or without 10 % serum for 24 hours. Pixel intensities of LATS1 over GAPDH (below panel 4) are indicated. (B) Immunoblot of YFP-tagged wild-type Amot130 or Amot130 (S175A) in lysates and immunoprecipitations of Myc-tagged AIP4 (anti-Myc) prepared from HEK 293T cells expressing the indicated combinations of proteins. (C) Immunoblot analysis of the levels of Flag-tagged Amot130 or mutant Amot130 (P-Y1,2,3F), where tyrosines of all three P-Y motifs are mutated to phenylalanines, that co-immunoprecipitate with Myc-tagged AIP4 from lysates of HEK 293T cells, grown to high confluence, expressing Flag-tagged LATS1 or control vector and other indicated proteins. Figure adapted from (Adler et al., 2013b).

4.2.3. Amot130 is Ubiquitinated by AIP4

Because AIP4 is a strong binding partner of Amot130, it was investigated as a substrate for the AIP4 ubiquitin ligase. For this purpose, HA-tagged Lys-0 Ubiquitin, where all 7 lysines are mutated to arginines to prevent ubiquitin chain extension, was used to monitor the capacity of Amot130 to be ubiquitinated. HA-tagged Lys-0 Ubiquitin was co-transfected with combinations of Myc-tagged AIP4 and YFP-tagged Amot130 into HEK 293T cells. Ubiquitinated proteins were immunoprecipitated with an anti-HA antibody (Figure 4-4A). Immunoblot analysis showed an enhanced ubiquitination of Amot130, when it was co-expressed with AIP4. That Amot130 is a physiologic substrate of AIP4 was further supported by the over three-fold increase in ubiquitination of endogenous immunoprecipitated Amot130 from lysates prepared from HEK 293T cells co-expressing HA-tagged Ubiquitin and Myc-tagged AIP4 versus the catalytically inactive AIP4 mutant, where the catalytic cysteine-830 is substituted for an alanine (C830A), or control vector (Figure 4-4B). Because Amot130 migrated with a single gel shifted band that was similar in intensity and position when it incorporated wild-type ubiquitin, mutant (K48R) ubiquitin, or mutant (K63R) ubiquitin, Amot130 does not seem to be commonly polyubiquitinated by AIP4 (Figure 4-4C). If it were polyubiquitinated by either of these chain extensions (Lys-63 or Lys-48), the mutation of these lysines should prevent such events. Further, the presence of an analogous Amot130 gel shifted band in cells grown to high density (Adler et al., 2013a) compared to the lack of in cells grown to low density (Ranahan et al., 2011), further suggests that Amot130 is often similarly ubiquitinated as cell-cell contacts are formed.

Based upon LATS1 activity increasing Amot130-AIP4 complex formation, the impact of LATS1 activity on Amot130 ubiquitination by AIP4 was examined in cells grown to high confluence, where LATS1 expression promoted the AIP4-dependent ubiquitination of Amot130 and interestingly, itself (Figure 4-5). This self-ubiquitination of AIP4 is similar to that seen for ligases that are activated by adapter proteins. The activity of Nedd4 family ligases is often enhanced by binding to adapter proteins containing P-Y motifs (Hooper et al., 2010; Mund and

Pelham, 2009). The impact of Amot130 expression on AIP4 activity was therefore examined, and revealed an increase in self-ubiquitination of AIP4 in the presence of Amot130 and LATS1 (Figure 4-5). This self-ubiquitination of AIP4 consistently resulted in a slower migrating gel shifted form of Myc-tagged AIP4, but not the catalytically inactive mutant AIP4 (C830A) (Figure 4-6A). This gel shifted upper band had more incorporated HA-tagged Ubiquitin than the lower band. Because the self-ubiquitinated form of AIP4 is reported to indicate active ligase, Amot130 is likely promoting the ligase activity of AIP4. Therefore, whether this AIP4 activation results in changes in its ubiquitination of total cellular proteins was also measured. Co-expression of Flag-tagged Amot130 with Myc-tagged AIP4, but not catalytically inactive mutant AIP4 (C830A) resulted in a synergistic increase in the levels of ubiquitin incorporation into cellular proteins extracted with PLC lysis buffer from HEK 293T cells (Figure 4-6B). Because this effect occurs in the absence of proteasome inhibitors, these substrates are likely stable following ubiquitination. The absence of this effect in cells expressing Amot130 (P-Y2,3F) double mutant (Adler et al., 2013a), further indicates that the direct association of Amot130 with AIP4 induces the activation of its ligase domain. Together, Amot130 is able to activate AIP4 ligase activity and this leads to the direct ubiquitination of Amot130. The ubiquitination of Amot130 is increased in response to LATS1 activity. The location of this ubiquitination on Amot130 and the impact of this ubiquitination will be addressed in the next sections.

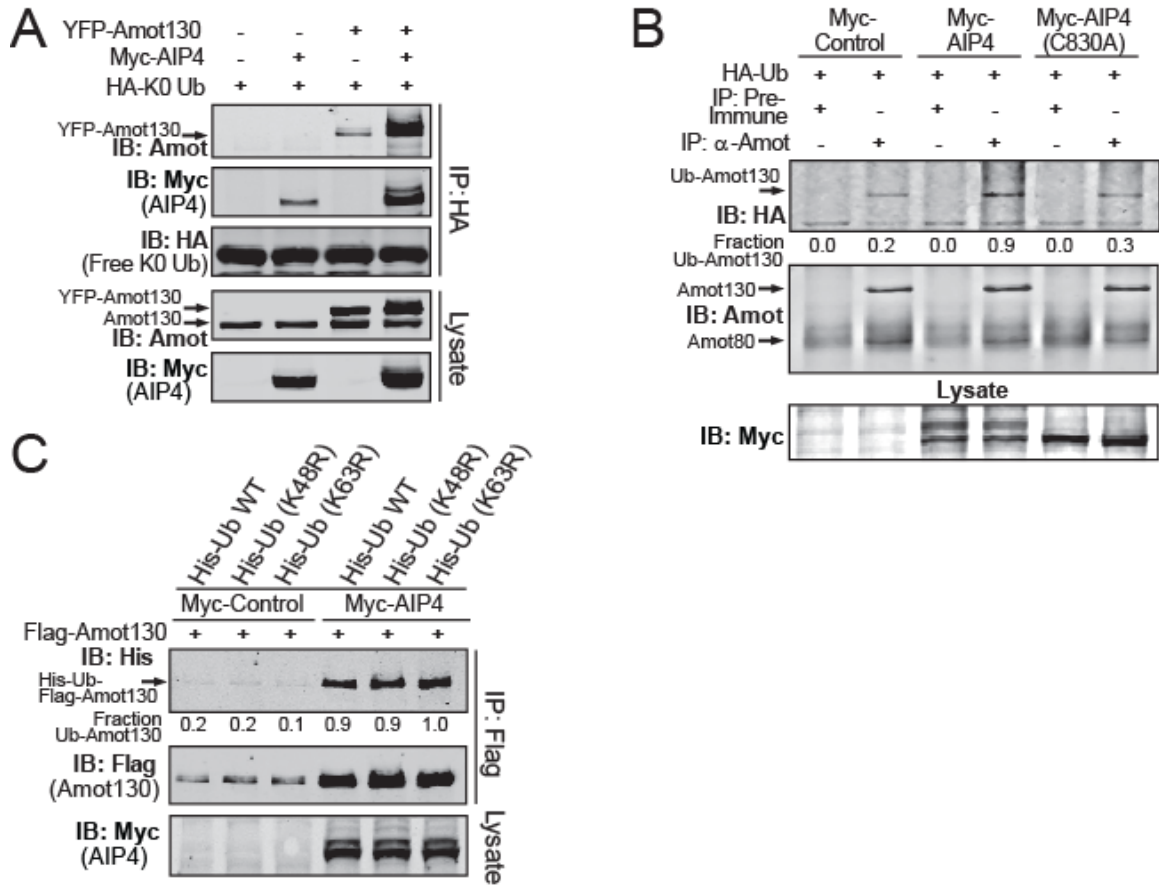


Figure 4-4 AIP4 Ubiquitinates Amot130.

(A) The relative levels of ubiquitinated Amot130 and AIP4 following immunoprecipitation of HA-tagged Lys-0 Ubiquitin (HA-K0 Ub) in HEK 293T cells co-expressing YFP-tagged Amot130, Myc-tagged AIP4, or control vectors were detected by immunoblot. (B) Endogenous Angiotensin (Amot) was immunoprecipitated from HEK 293T cells expressing HA-tagged Ubiquitin (HA-Ub) and Myc-tagged AIP4 or the catalytically inactive AIP4 (C830A). The levels of total and ubiquitinated Amot130 were detected by immunoblot. The ratios of pixel intensities of ubiquitinated Amot130 over total Amot130 are indicated. (C) Flag-tagged Amot130 was immunoprecipitated from HEK 293T cells co-expressing with and without Myc-tagged AIP4, His-tagged wild-type (WT) Ubiquitin, mutant (K48R) Ubiquitin, or mutant (K63R) Ubiquitin. The ratios of pixel intensities of ubiquitinated Flag-tagged Amot130 over total Flag-tagged Amot130 are indicated below top panel. Figure adapted from (Adler et al., 2013a).

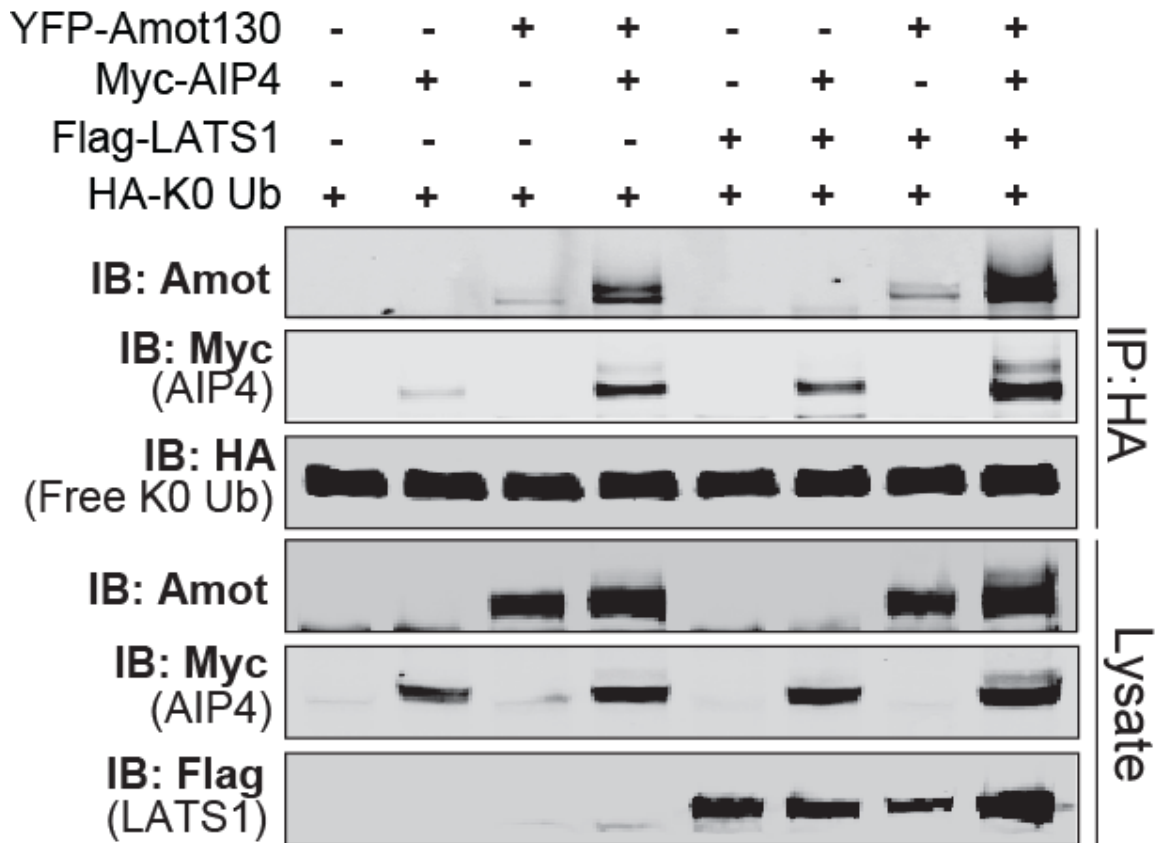


Figure 4-5 LATS1 Activity Enhances AIP4 Ubiquitination of Amot130.

Immunoblot of ubiquitinated Amot130 and AIP4 in immunoprecipitates of HA-tagged Lys-0 Ubiquitin (HA-K0 Ub) along with the indicated proteins in lysates from HEK 293T cells, grown to high confluence, expressing the indicated combinations of proteins. Figure adapted from (Adler et al., 2013b).

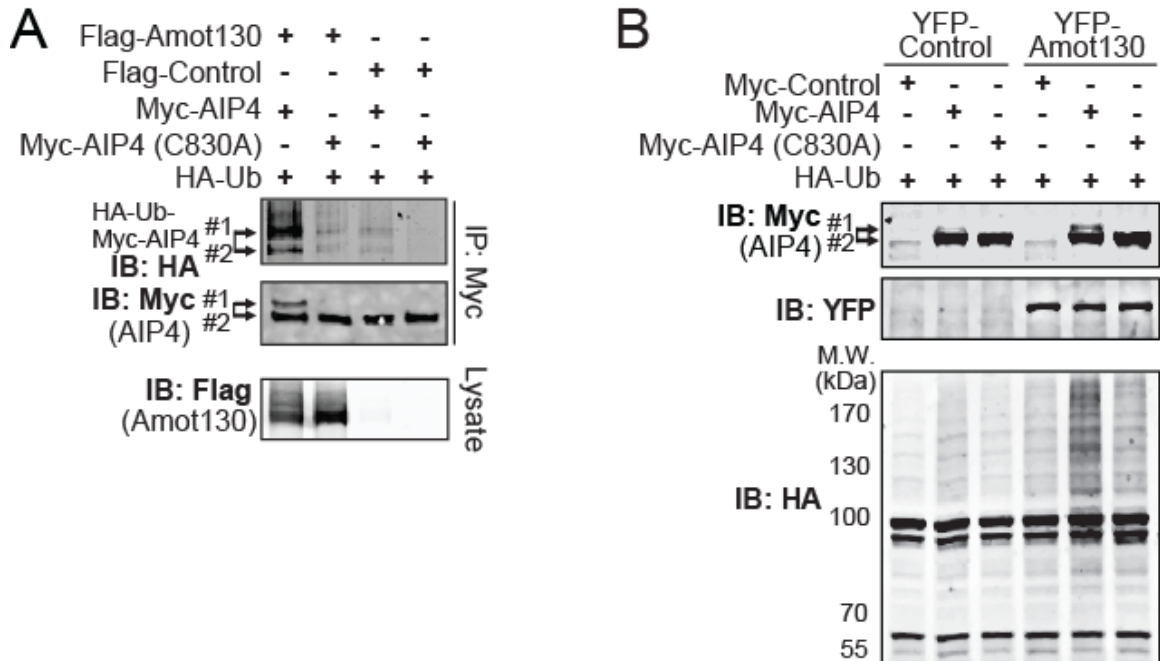


Figure 4-6 Amot130 Binding to AIP4 Activates the AIP4 Ligase.

(A) The relative incorporation of HA-tagged Ubiquitin (HA-Ub) into immunoprecipitated Myc-tagged AIP4 or mutant AIP4 (C830A) in HEK 293T cells following co-expression with Flag-tagged Amot130 was detected by immunoblot. Part A performed by Brigitte Heller. (B) HEK 293T cells expressing HA-Ub and Myc-tagged AIP4 or mutant AIP4 (C830A) as well as YFP-tagged Amot130 or control vector were lysed in PLC lysis buffer and soluble HA-Ub modified proteins were detected by immunoblot. Molecular mass standards (M.W.) (in kDa) are indicated for the bottom panel. Figure adapted from (Adler et al., 2013a).

4.2.4. Amot130 is Ubiquitinated at Lysine Residue 481

In an unbiased screen carried out by the laboratory of Mark Goebel to compare ubiquitination sites in all proteins in primary keratinocytes grown in differentiating (with calcium) conditions, a single Angiotensin peptide (VSEAYENLVKSSSKR) with a mass signature for ubiquitination at residue Lys-481 was identified; a site highly predicted to be ubiquitinated by the UbPred program (Adler et al., 2013a). The requirement of this lysine residue in Amot130 for its ubiquitination by AIP4 was then defined. For this purpose, HEK 293T cells were co-transfected with HA-tagged Ubiquitin, Myc-tagged AIP4 as well as YFP-tagged wild-type Amot130 or mutants of Amot130 (P-Y2,3F), (K481R), or (P-Y2,3F & K481R). The Amot130 (P-Y2,3F) mutant has a phenylalanine substituted for tyrosine at the second and third P-Y motifs. The Amot130 (K481R) mutant has an arginine substituted for Lys-481. Immunoblot of anti-YFP immunoprecipitates revealed that ubiquitination of Amot130 (P-Y2,3F) and (K481R) mutants was moderately reduced, while ubiquitination of the Amot130 (P-Y2,3F & K481R) mutant was undetectable (Figure 4-7A). This indicates that Lys-481 is a primary site for ubiquitination; however, other sites are likely ubiquitinated by AIP4, as the mutant that lacked binding to AIP4 showed less ubiquitination than the Amot130 (K481R) mutant. Consistent with Lys-481 being a primary site of ubiquitination, HA-tagged Ubiquitin was detected in gel shifted bands of Amot130 and AmotL1, but not AmotL2, which encodes an arginine at residue 364; the site that aligns with Lys-481/Lys-488 in Amot130/AmotL1 (Figure 4-7B). Together, Amot130 is strongly ubiquitinated at Lys-481 by AIP4. The effects of this Amot130 ubiquitination by AIP4 will be addressed in the next section.

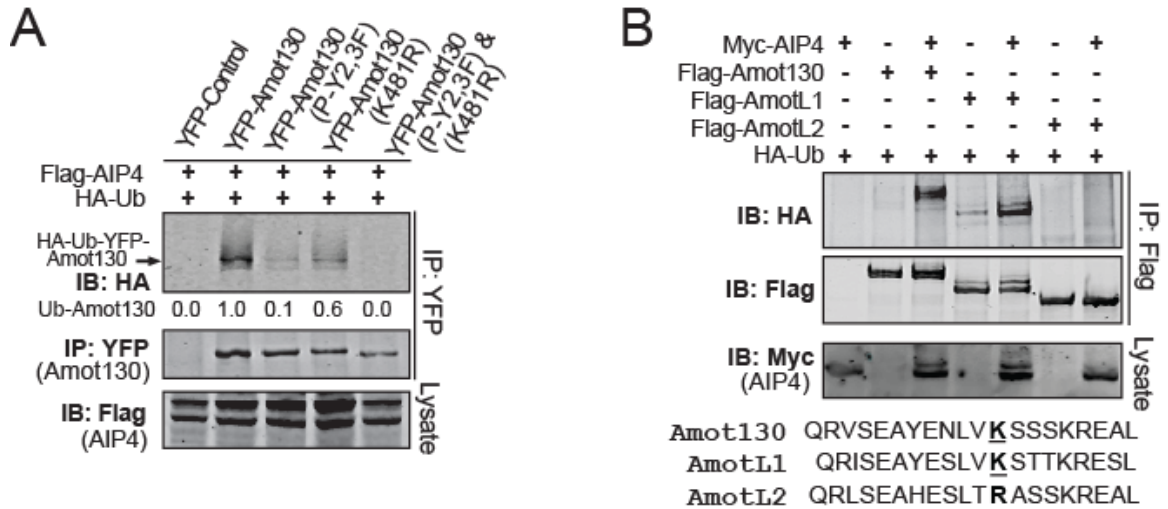


Figure 4-7 Amot130 is Ubiquitinated at Lysine-481 by AIP4.

(A) Ubiquitination of YFP-tagged Amot130 and Amot130 mutants (P-Y2,3F) (Y242F and Y287F), (K481R), and (P-Y2,3F & K481R) following co-expression with Flag-tagged AIP4 and HA-tagged Ubiquitin (HA-Ub) was examined following immunoprecipitation with an anti-YFP antibody and detected by immunoblot. The ratios of ubiquitinated over total YFP-tagged Amot130 pixel intensities are provided below top panel. (B) Flag-tagged Amot130, AmotL1, or AmotL2 were co-expressed with HA-Ub and with Myc-tagged AIP4 or control vector. Immunoblot of Myc-tagged AIP4 in lysates or immunoprecipitated Flag-tagged total (anti-Flag) or ubiquitinated (anti-HA) Angiomotin family members were detected by immunoblot. An alignment of the protein sequence encompassing Lys-481 in Amot130 with AmotL1 and AmotL2 is shown below the panels. Part B was performed by Brigitte Heller. Figure adapted from (Adler et al., 2013a).

4.2.5. Amot130 Protein Levels are Stabilized by AIP4

The consequences of ubiquitination of Amot130 on its protein stability were investigated. Overexpression of Myc-tagged AIP4 in HEK 293T cells caused the average steady state levels of endogenous Amot130 protein to be elevated over three-fold compared to cells expressing a control vector (Figure 4-8A). The AIP4-induced increase of Amot130 protein spurred an analysis of the effects of AIP4 expression on Amot130 protein stability. To this end, protein synthesis was blocked in MDA-MB-468 cells by treatment with cycloheximide, as previously described (Pervin et al., 2011), for the indicated times before being lysed. The relative levels of Amot130, AIP4, and GAPDH were then detected by immunoblot analysis. The average half-life derived from three independent experiments of endogenous Amot130 was about 4 hours in cells silenced for AIP4 compared to approximately 25 hours in control cells (Figure 4-8B). However, in an apparent contradiction, it was observed, similar to a previous report (Wang et al., 2012), that the steady state protein levels of Amot130 were increased in cells silenced for AIP4, previous to treatment with cycloheximide. Conversely, BT-474, HEK 293T, and MCF7 cells showed decreased steady state protein levels of Amot130 following silencing of AIP4 (Figure 4-8C-E). Given these conflicting effects, the impact of silencing AIP4 on *AMOT* mRNA transcript levels was measured by real time quantitative PCR. This revealed that *AMOT* transcript levels were about three-fold higher in MDA-MB-468 cells silenced for AIP4 versus control cells (Figure 4-8F). Thus, while AIP4 silencing directly reduces Amot130 protein stability, it can increase *AMOT* mRNA levels. The differing balances between these two effects in different cell types may therefore explain the overall impact of silencing AIP4 on Amot130 steady state levels.

Because silencing and overexpression of AIP4 has pleiotropic effects, the direct impact of ubiquitination of Amot130 on Amot130 stability was investigated. For this purpose, the stability of the Amot130 (K481R) mutant, which has substantially reduced ubiquitination by AIP4, was compared to that of wild-type Amot130. Consistent with ubiquitination having a significant stabilizing effect on Amot130, the half-life of wild-type YFP-tagged Amot130 was

about 30 hours in cycloheximide treated HEK 293T cells; whereas, YFP-tagged Amot130 (K481R) was about 8 hours (Figure 4-9A). Because LATS1 activity and the ability for Amot130 to be phosphorylated increases the association of Amot130 and AIP4 and thereby increases Amot130 ubiquitination (sections 4.2.2 and 4.2.3), the mutant of Amot130 (S175A), which has reduced phosphorylation by LATS, was also examined for changes in stability. Following the inhibition of translation with cycloheximide treatment, the rate of decay of Amot130 (S175A) protein was over two-fold higher than that of wild-type Amot130 in MDA-MB-468 cells (Figure 4-9B). Thus, Amot130 (S175A) likely is less stable, at least in part, due to its inability to bind and likely be ubiquitinated by AIP4. Further, comparison of the stability of the Amot130 (S175A) and Amot130 (K481R) mutants following cycloheximide treatment in MCF7 cells revealed similar significantly higher rates of decay versus wild-type Amot130 (over two-fold higher) (Figure 4-9C). Together, this leads to a possible connection between the LATS phosphorylation site (Ser-175) on Amot130 and the ubiquitination event on Lys-481 by AIP4 and consequent effects on protein stability.

Similar localization of Amot130 (K481R) and Amot130 (S175A) to actin also suggests that Amot130 phosphorylation by LATS regulates Amot130 ubiquitination. One possibility for the observed reduced stability of Amot130 (K481R) and Amot130 (S175A) is that they have altered subcellular distribution, possibly localizing them to a less stable location in the cell. Consistently, in over 60 % of live MCF7 cells, YFP-tagged wild-type Amot130 localized at intercellular contacts and at intracellular compartments that are likely endosomes (Heller et al., 2010) (Figure 4-10A). In agreement with this, Amot130-AIP4 complexes were found mainly in membrane fractions (Figure 4-10B). Interestingly, Amot130 (K481R) localized at cell-cell contacts in a significantly lower fraction of cells (around 20 %) and instead was mainly observed along actin fibers that were not on cell-cell contacts (Figure 4-10A, C-D). Because of the reduced stability connection between the Amot130 (K481R) and Amot130 (S175A) mutants, the localization of Amot130 (S175A) was also examined in the same experiment. This revealed an

even stronger phenotype of that seen with the Amot130 (K481R) (Figure 4-10E). The Amot130 (S175A) is seen tightly bundled with filamentous actin stress fibers and is rarely seen at junctions or at cortical actin. Together, similar localizations along with the decrease in stability of both mutants, reveal that the phosphorylation site and the ubiquitination site are likely connected in a common mechanism for regulating Amot130 stability.

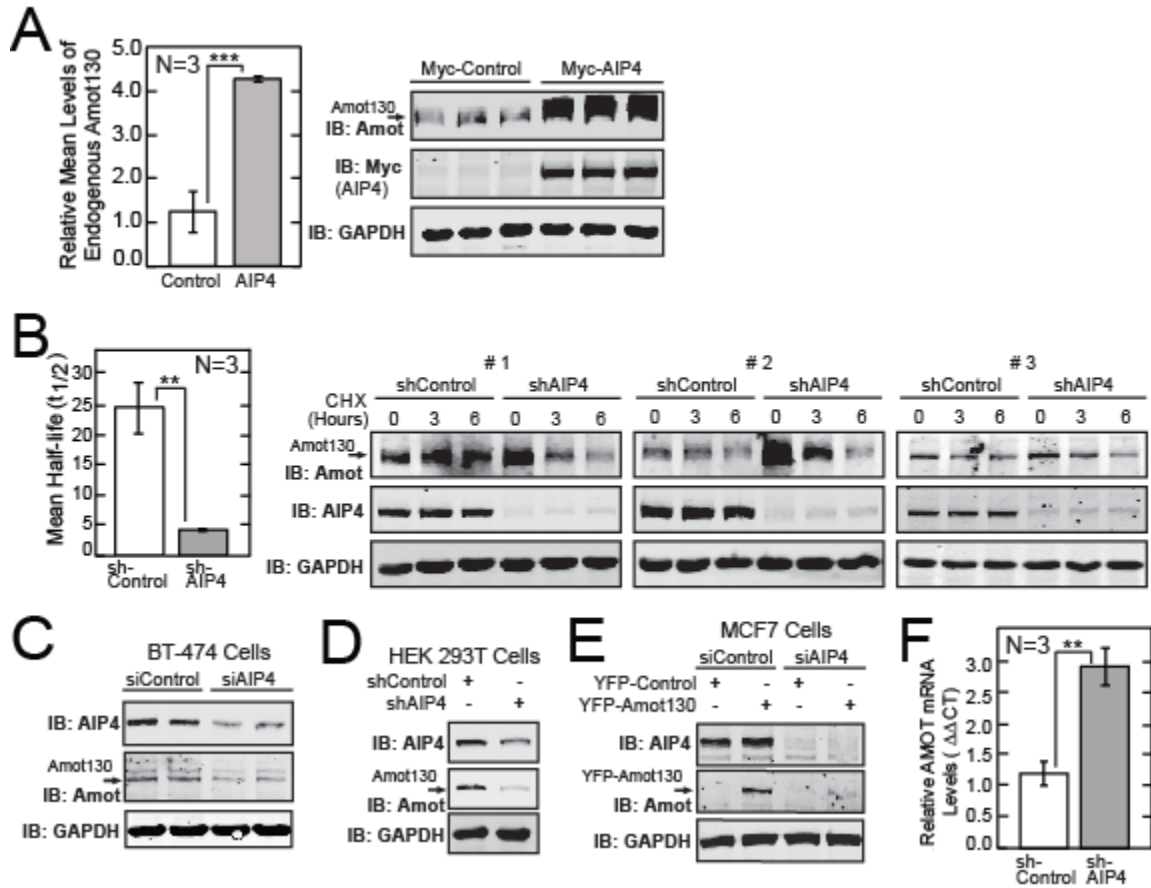


Figure 4-8 Amot130 Stability is Increased by AIP4.

(A) The levels of endogenous Amot130 were detected by immunoblot analysis from HEK 293T cells expressing Myc-tagged AIP4. The mean ratios of pixel intensities of endogenous Amot130 over GAPDH from three replicates were graphed (left). (B) The levels of endogenous Amot130 were detected by immunoblot from lysates derived from MDA-MB-468 cells expressing AIP4 or control shRNA and treated with vehicle (DMSO) or 200 $\mu\text{g}/\text{mL}$ of cycloheximide (CHX) for indicated times. The ratios of pixel intensities of endogenous Amot130 over GAPDH for both conditions were graphed with linear regression analysis. The mean half-lives were calculated from the three numbered independent experiments and graphed (left). (C) The levels of endogenous Amot130 were detected by immunoblot analysis of lysates from BT-474 cells transfected with AIP4 or control siRNA. (D) The levels of endogenous Amot130 were detected by immunoblot from lysates of HEK 293T cells infected with AIP4 or control shRNA. (E) The levels of YFP-tagged Amot130 were detected by immunoblot analysis of lysates from MCF7 cells transfected as in C. (F) The mRNA transcript levels of *AMOT* from MDA-MB-468 cells expressing AIP4 or control shRNA were measured from three independent experiments by real time quantitative PCR. Error bars represent \pm S. D. p-values: *** < 0.0005; ** < 0.005. Figure adapted from (Adler et al., 2013a).

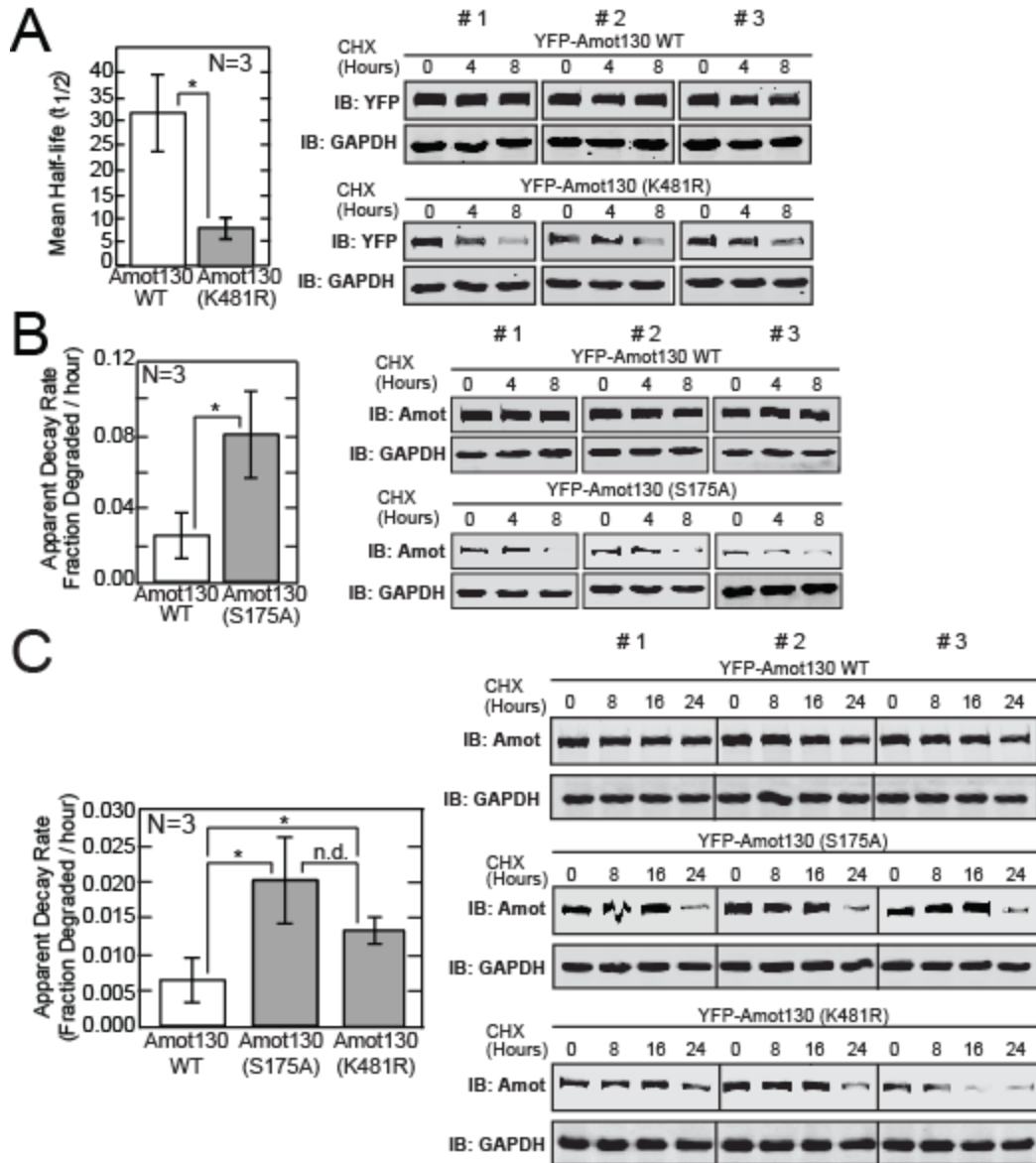


Figure 4-9 Two Amot130 Mutants, (K481R) and (S175A), Have Similarly Reduced Protein Stability.

(A) The levels of YFP-tagged wild-type (WT) Amot130 or Amot130 (K481R) were detected by immunoblot analysis of lysates prepared from HEK 293T cells treated with vehicle (DMSO) or 200 μ g/mL of cycloheximide (CHX) for the indicated times. The ratio of pixel intensities of YFP-tagged WT Amot130 or Amot130 (K481R) over GAPDH were graphed with linear regression plots. The mean half-lives were calculated from the three numbered independent experiments and graphed (left). (B) A graph (left) of the mean regression slopes from three numbered independent experiments of immunoblots of the levels of YFP-tagged WT Amot130 or Amot130 (S175A) in lysates of MDA-MB-468 cells treated as in A. (C) A graph (left) of the mean regression slopes from three numbered independent experiments of immunoblots of lysates prepared from MCF7 cells of the levels of YFP-tagged WT Amot130, Amot130 (S175A), or Amot130 (K481R) as described in B. Error bars represent \pm S. D. p-values: * < 0.05. Figure adapted from (Adler et al., 2013a) and (Adler et al., 2013b).

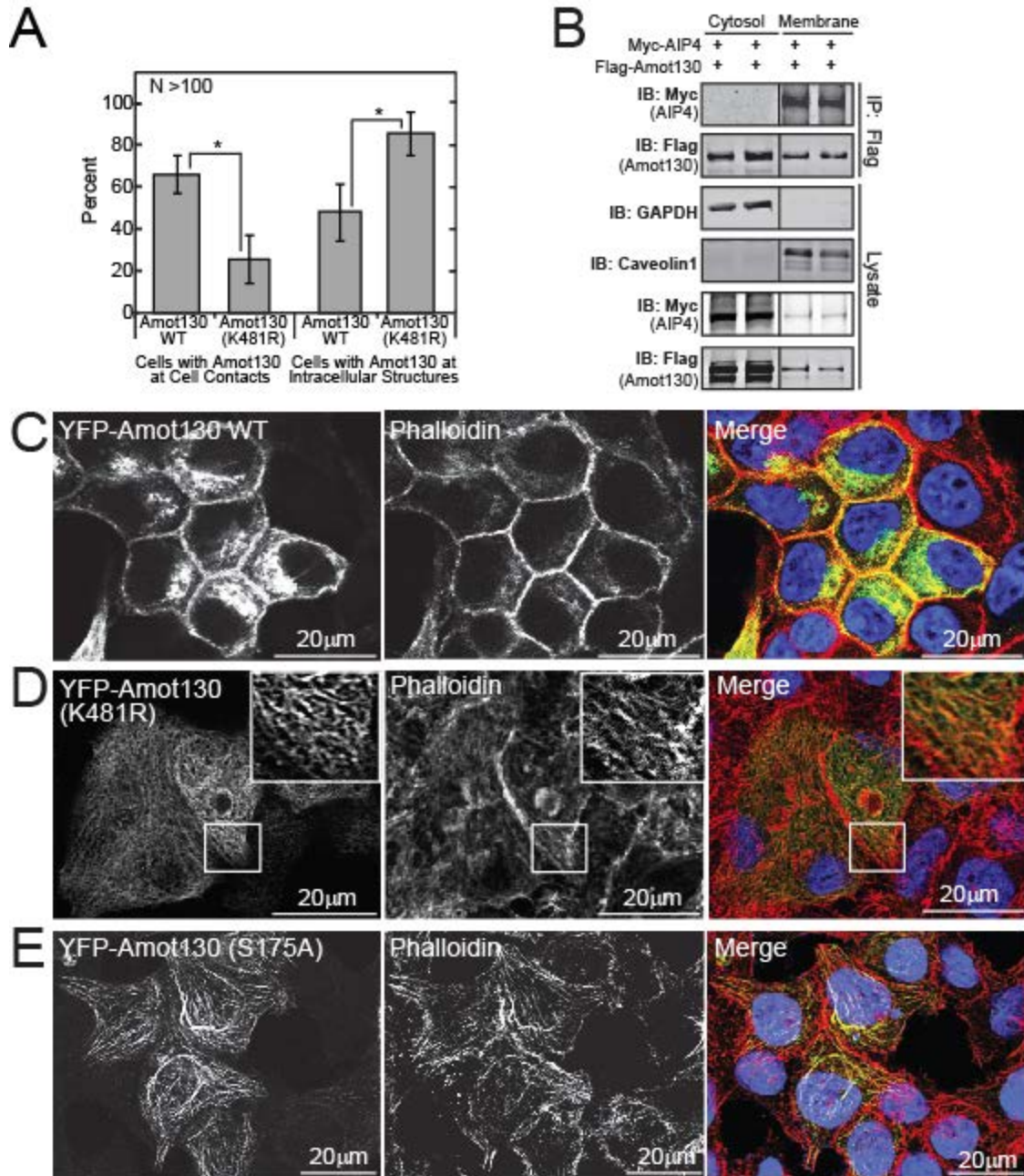


Figure 4-10 Two Amot130 Mutants, (K481R) and (S175A), Have Similarly Altered Subcellular Localization.

(A) The percent of live MCF7 cells that show wild-type (WT) Amot130 or (K481R) localization at intercellular contacts or at intracellular structures. (B) Immunoblot analysis of Myc-tagged AIP4 in lysates or immunoprecipitated Flag-tagged Amot130 (anti-Flag) after membrane fractionation of HEK 293T cells expressing indicated proteins. Fractionation indicated via immunoblot of lysates with Caveolin1 and GAPDH. (C-E) Confocal images of fixed MCF7 cells of (C) YFP-tagged wild-type Amot130, (D) YFP-tagged Amot130 (K481R), or (E) YFP-tagged Amot130 (S175A) (all three green) and Phalloidin-594 for actin (red). Nuclei were stained with Hoechst (blue). Parts C-E were in collaboration with Lauren Bringman. Error bars represent \pm S. D. p-values: * < 0.05. Figure adapted from (Adler et al., 2013a) and (Adler et al., 2013b).

4.3. Discussion

4.3.1. Stabilization of Amot130 by AIP4

Here, levels of Amot130 protein are seen to increase under conditions of high LATS activity (chapter 3). Increased Amot130 protein, in turn, is found to likely result from the induced binding of AIP4 to Amot130, leading to Amot130 ubiquitination and stabilization. The ubiquitination of Amot130 by AIP4 is thought to mainly be unchained, an event frequently associated with changes in cellular trafficking (Rotin et al., 2000). Thus, monoubiquitination of Amot130 is consistent with its observed changes in localization to the cell membrane, whereas, Amot130 (K481R) and Amot130 (S175A) both dominantly localize at enlarged actin stress fibers. The change in localization, in turn, through an unknown mechanism reduces Amot130 stability. Another possible mechanism for increased stability of Amot130 upon AIP4 binding could be the prevention of other Nedd4 ligases binding to Amot130, which are reported to lead to Amot130 polyubiquitination and degradation. An example of this is Nedd4-1, which reduces the stability of Amot130 via binding these same P-Y motifs of Amot130 (Wang et al., 2012).

Here, AIP4 is proposed to have a high-affinity interaction with Amot130 through binding both the P-Y2 and P-Y3 motifs through the first and second WW domains of AIP4. The interaction of Amot130 and AIP4 was demonstrated through a series of pull-downs and immunoprecipitation reactions (Adler et al., 2013a). A significant consequence of Amot130 binding to AIP4 is the induction of AIP4 ligase activity and self-ubiquitination of the ligase. Here, Amot130, like other adapters is able to initiate the self-ubiquitination of AIP4 via binding of its P-Y motifs, presumably relieving the inhibitory conformation of AIP4 (Hooper et al., 2010; Mund and Pelham, 2009). Interestingly, AmotL2, lacking the third functional P-Y motif, was unable to initiate the doublet-formation of AIP4 and thus appears unable to promote active AIP4. This indicates the importance of functional P-Y motifs for interactions with the ligase.

The Amot130-AIP4 complex further defines the substrate availability of AIP4 by providing Amot130 as a substrate. The result of the Amot130-AIP4 interaction and ubiquitination is the increased stability of Amot130. The stabilization of Amot130 by AIP4 is proposed to be a result of ubiquitinated Amot130 being targeted to intercellular contacts. While the finding that Amot130 is stabilized by AIP4 differs from a previous study (Wang et al., 2012), the findings here are supported by multiple approaches. First, the effects of silencing AIP4 both reduce Amot130 protein stability and also increases *AMOT* mRNA transcript levels. The cell type specific effects of silencing AIP4 on Amot130 steady state protein levels are therefore likely due to a dominance of either effect. Further, while silencing AIP4 is a fairly non-specific approach, the reduced stability of the Amot130 (K481R) and Amot130 (S175A) is a more direct indicator that the phosphorylation and ubiquitination generally enhances Amot130 stability. Further, Amot130 is reported to be more stable in cells at high confluence (Bratt et al., 2005), where it is found here that Amot130 is more likely to be ubiquitinated. For instance, an ubiquitinated peptide of Angiotensin was identified in differentiated keratinocytes in 4 out of 5 mass spectrometry experiments, but was never detected in undifferentiated keratinocytes (Adler et al., 2013a). Further, a gel shifted band of Amot130, which is associated with its ubiquitination, is strongly seen across mammary epithelial cells grown to high density (Adler et al., 2013a), but not in cells at low density (Ranahan et al., 2011). This change in stability is also consistent with the finding that wild-type Amot130, but not the ubiquitination-reduced mutant (K481R) nor the LATS phosphorylation site deficient mutant (S175A), localized to a much greater extent to intercellular contacts.

4.3.2. Amot130 Phosphorylation by LATS1 Increases the Stability of Amot130 by Promoting AIP4 Binding and Ubiquitination of Amot130

Importantly, this is the first report of any protein enzymatically increasing Amot130 steady state protein levels. Further, the interaction between Amot130 and AIP4 is increased by the ability of Amot130 to be phosphorylated at Ser-175 by LATS1. Thus, a downstream effect of Amot130 phosphorylation is demonstrated to increase the steady state protein levels of Amot130 (Figure 4-11). This outcome is not surprising in the context of physiological effects of serum starvation to inhibit cellular growth. The mammary epithelial cells, upon serum starvation, signal to shut down their pro-growth pathways, which should include YAP and TAZ nuclear activities. LATS is a potent inhibitor of cell growth, and by stabilizing Amot130, enhances the ability LATS to be a tumor suppressor. In order to understand how these proteins (LATS and Amot130) influence cell growth, an examination of their reported roles as potent inhibitors of YAP and TAZ is warranted, and will be examined in the next chapter.

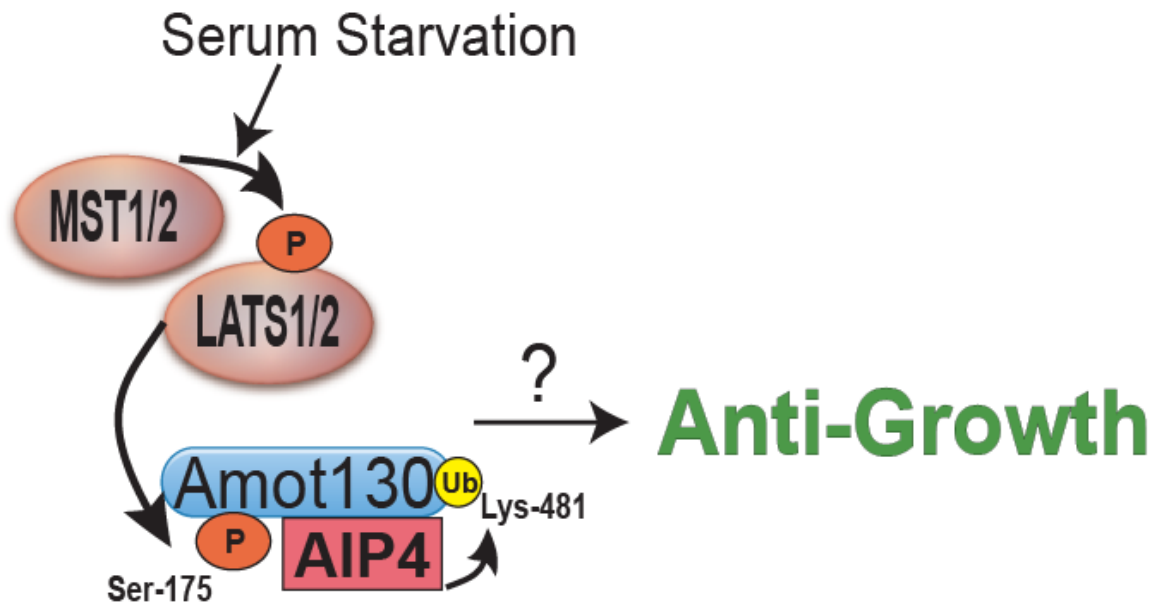


Figure 4-11 Working Model for Serum Starvation Inhibition of Cell Growth.

Amot130 is a major contributor to the anti-growth phenotype in mammary epithelial cells. LATS1 is activated in breast cancer cells upon serum starvation. Active LATS1 phosphorylation of Amot130 promotes Amot130 binding to and ubiquitination by AIP4. The ubiquitination occurs in part at Lys-481 of Amot130. This ubiquitination, in turn, increases the stability of Amot130. How the Amot130-AIP4 complex modulates growth arrest will be examined in the next chapter.

**CHAPTER 5. THE LONG ISOFORM OF ANGIOMOTIN AND AIP4 COOPERATIVELY
INHIBIT THE TRANSCRIPTION OF YAP-DEPENDENT GENES**

Some text in this chapter was originally published in The Journal of Biological Chemistry and the Proceedings of the National Academy of Sciences USA. Adler et al. Amot130 Adapts Atrophin-1 Interacting Protein 4 to Inhibit Yes-Associated Protein Signaling and Cell Growth. *Journal of Biological Chemistry*. 2013; Vol: 288, 25: 15181-15193. © the American Society for Biochemistry and Molecular Biology. Adler et al. Serum deprivation inhibits the transcriptional co-activator YAP and cell growth via phosphorylation of the 130-kDa isoform of Angiotensin II by the LATS1/2 protein kinases. *Proceedings of the National Academy of Sciences*. 2013; Vol: 110, 43: 17368-17373. © Proceedings of the National Academy of Sciences USA.

5.1. Introduction

Hippo signaling mainly functions to inhibit YAP and TAZ, co-activators of the transcription of genes involved in growth and survival. YAP and TAZ are functional homologues that promote cell growth and survival by activating transcription factors that in turn drive the expression of genes like, *connective tissue growth factor (CTGF)*. Typically, inhibition of the nuclear localization of YAP and TAZ results in cellular growth arrest. This is generally accomplished through their phosphorylation by LATS1/2 protein kinases. Recently, the Angiomotin family of proteins was also demonstrated by several groups to inhibit YAP and TAZ nuclear activities (Chan et al., 2011; Wang et al., 2011; Zhao et al., 2011a). However, the primary mechanisms of how Angiomotins inhibit YAP and TAZ are uncertain.

Here, a novel complex is identified containing YAP and the ubiquitin ligase AIP4, through their binding to Amot130. This complex leads to the ubiquitination and decreased steady state protein levels of YAP. This, in turn, inhibits the nuclear functions of YAP, as seen by decreased endogenous *CTGF* transcript levels. Importantly, the formation of this complex is induced by the phosphorylation of Amot130 by LATS1 upon serum starvation.

Amot130 binding to AIP4 may also affect YAP signaling, by preventing AIP4 interaction with LATS1. Typically, LATS1 is targeted for degradation by AIP4, but Amot130 is able to dominantly bind AIP4, preventing LATS1 degradation. Together, the Amot130-AIP4 complex likely inhibits YAP signaling, via multiple approaches, in response to serum starvation and LATS activity.

5.2. Results

5.2.1. Amot130 Repurposes AIP4 from LATS1 Degradation to the Ubiquitination of YAP

Due to the individual important functions of AIP4 and Amot130 in Hippo signaling, the impact of the Amot130-AIP4 complex (described in section 4.2.1) on Hippo signaling was examined. Because AIP4 binds to P-Y motifs in both Amot130 and LATS1 via the WW domains of AIP4, their competition for binding to AIP4 was explored. Myc-tagged AIP4 was immunoprecipitated from HEK 293T cells that also expressed a control vector and Flag-tagged LATS1 or YFP-tagged Amot130 and Flag-tagged LATS1. Immunoblot analysis revealed that YFP-tagged Amot130 expression resulted in dramatically less LATS1 being precipitated by AIP4 and concomitant binding to Amot130 (Figure 5-1A). Consistent with AIP4 mediating the degradation of LATS1 (Salah et al., 2011), the steady state protein levels of endogenous LATS1 were reduced upon expression of AIP4 (Figure 5-1B). However, expression of Amot130 increased the levels of endogenous LATS1 protein even when AIP4 was co-expressed. Amot130 is therefore proposed to uncouple AIP4 from binding and inducing the degradation of LATS1. This is important, because LATS1 phosphorylation of YAP and TAZ prevents their nuclear activities. Therefore, Amot130 by preventing LATS1 degradation likely promotes LATS1 activity.

Amot130 also robustly binds YAP2 (containing two WW domains) but not with YAP1 (containing one WW domain) (Oka et al., 2012). Therefore, only YAP2 was examined for all overexpressed YAP studies and is commonly referred to as YAP, for simplicity.

It was investigated whether AIP4 is part of a complex with YAP and Amot130. In examination of this, Myc-tagged AIP4 and YFP-tagged Amot130 strongly co-precipitated with Flag-tagged YAP, whereas only trace levels of Myc-tagged AIP4 (along with endogenous Amot130) bound Flag-tagged YAP in the absence of YFP-tagged Amot130, when expressed in

HEK 293T cells (Figure 5-2A). Thus, YAP and AIP4 are likely scaffolded by Amot130 into a single protein complex. This indicates that YAP and AIP4 are brought together by the adapter protein Amot130.

Because AIP4 and YAP potentially bind to overlapping P-Y motifs in Amot130, the mechanisms of interaction of YAP with Amot130 were further examined. The mutation of Amot130 P-Y motifs (P-Y1F or P-Y2F), both showed almost no detectable association with exogenous YAP in HEK 293T cells (Figure 5-2B), this along with additional binding experiments revealed that there is a likely preference of the WW1 of YAP for P-Y1 motif of Amot130 and the WW2 of YAP for P-Y2 motif of Amot130 (Adler et al., 2013a). The P-Y3 motif of Amot130 was not examined, as this was previously reported not to bind to YAP (Skouloudaki and Walz, 2012). Together, this data points to a possible competition for the P-Y2 motif of Amot130 between YAP and AIP4, as both need this P-Y2 motif to bind Amot130 (section 4.2.1) (Figure 5-2B). Simplistically, this should inhibit AIP4 and YAP from simultaneously being in a complex with Amot130. However, because the Angiomotins homo- and hetero-dimerize (Ernkvist et al., 2008; Gagné et al., 2009), this may result in AIP4 and YAP both binding separate Amot130 proteins, yet remain in a single complex (Figure 5-2C).

Based upon the evidence that Amot130 brings YAP and AIP4 into a common complex, the effects of Amot130 on the ubiquitination of YAP by AIP4 were measured. Ubiquitinated Flag-tagged YAP was immunoprecipitated from HEK 293T cells expressing HA-tagged Lys-0 Ubiquitin with an anti-HA antibody. While ubiquitinated YAP was undetectable in samples not expressing Amot130 or AIP4, the expression of either Amot130 or AIP4 alone modestly increased the levels of ubiquitinated YAP. However, co-expression of AIP4 and Amot130 resulted in a strong synergistic increase in the levels of ubiquitinated YAP, indicating the importance of Amot130 in adapting YAP as a substrate for AIP4 (Figure 5-3A). This effect requires catalytically active AIP4, as co-expression of Amot130 and the catalytically inactive mutant of AIP4 (C830A) did not induce the ubiquitination of YAP (Figure 5-3B).

The differential effects of incorporation of HA-tagged wild-type Ubiquitin versus Lys-0 Ubiquitin induced by Amot130 and AIP4 into YAP were compared in HEK 293T cells (Figure 5-3C). Lys-0 Ubiquitin has all seven lysines mutated to arginines and thus is incapable of ubiquitin chain extension. Expression of Amot130 with AIP4 resulted in a gel shifted weak smear of wild-type ubiquitinated YAP, which is consistent with polyubiquitination and therefore potential targeting for degradation. Whereas, Lys-0-ubiquitinated YAP, induced by expression of Amot130 and AIP4 migrated as a faster/smaller and much stronger single band. The absence of this lower band with wild-type Ubiquitin supports that AIP4-catalyzed ubiquitination of YAP could be coupled to polyubiquitination. This may also indicate that the ubiquitination of YAP by AIP4 leads to rapid degradation, as preventing AIP4-mediated chain extension of ubiquitin moieties enhances the levels of ubiquitinated protein.

The role of LATS in promoting Amot130-AIP4 complex-mediated ubiquitination of YAP was examined. The ubiquitination of Flag-tagged YAP was increased in HEK 293T cells under serum starvation conditions versus control cells in a manner promoted by expression of AIP4 (Figure 5-4A). Thus, AIP4 ubiquitinates YAP in response to serum starvation. Further, the ubiquitination of YAP was dependent on LATS phosphorylation of Amot130. While YAP was able to bind the Amot130 (S175A) mutant as effectively as wild-type Amot130 under active LATS1 conditions (Figure 5-4B), Amot130 (S175A) was unable to increase the ubiquitination of YAP following serum starvation (Figure 5-4C). Therefore, a role exists for Amot130 to promote YAP ubiquitination in response to serum starvation and likely LATS activity. Together, the Amot130-AIP4 complex promotes the ubiquitination of YAP in a manner that is dependent on the ability of Amot130 to be phosphorylated by LATS.

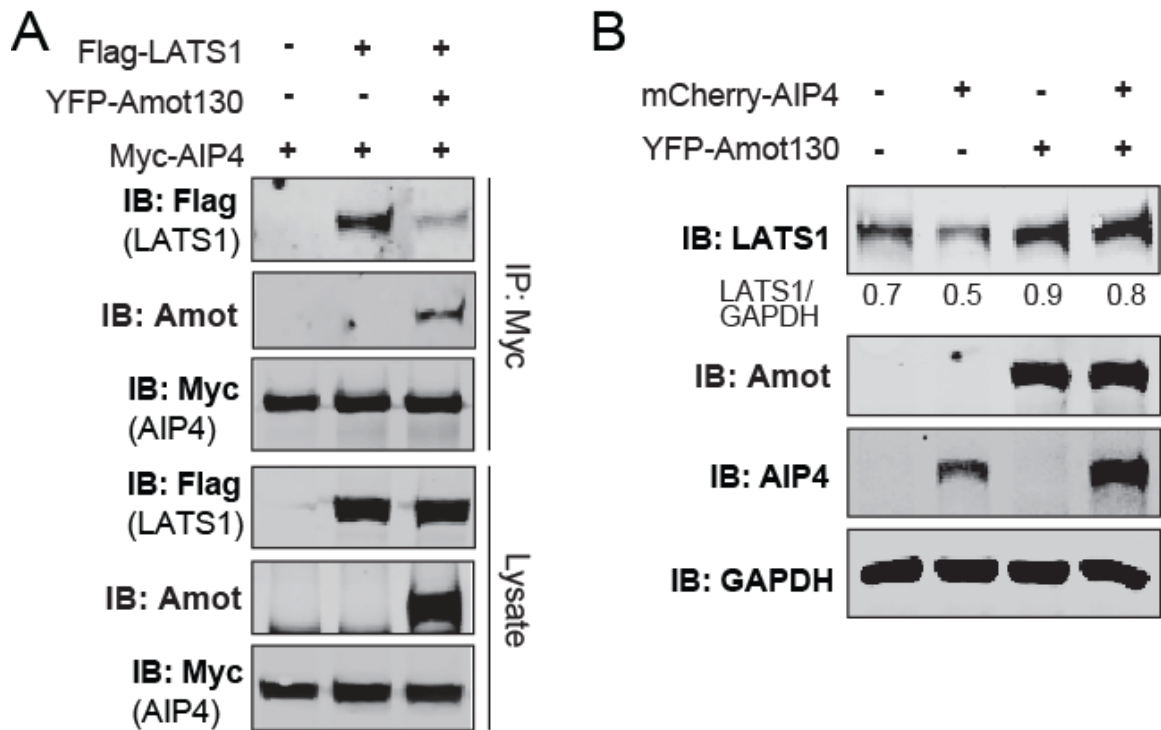


Figure 5-1 Amot130 Prevents AIP4-Mediated LATS1 Degradation.

(A) The levels of Myc-tagged AIP4, Flag-tagged LATS1, and YFP-tagged Amot130 were detected by immunoblot from lysates and immunoprecipitations (anti-Myc) prepared from HEK 293T cells expressing these proteins in the indicate combinations. (B) The levels of endogenous LATS1 were measured by immunoblot in MDA-MB-468 cells expressing mCherry-tagged AIP4 and YFP-tagged Amot130 alone or in combination. The ratios of pixel intensities of LATS1 over GAPDH are presented below top panel. Figure adapted from (Adler et al., 2013b).

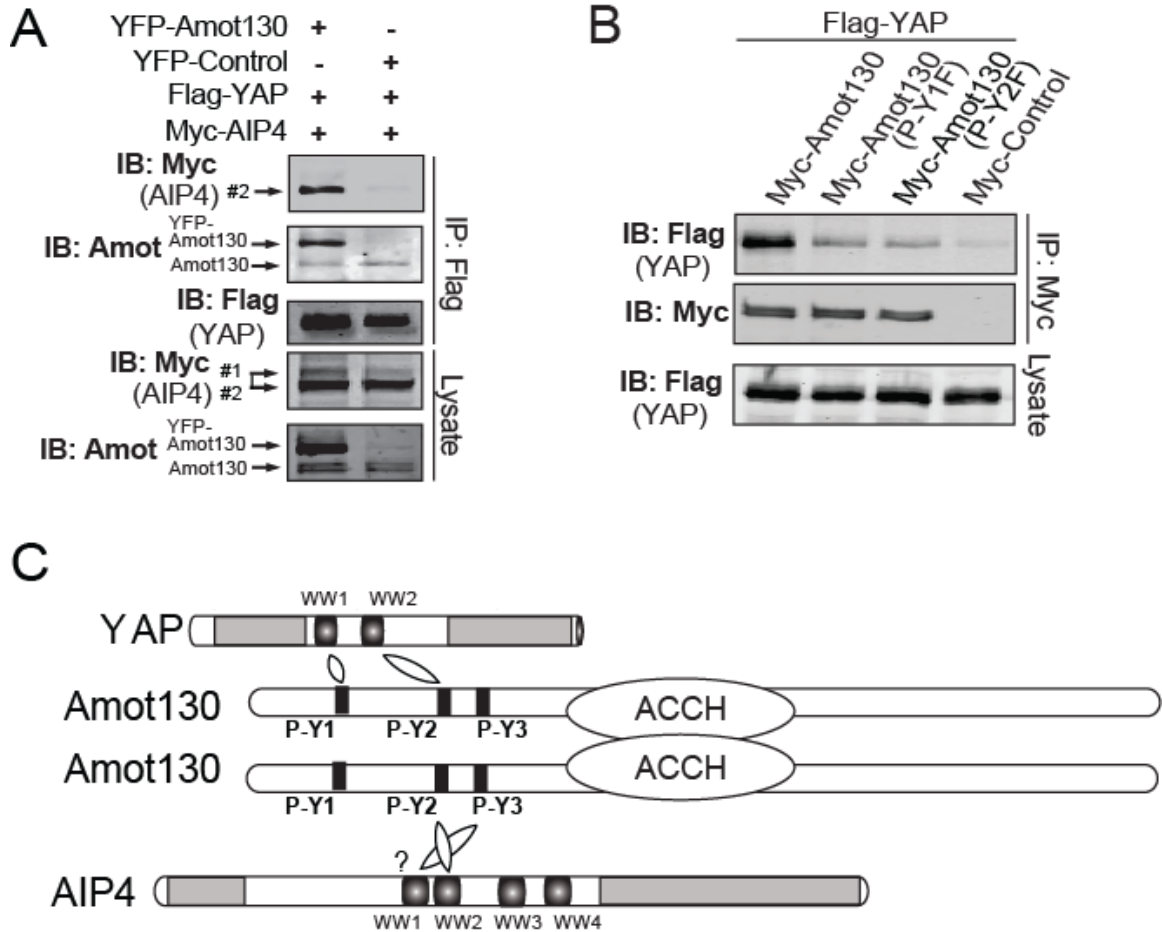


Figure 5-2 YAP is in a Complex with AIP4 and Amot130.

(A) The levels of Myc-tagged AIP4, YFP-tagged Amot130, and Flag-tagged YAP were detected by immunoblot from lysates and immunoprecipitations (anti-Flag) prepared from HEK 293T cells expressing these three proteins in the indicated combinations. (B) The levels of Flag-tagged YAP and Myc-tagged wild-type Amot130, Amot130 (P-Y1F) (Y109F), Amot130 (P-Y2F) (Y242F) mutants, or control vector were detected by immunoblot from lysates and immunoprecipitations (anti-Myc) prepared from HEK 293T cells expressing these proteins in the indicated combinations. Part B performed by Brigitte Heller. (C) Model of the binding relationships of the YAP-Amot130-AIP4 complex. A (?) denotes unknown sites of binding. Figure adapted from (Adler et al., 2013a).

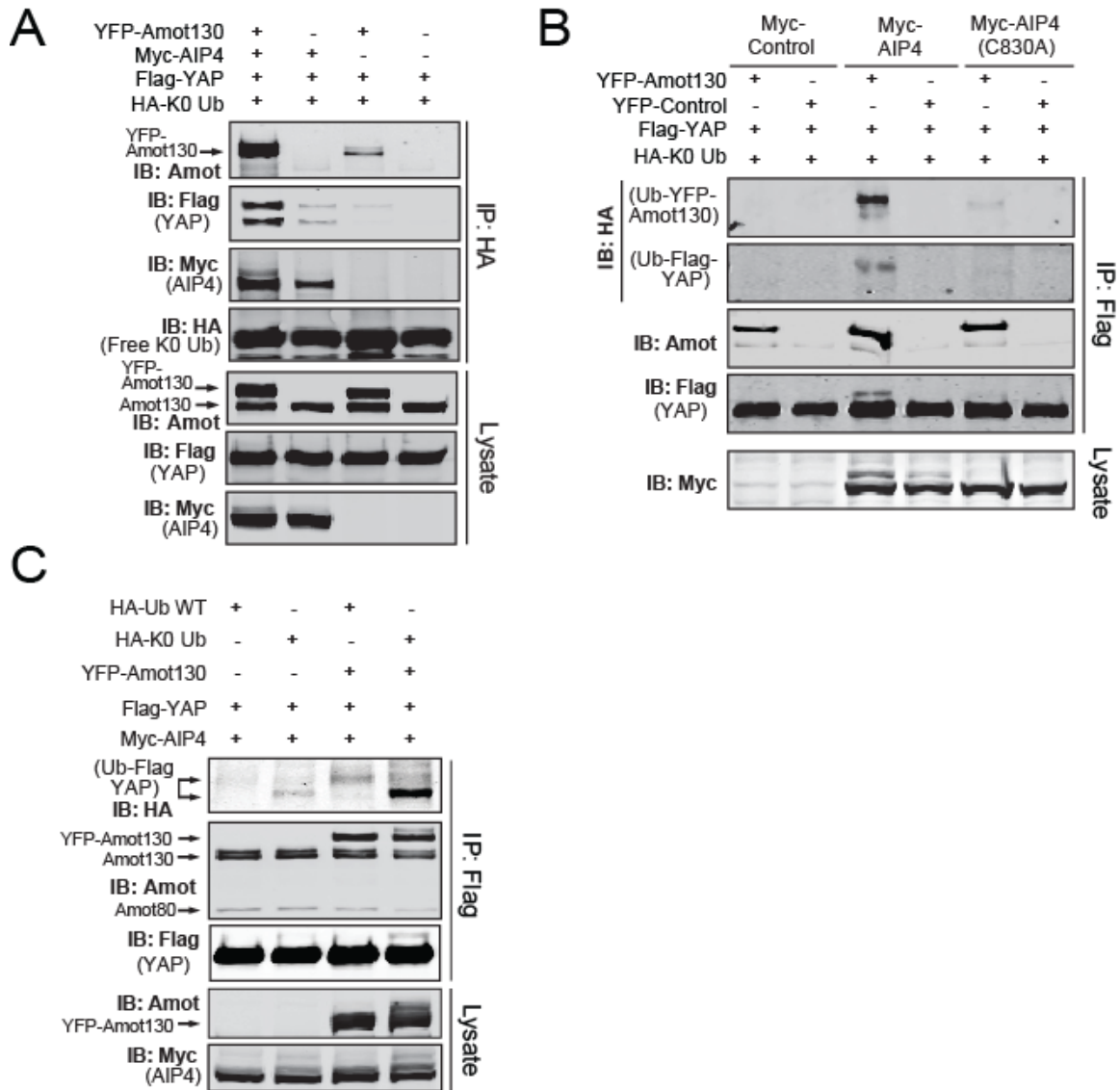


Figure 5-3 YAP is Ubiquitinated by the Amot130-AIP4 Complex.

(A) The levels of ubiquitinated Flag-tagged YAP were detected by immunoblot following immunoprecipitation (anti-HA) from HEK 293T cells expressing HA-tagged Lys-0 Ubiquitin (HA-K0 Ub) in combination with YFP-tagged Amot130 or control vector as well as Myc-tagged AIP4 and Flag-tagged YAP. (B) The relative incorporation of HA-K0 Ub into immunoprecipitated Flag-tagged YAP in HEK 293T cells co-expressing YFP-tagged Amot130, Myc-tagged AIP4, mutant AIP4 (C830A), or control vectors was detected by immunoblot. (C) The levels of total and ubiquitinated Flag-tagged YAP were detected by immunoblot following immunoprecipitation from HEK 293T cells expressing HA-tagged wild-type (WT) or K0 Ubiquitin in combination with YFP-tagged Amot130 or control vector as well as Myc-tagged AIP4 and Flag-tagged YAP. Figure adapted from (Adler et al., 2013a).

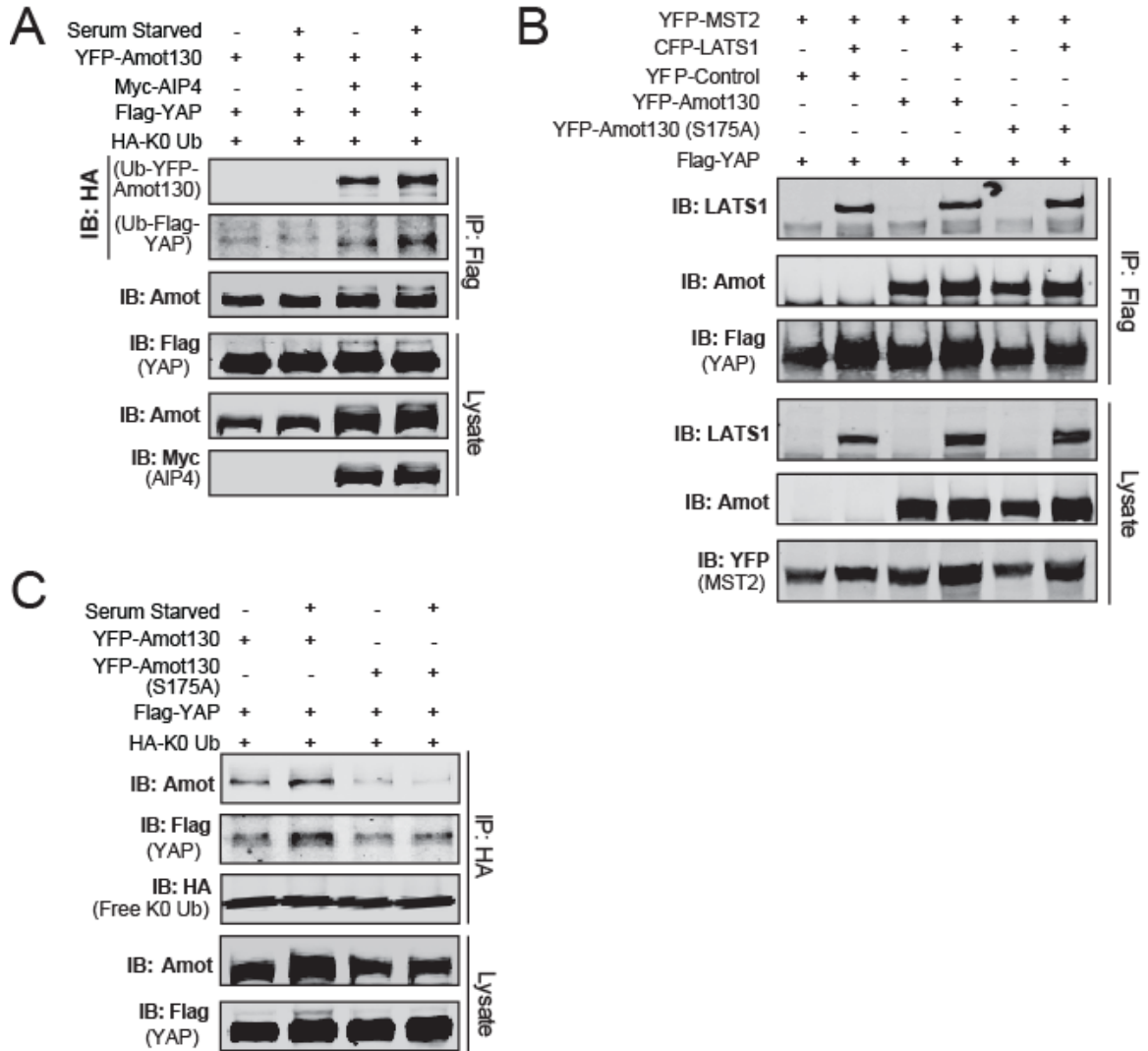


Figure 5-4 Serum Starvation and Ability of Amot130 to be Phosphorylated at Serine-175 Enhances YAP Ubiquitination by the Amot130-AIP4 Complex.

(A) Immunoblot with an anti-HA antibody was used to detect ubiquitinated Flag-tagged YAP and YFP-tagged Amot130 in immunoprecipitations with an anti-Flag antibody from HEK 293T cells expressing HA-Lys-0 Ubiquitin (HA-K0 Ub) and the indicated combinations of proteins. Before lysis, cells were cultured in DMEM with 10 % serum or serum starved for 24 hours. (B) Immunoblot of LATS1 and Amot130 in lysates or immunoprecipitated Flag-tagged YAP (anti-Flag) from HEK 293T cells transiently expressing proteins in indicated combinations. (C) Ubiquitinated proteins were immunoprecipitated with an anti-HA antibody from HEK 293T cells expressing the indicated combinations of recombinant proteins. Individual proteins were then detected by immunoblot as indicated. Figure adapted from (Adler et al., 2013b).

5.2.2. The Ability of Amot130 to be Phosphorylated at Serine Residue 175 Allows for Amot130 to Reduce the Stability of YAP

Taking into account that the Amot130-AIP4 complex ubiquitinates YAP, the ability of the complex to influence the stability of YAP was examined. Initially, the effects of Amot130 expression on the endogenous stability of YAP protein in the presence or absence of AIP4 were defined. For this, MDA-MB-468 cells stably expressing YFP-tagged Amot130 or control vector in combination with shRNA control or shRNA targeting AIP4 were lysed at the indicated times following treatments with cycloheximide (Figure 5-5A). Unlike control cells, which showed no reduction of endogenous YAP by 8 hours, cells expressing YFP-tagged Amot130 showed a 40 % loss of YAP (Figure 5-5A, top left). Further, as previously reported (Salah et al., 2011), silencing of AIP4 reduced the levels of YAP by over 80 % over this time, likely via stabilized LATS1. Consistent with Amot130 uncoupling YAP from regulation by LATS (Hao et al., 2008; Zhao et al., 2010), the expression of Amot130 partially reversed the effects of silencing AIP4 (Figure 5-5A, top right). However, the reported destabilization of LATS1 by AIP4 likely explains the inability to see a reversal of the inhibition of YAP by Amot130 expression upon the silencing of AIP4. This event is also complicated by the potential for Amot130 to regulate other Nedd4 family members (Wang et al., 2012). However, because co-expression of Amot130 and AIP4 results in a synergistic reduction in the steady state protein levels of YAP, there appears to be some role for AIP4 in directing Amot130-mediated reduction of YAP protein levels (Figure 5-5B). Thus, the inhibition of YAP is complicated by multiple roles of AIP4.

Based upon the differences in wild-type Amot130 versus Amot130 (S175A) to induce YAP ubiquitination (section 5.1), their effects on YAP stability were defined. This analysis was carried out in MCF7 cells due to their high AIP4 levels (Adler et al., 2013a), which sensitizes them to effects of phosphorylation of Amot130. Expression of wild-type Amot130 reduced the half-life of CFP-tagged YAP to 8.9 hours, following incubation with cycloheximide. However, cells expressing Amot130 (S175A) showed no detectable reduction of YAP stability over this

period (Figure 5-5C). Thus, the ability of Amot130 to be phosphorylated at Ser-175 appears to be important for Amot130 to promote the degradation of YAP.

Actin stress fibers are highly implicated in the activation of YAP and TAZ (Wada et al., 2011). Further, the mutants Amot130 (K481R) and Amot130 (S175A) localize to actin stress fibers; unlike wild-type Amot130 (section 4.2.5). Therefore, the redistribution of YAP to actin stress fibers by Amot130 (S175A) (Figure 5-6A-B) is consistent with Amot130 (S175A) having robust YAP binding (section 5.2.1), but not playing a role in suppressing YAP signaling. Overall, phosphorylation of Amot130 is likely central to the ability of Amot130 to redirect YAP away from actin stress fibers to trigger the destruction of YAP, likely via coupling YAP to an Amot130-AIP4 complex.

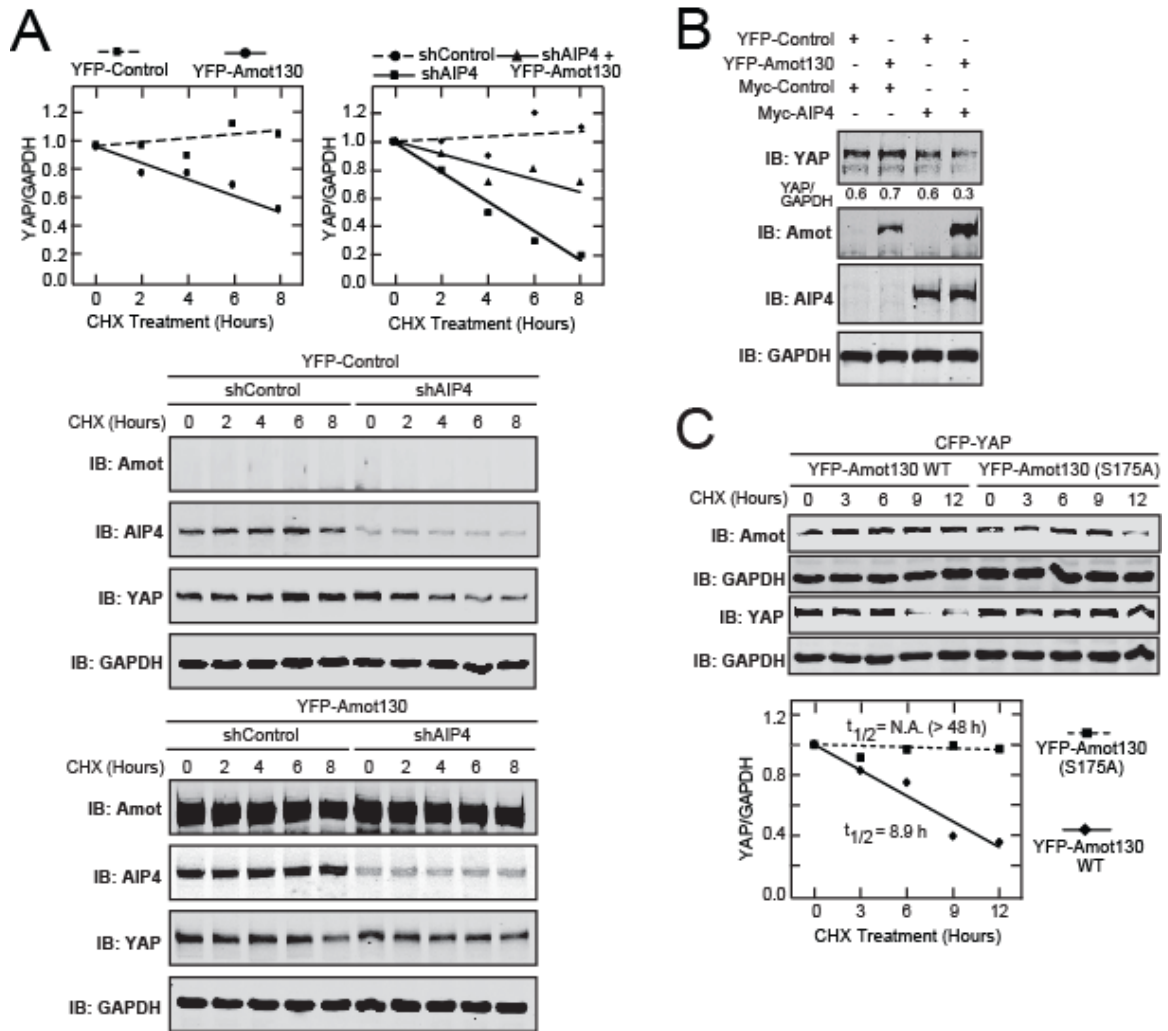


Figure 5-5 Amot130 Expression Induces YAP Degradation.

(A) The levels of YFP-tagged Amot130 as well as endogenous AIP4, YAP, and GAPDH were detected in lysates from MDA-MB-468 cells stably expressing control or AIP4 shRNA in combination with YFP-tagged Amot130 or control vector and treated for the indicated times with vehicle (DMSO) or 200 $\mu\text{g}/\text{mL}$ cycloheximide (CHX). The ratio of pixel intensities with linear regression analysis was plotted from the immunoblots, where the YAP/GAPDH levels in cells expressing (■) YFP-Control or (●) YFP-Amot130 are depicted (left graph) and the YAP/GAPDH levels in cells expressing (●) shControl, (■) shAIP4, or (▲) YFP-tagged Amot130 and shAIP4 are shown (right graph). (B) The levels of endogenous YAP were detected by immunoblot analysis of lysates from HEK 293T cells expressing combinations of YFP-tagged Amot130 and Myc-tagged AIP4. The ratios of pixel intensities of endogenous YAP over GAPDH bands are below the top panel. (C) The levels of YFP-tagged Amot130, YFP-tagged Amot130 (S175A), CFP-tagged YAP, and endogenous GAPDH were detected by immunoblot of lysates from MCF7 cells stably expressing these proteins following treatment for the indicated times, as described in A. Below, a graph of the ratios of CFP-tagged YAP over GAPDH and the resulting half-lives in cells expressing (■) YFP-tagged Amot130 (S175A) or (♦) YFP-tagged wild-type Amot130. Figure adapted from (Adler et al., 2013a) and (Adler et al., 2013b).

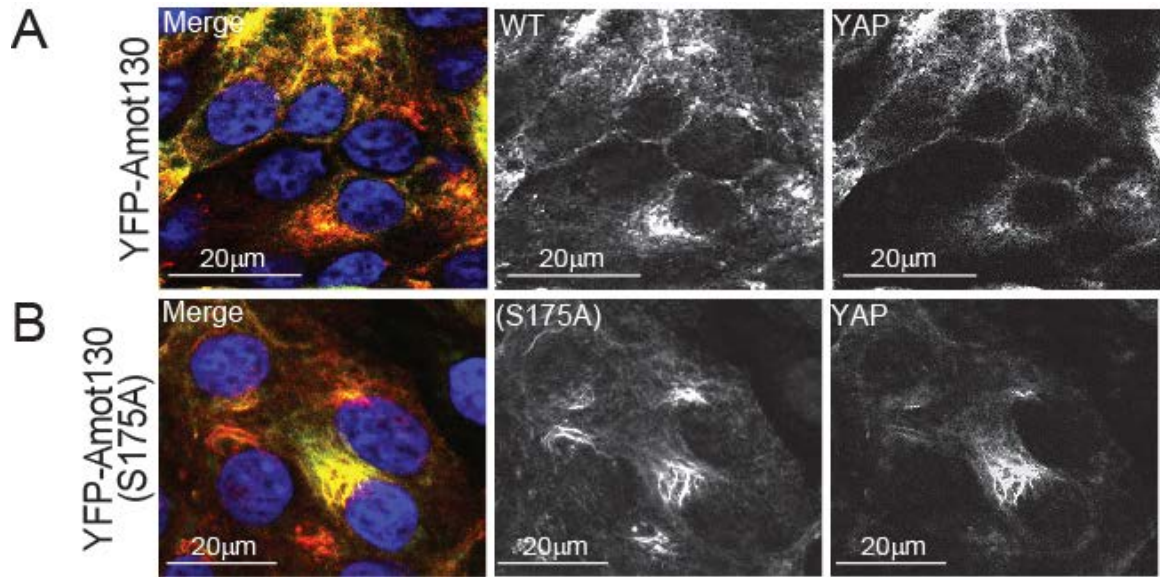


Figure 5-6 Wild-type Amot130 and Mutant Amot130 (S175A) Promote Different Subcellular Distributions of YAP.

(A-B) Confocal images of fixed MCF7 cells examining endogenous YAP using an anti-YAP antibody (red) and expressing (A) YFP-tagged wild-type (WT) Amot130 or (B) YFP-tagged Amot130 (S175A) (both in green). Nuclei are stained with Hoechst (blue). Figure in collaboration with Lauren Bringman. Figure adapted from (Adler et al., 2013b).

5.2.3. The Amot130-AIP4 Complex Mediates the Inhibition of YAP by LATS

Given the complex effects of AIP4 and Amot130 on YAP stability, functional analysis was undertaken to determine the role of AIP4 in mediating Amot130 induced inhibition of YAP-dependent transcription. The transcription of *CTGF* and *Cyr61* are regulated by TEAD transcription factors that, in turn, are under the control of YAP (Lai et al., 2011; Zhao et al., 2008b). The endogenous levels of *CTGF* and *Cyr61* transcripts were examined in MDA-MB-468 cancer cells, which have an average basal YAP levels and relatively high Angiotensin (Adler et al., 2013a). These cells were grown to conditions conducive to low Hippo signaling (10 % serum or low confluence) or high Hippo signaling (serum starved or high confluence). Representative brightfield images were taken of cells at both high and low confluence, so that a reference of what constitutes high and low confluence is established (Figure 5-7A). Initially, the effects of AIP4 silencing in combination with Amot130 expression on both the endogenous *CTGF* and *Cyr61* mRNA levels was measured by real time PCR under conditions of serum starvation and low confluence, where Hippo signaling should be active (Figure 5-7B). Analysis revealed that cells stably expressing Amot130 had more than an 85 % reduction in *CTGF* transcript, while *CTGF* mRNA levels in AIP4 stably silenced cells were reduced by roughly 50 %. The inhibition of *CTGF* mRNA levels in AIP4 silenced cells is likely via gain of LATS activity (Salah et al., 2011). However, *CTGF* mRNA levels were reduced by less than 45 % in cells simultaneously silenced for AIP4 expression and expressing YFP-tagged Amot130. Similar effects were seen with *Cyr61* transcript levels. Thus, AIP4 appears to be at least partially required for Amot130 to suppress the transcript levels of *CTGF* and *Cyr61*.

Next, the role of Amot130 on LATS reported inhibition of YAP activity was examined. These cells were grown in 10 % serum to low confluence, where Hippo signaling should be low. Here, following infection of these cells with shRNA targeting Angiotensin for 24 hours, there is an isoform selective silencing of Amot130 but not Amot80. Cells expressing CFP-tagged LATS1 and a control shRNA showed a significant reduction in *CTGF* levels, as expected with active

LATS1 (Figure 5-8A); whereas, there was no significant loss of *CTGF* transcription in LATS1 expressing cells with silenced Amot130 levels. Interestingly, silencing of Amot130 without LATS1 expression resulted in a significant increase in *CTGF* levels. Thus, Amot130 is required to transmit the inhibition of YAP by LATS1 in these cells.

The roles of phosphorylation of Amot130 on YAP phosphorylation and YAP-dependent transcription were then investigated. MDA-MB-468 cells were grown in 10 % serum, to high confluence, therefore placing them in presumably active Hippo signaling. Exogenous expression of wild-type Amot130 showed increased levels of phosphorylation of Ser-127 on YAP versus control cells, as previously reported (Figure 5-8B) (Zhao et al., 2011a). Conversely, Amot130 (S175A) expression reduced phosphorylation of YAP at Ser-127 versus control cells. To determine if the change in phosphorylation of YAP translated into reduced levels of YAP-regulated transcripts, *CTGF* mRNA levels were measured in similarly stably expressing cells under presumably low Hippo signaling (10 % serum and low confluence) or high Hippo signaling (10 % serum and high confluence) (Figure 5-8C). The expression of wild-type Amot130, but not Amot130 (S175A) significantly reduced the levels of *CTGF* transcript in cells with low Hippo signaling. Alternatively, cells with high levels of intercellular contacts showed modestly reduced *CTGF* levels upon wild-type Amot130 expression from presumably already low basal levels of YAP activity. However, Amot130 (S175A) expression increased *CTGF* levels significantly above those of control cells. This is consistent with it exerting a dominant negative effect in cells with active Hippo signaling. Together, these studies indicate an important role of Amot130 inhibition of YAP-dependent transcription. These include an important requirement for AIP4 and the ability of LATS to phosphorylate Amot130 at Ser-175 to drive the inhibition of YAP.

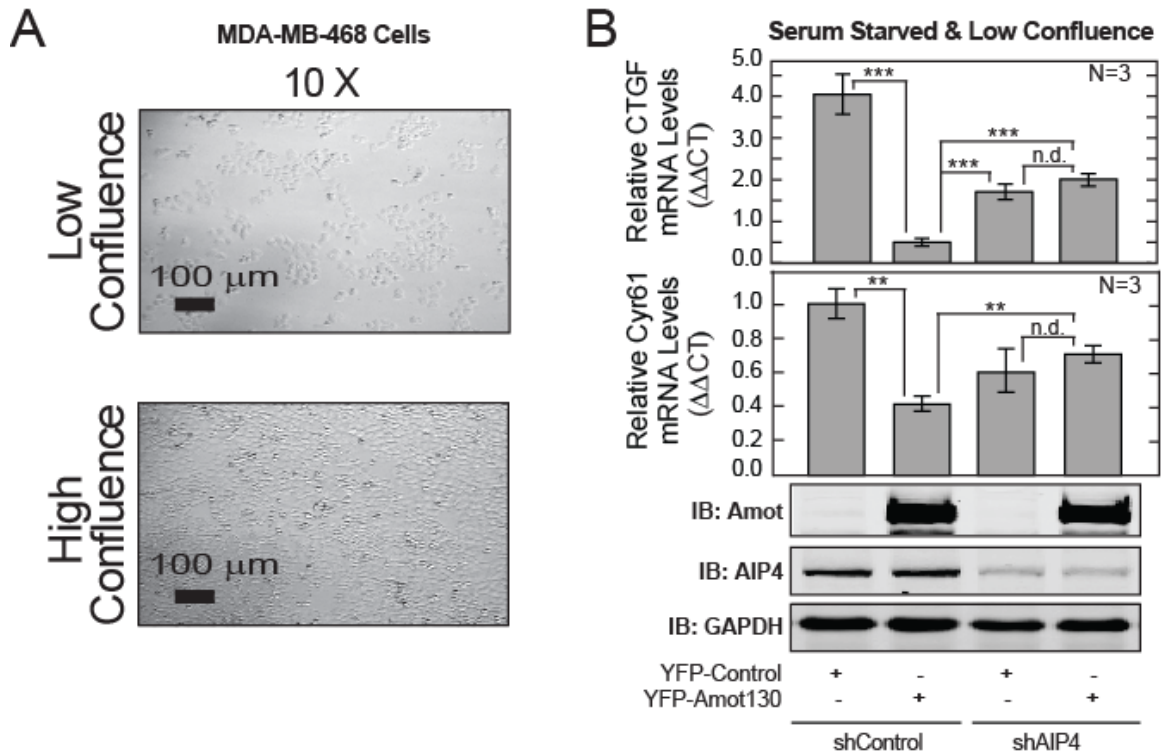


Figure 5-7 Amot130 Inhibits YAP-Dependent Transcription Cooperatively with AIP4.

(A) Stereoscopic brightfield images of representative fields of MDA-MB-468 cells grown to low and high confluence before harvest at 10 X magnification are presented to illustrate the density of cells termed low and high confluence in the real time PCR experiments. (B) MDA-MB-468 cells stably expressing YFP-tagged Amot130 or control vector in combination with control or AIP4 shRNA. Cells were grown under serum starvation conditions 24 hours prior to harvest. The mRNA transcript levels from cells of *CTGF* (upper plot) and *Cyr61* (lower plot) are presented for conditions indicated. Data represents three experimental replicates ($n = 3$). Below, immunoblots from paired cells validating AIP4 silencing and Amot130 expression are presented. Error bars represent \pm S. D. p-values: *** < 0.00001 ; ** < 0.01 . Figure adapted from (Adler et al., 2013a) and (Adler et al., 2013b).

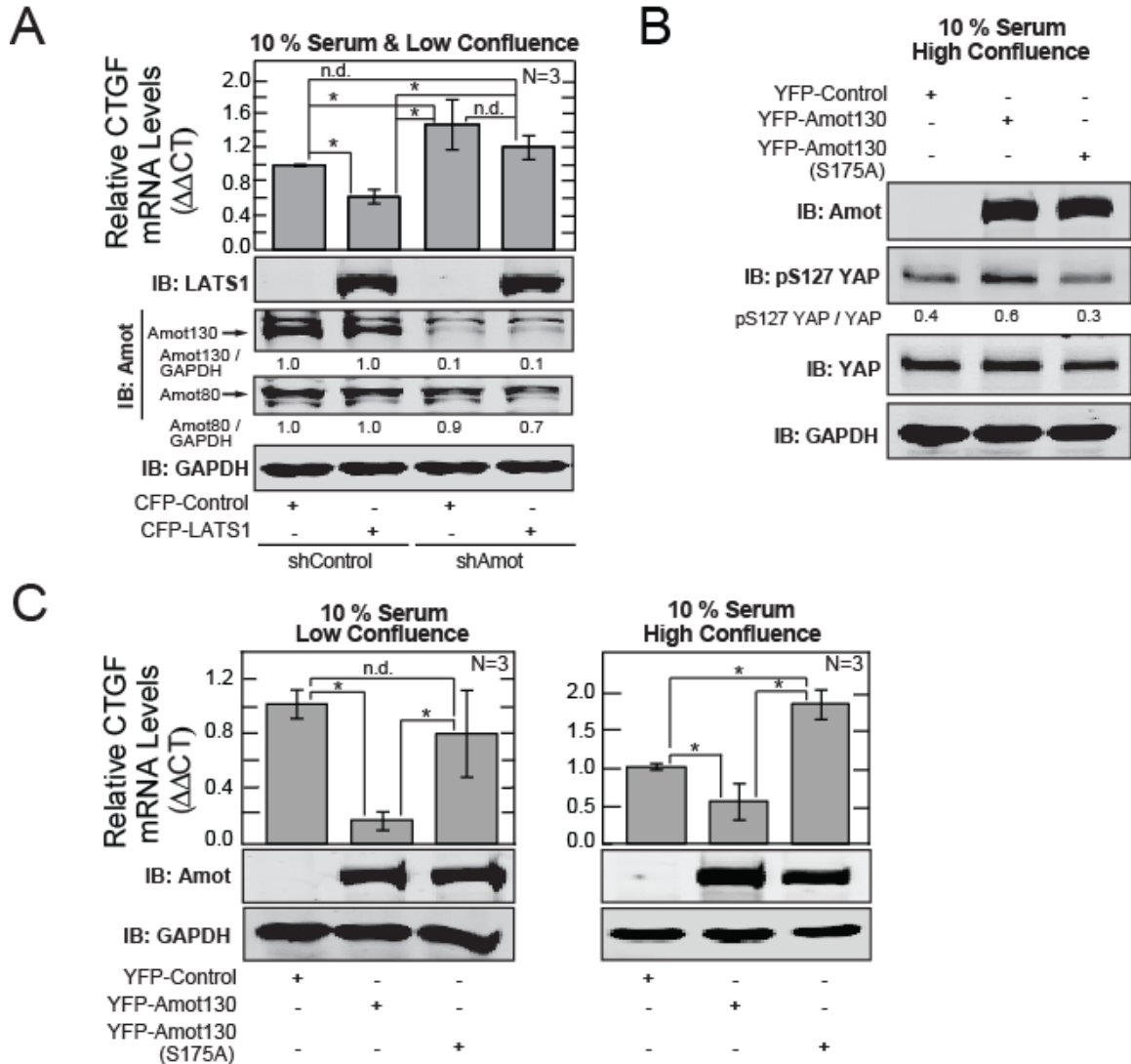


Figure 5-8 Amot130 Mediates the Inhibition of YAP-Dependent Transcription by LATS.

(A) Real time quantitative PCR measurements of the levels of *CTGF* mRNA in MDA-MB-468 cells co-infected for 24 hours with lentivirus encoding combinations of Angiotensin II receptor type 1 shRNA (shAmot), CFP-tagged LATS1, or the indicated controls. Below, immunoblots from paired cells validating Amot130 selective silencing and CFP-tagged LATS1 expression with pixel intensity values of Amot130 and Amot80 levels normalized to GAPDH. Data represents three biological replicates ($n = 3$). (B) Immunoblot of phosphorylated YAP at Ser-127 (pS127), total YAP, and GAPDH from MDA-MB-468 cells expressing YFP-tagged wild-type Amot130, Amot130 (S175A), or control vector grown to high confluence prior to harvest. The ratios of pixel intensities of pS127 YAP to total YAP are presented below second panel. (C) Real time quantitative PCR measurements of *CTGF* mRNA levels in MDA-MB-468 cells described in B and harvested at low (left) or high confluence (right). Data represents three biological replicates ($n = 3$). Error bars represent \pm S. D. p-values: * < 0.05 ; n.d. no statistical difference. Figure adapted from (Adler et al., 2013b).

5.3. Discussion

5.3.1. The YAP-Amot130-AIP4 Complex Formation and Its Inhibition of YAP Activity

The inhibition of YAP-dependent transcription by the Hippo kinases is a key element in growth control. The Amot130-AIP4 complex is an alternative mechanism to relay Hippo signaling to inhibit YAP activity. Importantly, YAP is a novel target for the ubiquitin ligase AIP4, when both proteins are bound to Amot130. The YAP-Amot130-AIP4 complex is promoted by LATS-dependent Amot130 phosphorylation at Ser-175, that both increases Amot130 stability and drives the Amot130-AIP4 complex ubiquitination and degradation of YAP. Further, phosphorylation of Amot130 and AIP4 binding is required for them to inhibit YAP activity. Together, this comprises a novel mechanism for Hippo signaling to inhibit YAP nuclear activity.

YAP binding to Amot130 utilizes two P-Y motifs for a high affinity interaction, as does AIP4. The complex containing both AIP4 and YAP is proposed to involve Amot130 homodimerization. In effect, the dimerization of the Angiomotins provides double the number of available P-Y motifs in a single complex, allowing both proteins to bind the second P-Y motif to achieve a high affinity association. Importantly, an interaction between AIP4 and YAP was not seen without Amot130 expression, which indicates the importance of the Amot130 adapter protein for providing the docking sites for the ubiquitin ligase and the substrate into a common complex. Further, the complex formation and YAP ubiquitination is highly dependent on the ability of Amot130 to be phosphorylated at Ser-175.

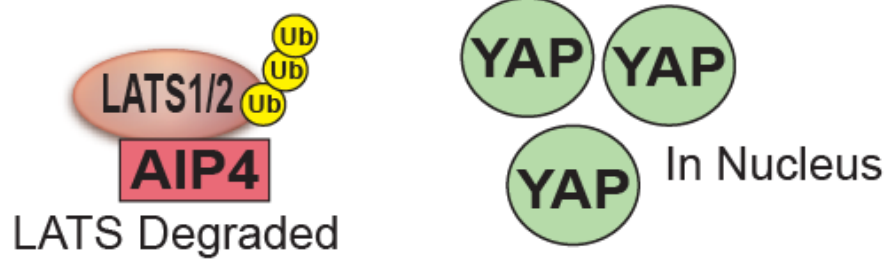
5.3.2. The Essential Role of Amot130 in Reinforcing YAP Inhibition

The formation of an Amot130-AIP4 complex also prevents AIP4 from binding and targeting LATS1 for degradation. Amot130 likely competes for binding to AIP4, with LATS1, and thereby prevent LATS1 degradation via the 26S Proteasome (Salah et al., 2011). LATS1

remains free to phosphorylate and inhibit YAP activity. Likely, this is one of the multifactorial effects of Amot130 in promoting the degradation of YAP.

Overall, Amot130 is proposed to both activate and transmit Hippo signaling to strongly induce the inhibition of YAP activity and cell growth (Figure 5-9). The inhibition of YAP in response to Amot130 is likely self-reinforcing, whereby Amot130 directly activates LATS1/2 (Paramasivam et al., 2011) that, in turn, promotes Amot130 stabilization by driving Amot130 association with AIP4. Together, these events likely drive the rapid accumulation of active LATS1/2 and Amot130 to directly inhibit YAP nuclear activity. The inhibition of YAP is predicted to occur by both targeting YAP for phosphorylation by LATS1/2 and ubiquitination by SCF-(β)-TRCP (Zhao et al., 2010), as well as by AIP4-induced ubiquitination and degradation.

(-) Amot130



(+) Amot130

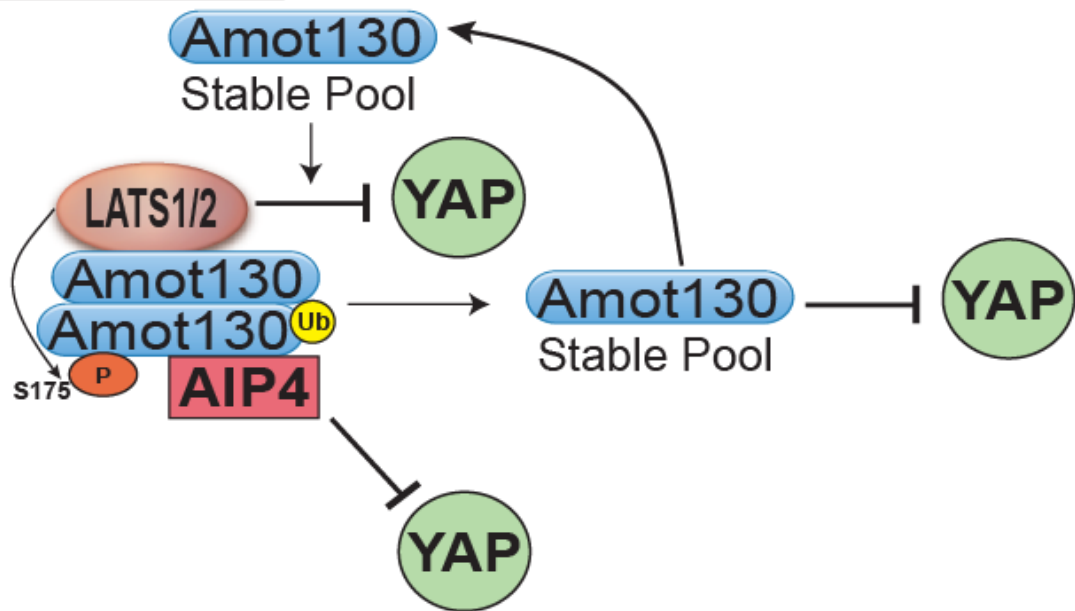


Figure 5-9 Proposed Cyclic Model for Amot130 and LATS1 Inhibition of YAP-Dependent Transcription.

Under conditions of low Amot130 protein levels (above), LATS is degraded by AIP4 and YAP is ultimately in the nucleus, where it can activate pro-growth transcription events. However, upon increasing Amot130 protein levels (below), it creates a self-reinforcing cycle of LATS and Amot130 stability, which ultimately leads to inhibition of YAP. First, LATS, upon activation, phosphorylates Amot130, which leads to AIP4 binding and stabilization of Amot130. This complex inhibits YAP via its ubiquitination and targeting for degradation by AIP4. Second, stable Amot130 is able to inhibit YAP via sequestration mechanisms. Third, Amot130 is able to increase the phosphorylation of YAP and inhibition, likely via preferential binding of AIP4 away from LATS, creating a stable pool of both LATS and Amot130 to inhibit growth. Upon external pro-growth signals, this loop breaks down and YAP can enter the nucleus again.

5.3.3. Phosphorylation of Serine Residue 127 on YAP is not Sufficient for YAP

Inhibition via Serum Starvation

Recent published evidence indicates that factors can work outside of the phosphorylation status of YAP at Ser-127 to inhibit YAP. Importantly, the phosphorylation at Ser-127 is not sufficient to exclude YAP from the nucleus (Wada et al., 2011). This same study indicates that there is major uncertainty about the location of LATS in the pathway of YAP inhibition. Further, where growth was inhibited, under serum starvation conditions, the phosphorylation of YAP at Ser-127 was differentially regulated in a panel of adenocarcinoma cell lines (Levin et al., 2009). In some cases, serum starvation increased YAP phosphorylation at Ser-127, while in other cell lines it decreased. Together, these two studies give evidence to an alternative model of LATS inhibiting YAP via the phosphorylation of Amot130 and not directly on YAP. The ability of LATS to phosphorylate both YAP and Amot130 provides an alternative explanation for inhibition of YAP regulation that supports Amot130 and LATS as dual-inhibitors of YAP. Overall, Amot130 likely inhibits YAP through a combination of mechanisms that likely include both direct activation of LATS (Paramasivam et al., 2011) and independent effects via AIP4 (Figure 5-10).

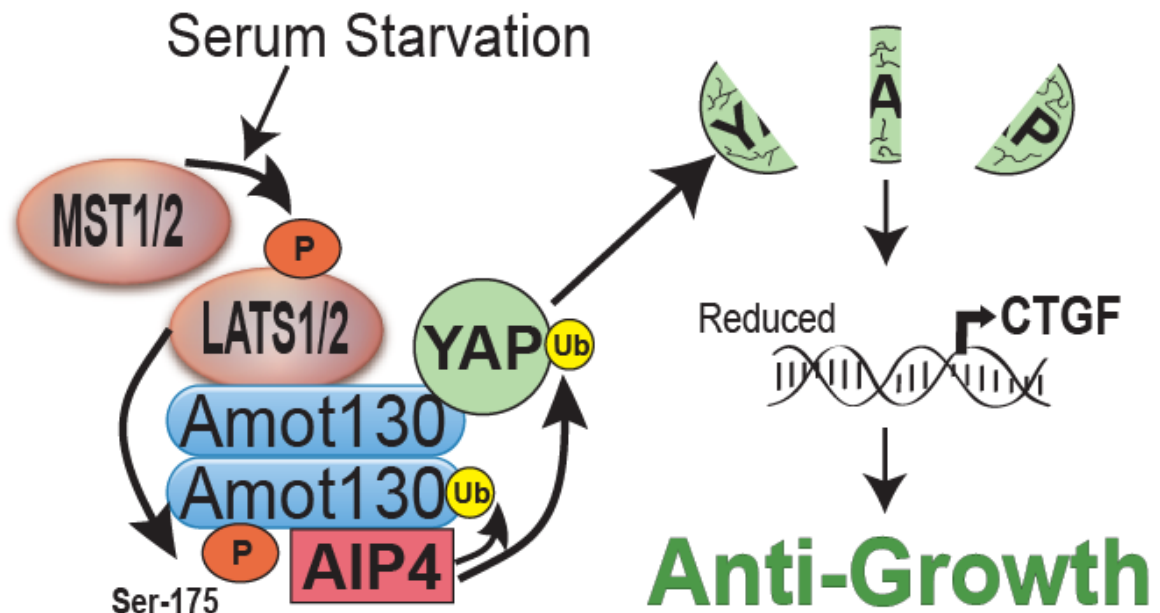


Figure 5-10 An Alternative Mechanism for Serum Starvation Inhibition of Cellular Growth.

The ability of Amot130 to homo-dimerize allows for multiple binding partners to exist in a complex together. This homo-dimerization may allow for both YAP and AIP4 to form a complex, which leads to the ubiquitination and degradation of YAP. The end result of the Amot130-AIP4 complex is reduced *CTGF* transcript levels, which likely explains how Amot130 is able to inhibit cellular growth. Additionally, the phosphorylation of Amot130 by LATS1 is required for YAP ubiquitination by AIP4 in response to serum starvation. Further, the inhibition of *CTGF* transcription by Amot130 requires the ability of Amot130 to be phosphorylated at Ser-175. Together, these data suggest an alternative mechanism for growth inhibition in mammary epithelial cells that is independent of the canonical phosphorylation of YAP, through the YAP-Amot130-AIP4 complex.

CHAPTER 6. CONCLUDING REMARKS ON THE ROLE OF THE LONG ISOFORM OF ANGIOMOTIN IN GROWTH SIGNALING IN MAMMARY EPITHELIAL CELLS

Some text in this chapter was originally published in The Journal of Biological Chemistry and the Proceedings of the National Academy of Sciences USA. Adler et al. Amot130 Adapts Atrophin-1 Interacting Protein 4 to Inhibit Yes-Associated Protein Signaling and Cell Growth. *Journal of Biological Chemistry*. 2013; Vol: 288, 25: 15181-15193. © the American Society for Biochemistry and Molecular Biology. Adler et al. Serum deprivation inhibits the transcriptional co-activator YAP and cell growth via phosphorylation of the 130-kDa isoform of Angiotensin II by the LATS1/2 protein kinases. *Proceedings of the National Academy of Sciences*. 2013; Vol: 110, 43: 17368-17373. © Proceedings of the National Academy of Sciences USA.

6.1. Introduction

A novel mechanism for the inhibition of YAP activity by Amot130 and the Nedd4 ligase AIP4 is presented in this study. Deeper understanding of how microenvironmental factors regulate the Hippo pathway is of great importance. Unfortunately, understanding the roles of specific Angiotensins and Nedd4 ligases is complicated by the multiple overlapping, redundant, and non-overlapping roles of these proteins. Further, the regulation of their expression in normal and pathologic contexts is largely unknown. This thesis suggests possible routes by which Angiotensins and Nedd4 ligases may transduce microenvironmental cues as part of the Hippo signaling pathway.

6.2. Influencing Angiotensins and Their Impact on Signaling

6.2.1. The Role of Serum Factors in Angiotensin Signaling

While the role of specific serum factors in the microenvironment of the cell was not discussed in this thesis, the deprivation of these and other unknown factors is clearly an important signal for cells to cease cell division and growth. Evidence is presented here that illustrates how serum deprivation at least in part increases the protein steady state levels of Amot130 to induce growth arrest. The response to serum deprivation was found to be specific to Amot130 and not AmotL1. This information further led to the investigation of how Amot130 in response to serum deprivation is at the heart of a novel mechanism by which Hippo signaling inhibits YAP and cellular growth. Interestingly and surprisingly, throughout this investigation of Amot130, the short isoform of Angiotensin (Amot80) also had a robust increase in its protein steady state levels in response to serum deprivation (Figure 6-1A). However, this increase in protein steady state levels was not as consistent as those seen with Amot130 (Figure 6-1B). The explanation for this increase is not clear because Amot80 lacks the N-terminal P-Y motifs, thus cannot directly bind,

be ubiquitinated, or stabilized by AIP4. Additionally, the predicted LATS binding site also is lacking in Amot80. Based upon the absence of important binding relationships, the increase in steady state protein levels of Amot80 in response to serum deprivation is likely indirect. A possible explanation lies in the ability of Amot80 to hetero-dimerize with other Angiotomins, which have these functional N-terminal regions. Depending upon what Angiotomin Amot80 dimerizes with (AmotL1, Amot130, or AmotL2) could greatly impact if Amot80 is influenced by serum deprivation. For example, AmotL1 steady state protein levels are not influenced by serum deprivation, thus if Amot80 dimerizes with AmotL1, it is likewise hypothesized to not be influenced. However, if Amot130 dimerizes with Amot80, it would allow Amot80 to be in the same complex with AIP4, which increases the ubiquitination and stability of Amot130, and thus also possibly bound Amot80. Regardless, Amot80 increases sometimes in response to serum deprivation. Further analysis of the Amot80 response to serum deprivation and its relationship with cell growth remains to be investigated. Perhaps serum deprivation is generally trying to achieve a balance of the Angiotomins to inhibit cellular growth. The action of increasing steady state protein levels of Angiotomin versus AmotL1 is likely a signal for other growth and survival related pathways, with unknown outcomes. Overall, specific Angiotomins are influenced by serum deprivation and this action is likely a key mediator of their abilities to influence growth control.

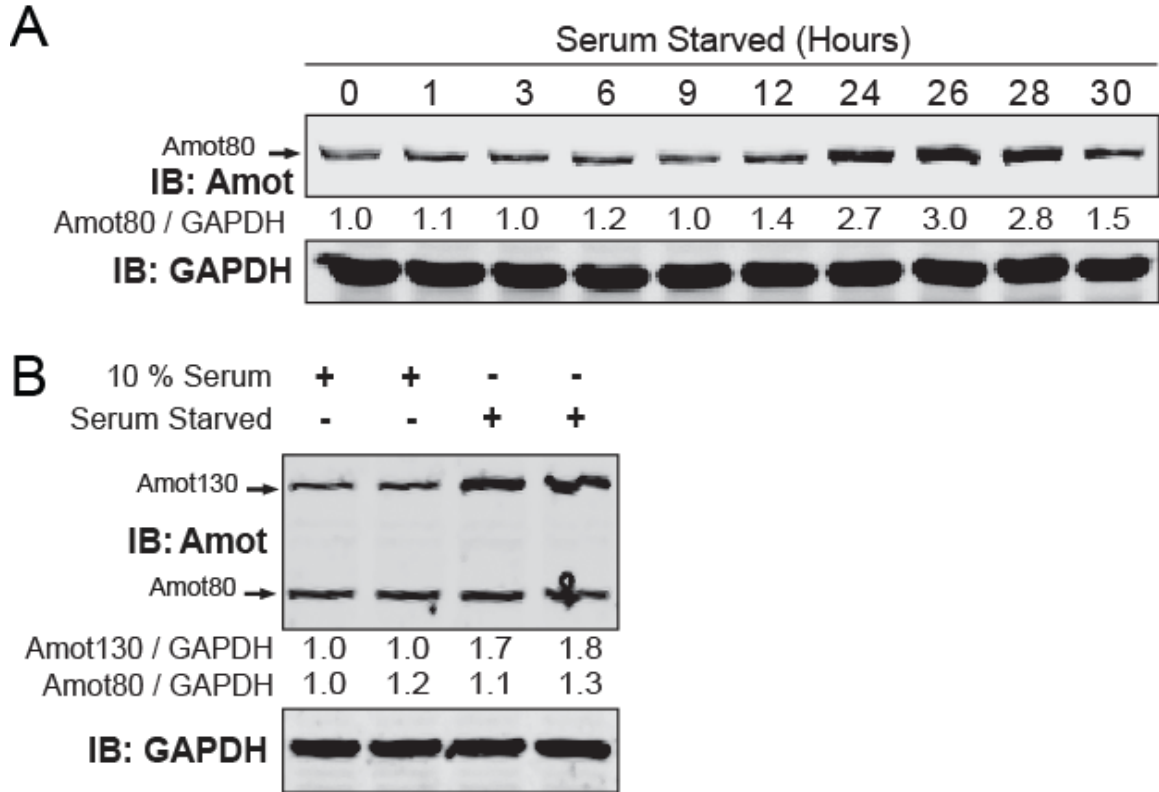


Figure 6-1 Serum Starvation Increases Amot80 Steady State Protein Levels.

(A) Amot80 and GAPDH steady state protein levels were analyzed via immunoblot of lysates from MDA-MB-468 cells subjected to serum starvation for times indicated. The normalized pixel intensities of Amot80 over GAPDH for each condition are indicated. (B) Immunoblot of Amot130, Amot80, and GAPDH protein steady state levels as analyzed in A in MDA-MB-468 cells after 24 hour serum starvation or with 10 % serum.

6.2.2. The Similarities and Differences Between the Angiomotins

Upon initial structural examination of the long Angiomotins, they appear very similar. All contain a PDZ-binding motif, P-Y motifs, and an ACCH domain, among other features. This could lead to the assumption that all of the Angiomotins are functionally redundant. Further, this is enforced by the overlapping role of the long Angiomotins to inhibit YAP and TAZ. While redundant roles have been demonstrated, this thesis provides important differences between these family members. Further, these differences are likely important for understanding their general roles as adapter proteins and their non-overlapping roles.

Amot130 and likely AmotL1 are phosphorylated by LATS2. However, AmotL2 does not appear to be able to be phosphorylated, based upon the peptide *in vitro* kinase assays. The inability of AmotL2 to be phosphorylated by LATS2 may help explain why AmotL2 also failed to be ubiquitinated by AIP4, unlike both AmotL1 and Amot130. The amino acids that surround the LATS consensus motif of AmotL2 are more diverse when compared to AmotL1 and Amot130. Thus, it is not surprising that AmotL2 would have the greatest difference in phosphorylation compared to the other Angiomotins. Further establishing the uniqueness of AmotL2, it contains an arginine residue in the site that aligns with the lysine ubiquitination sites of Amot130/AmotL1. In support of the inability of AmotL2 to be ubiquitinated by AIP4, AmotL2 lacks a third conserved P-Y motif seen in both Amot130 and AmotL1. This motif is required for Amot130 to bind to AIP4. The inability to have this third functional P-Y motif, may in part explain the inability of AmotL2 to be ubiquitinated by AIP4. Together, AmotL2 lacks key functional residues seen in AmotL1 and Amot130, which prevent the ability of AmotL2 to be phosphorylated at its predicted LATS consensus motif and lacks ubiquitination by AIP4. Given the evidence above, it is likely that AmotL2 would also not respond to serum deprivation nor be able to transmit Hippo signaling through this particular growth-arrest mechanism.

Based upon the similarities presented thus far between Amot130 and AmotL1, it is tempting to conclude that both are functionally the same. However, the increase in Amot130

steady state protein levels upon serum deprivation was not seen for AmotL1. Interestingly, both seem capable of being phosphorylated by the LATS2 protein kinase. Thus, the specificity of Amot130 in response to serum deprivation remains to be answered. This could possibly be answered by observations that AmotL1 seems to preferentially bind another Nedd4 ubiquitin ligase, Nedd4-1, better than AIP4. Nedd4-1 leads to the ubiquitination and degradation of both AmotL1 and Amot130 (Wang et al., 2012), whereas AIP4 increases the steady state protein levels of Amot130 (Adler et al., 2013a). Thus, if AmotL1 preferentially binds Nedd4-1, it will not be able to also bind AIP4, and thus prevents an AIP4-dependent increase in steady state protein levels of AmotL1. Together, AmotL1 steady state protein levels are not influenced in response to serum deprivation and LATS phosphorylation likely because these events do not lead to binding of AIP4, which is shown here to be critical for stabilizing Amot130 protein. Future studies examining the specificity of Nedd4 ligases for binding with specific Angiomotins may clarify their functioning in cells.

Taken together, AmotL2 and AmotL1 are not regulated the same as Amot130 in epithelial cells. Clearly, these Angiomotins are not completely functionally redundant and future studies will help differentiate the family members in the context of epithelial cell signaling.

6.2.3. The Role of Angiomotin in Mammary Tissue

In normal breast development, especially during the pregnancy lactation cycle, major changes in tissue architecture in the breast occur via the regulation of cell growth, migration, and cell death pathways. These are especially apparent during the process of involution. During this time, changes in the cellular microenvironment modify cellular polarity and lead to signaling that promotes physiological changes in the architecture of the breast. In mouse models, mRNA profiles identified prolonged *AMOT* signatures at day 3 of involution (Stein et al., 2009). This upregulation of *AMOT* was correlated with the highest level of metastasis and cell movement. This physiological correlation best associates with the reported functions of Amot80 and not

Amot130 (Bratt et al., 2005). However, based upon the functions of Amot130 presented in this study it is likely that Amot130 also plays a role in tissue remodeling. A major function of Amot130 presented here is its ability to inhibit growth signaling pathways in mammary epithelial cells. Thus, Amot130 is predicted to be involved in cellular differentiation. Evidence of Amot130 inducing cellular differentiation is seen upon expression of Amot130 in MCF10A acini, which appears to force the acini into early differentiation, yielding a structure likely incapable of physiological function. Further, Amot130 is associated with control of differentiation of the inner cell mass cells in pre-implantation mouse embryos (Leung and Zernicka-Goetz, 2013). Together, it is hypothesized that Amot130 likely has an opposing role to Amot80 in tissue architecture. However, the exact roles of Amot130 versus Amot80 in tissue remodeling are currently unknown. A balance between the pro-growth and migratory functions of Amot80 and the differentiation and growth-arrest functions of Amot130 likely underlies a critical mechanism for tissue remodeling in the breast. Future understanding of the roles of all the Angiomotins in normal tissue remodeling processes, including involution, where Angiomotin appears to play an important role, will shed light into the key physiological functions of these proteins.

6.2.4. The Involvement of the Angiomotins in Viral Signaling

The roles of specific Nedd4 ligases and Angiomotins in transducing changes from the microenvironment of mammary epithelial cells to Hippo signaling and growth control was an important aspect of this study. Specifically, the role of factors in serum was examined; however, other potential microenvironmental effectors are likely impacting Hippo signaling and this specific mechanistic pathway. These factors include viruses, which have underappreciated roles in Hippo signaling.

The microenvironment of the breast can contain viruses, which may potentially impact the growth and survival of cells. Viruses account for about 12 % of all cancers (Moore and Chang, 2010) and act on numerous signaling pathways within epithelial cells, regulating

processes of cell division, cell polarity, and Hippo signaling (Banks et al., 2012). For example, the Par and Crb polarity proteins complexes, which associate with Angiomotin, are hijacked by viruses to promote replication of infected cells (Banks et al., 2012). Fortunately, there are inhibitory pathways to prevent viral production. One such pathway utilizes AmotL1 to interact with and inhibit the activity of a protein involved with virus production (Pei et al., 2010). Interestingly, this same process has been thought to involve disassembly of the actin cytoskeleton (Lamb et al., 1976; Pei et al., 2010) and recruitment of Nedd4 ubiquitin ligases (Martin-Serrano et al., 2005; Rauch and Martin-Serrano, 2011). Additionally, Nedd4 proteins can promote actin assembly in yeast cells (Stawiecka-Mirota et al., 2008). Further, this thesis reinforces connections between the Angiomotins, Nedd4 ligases, and actin rearrangements and their impact on cell growth. Together, it is hypothesized that a mechanism of Nedd4 recruitment and actin remodeling in virus production could be through the Angiomotins in processes similar to that presented herein. For example, Amot130 is able to remodel actin through its ability to be phosphorylated by LATS. Further, the Nedd4 ligase AIP4 is recruited to bind to Amot130, which changes its cellular localization and availability for substrates. Therefore, inhibition of viral signaling could occur through sets of Angiomotins and their unique abilities to anchor Nedd4 ligases and rearrange actin. However, the precise role of these proteins in viral budding and virus production is unclear. Regardless, the links between the Angiomotins with the microenvironment and Hippo signaling yields room for future studies to identify how the Angiomotins are utilized in viral signaling for growth regulation.

6.2.5. Promoting *AMOT* Transcription via Microenvironmental Elements in Mammary Tissue

The paracrine microenvironment of mammary tissue contains growth regulatory elements including various cytokines and chemokines secreted by inflammatory cells, many of which are associated with breast cancer development, particularly in inflammatory breast cancers (Hussein

and Hassan, 2006; Lieblein et al., 2008; O'Shea and Murray, 2008). Specifically, the cytokine interleukin-6 (IL-6), promotes the accumulation of the signal transducer and activator of transcription (STAT) 3 and nuclear factor- κ B (NF κ B) transcription factors (Yang et al., 2007). IL-6 activates transcription, which promotes the oncogenic transformation of mammary epithelial cells (Hodge et al., 2005; Mohankumar et al., 2008). Interestingly, these physiological effects are similar to those seen upon exogenous Amot80 expression in mammary epithelial cells (Ranahan et al., 2011). Further, expression array studies implicate IL-6 and STAT3 in the induction of *AMOT* transcription (Yang et al., 2007). Sequence analysis of the 5'-upstream region of the *AMOT* gene indicates several potential STAT and NF κ B binding sites (Figure 6-2). Thus, *AMOT* transcription is hypothesized to be under control of these transcription factors, and thus under control of cytokines, such as IL-6. Future studies examining the response to microenvironmental factors, will likely give clues to the control of growth via the microenvironment of the breast tissue. Based upon the opposing roles of Amot80 versus Amot130, these factors that control the transcription of *AMOT* are likely isoform specific. Thus, understanding the isoform specific regulation of their transcription could unlock clues to understanding the balance of growth control via gene expression in mammary epithelial cells. This would point at an interesting role for the microenvironment in the control of cell growth.



5' of EXON 1	Base Pairs 5' Upstream of EXON 1	Prediction Program Algorithm
STAT	5353	P-Match by D.S. Chekmenev
NFκB	180	AliBaba2 by N. Grabe

Between EXON 1 and 2	Base Pairs 5' Upstream of EXON 2	Prediction Program Algorithm
NFκB	4802	AliBaba2 by N. Grabe
STAT	4801	P-Match by D.S. Chekmenev
NFκB	2897	AliBaba2 by N. Grabe
NFκB	1814	AliBaba2 by N. Grabe

Figure 6-2 Possible Transcription Factor Binding Sites for Promoting *AMOT* Transcription.

Prediction programs designed to identify transcription factor binding sites in DNA sequences were utilized for the sequences upstream of *AMOT* and between its first two exons. These programs utilize the set of binding sites available from TRANSFAC® to predict future unknown binding sites. Two prediction programs revealed several potential STAT and NFκB binding sites in these regions. The diagonal double lines indicate that this is a selection of a much longer DNA sequence.

6.2.6. Regulation of the Angiotensins into the Nucleus

Understanding how the microenvironment influences the nuclear functions of YAP was a major goal of this study. One important aspect of YAP function not examined in this study was how YAP does or does not enter the nucleus. However, this study and some unpublished work present a possible role of Angiotensin in YAP nuclear import. Previous work with Zona Occludin 2 (ZO-2) implicates it as a known positive regulator of YAP activity, via shuttling YAP into the nucleus (Oka et al., 2010). No other protein is reported to have this unique shuttling ability. However, recent work with Amot80 shows the ability of it to activate cellular growth and have similar properties to overexpression of YAP in mammary epithelial cells (Ranahan et al., 2011; Yi et al., 2011). The precise mechanism by which Amot80 is able to promote cellular growth has not been reported. However, in unpublished work by William Ranahan, YAP presents itself in a complex with Amot80, via hetero-dimerization with Amot130. Amot80 is then able to dominantly redistribute Amot130, along with its associated YAP, away from cell contacts and actin and into compartments surrounding the nucleus. Finally, Amot80 was able to increase the nuclear activity of YAP. However, the mechanism for this Angiotensin activation of YAP is unknown. A proposed direct import of YAP via Amot130 is hypothesized based upon several observations. First, Amot130 contains a canonical nuclear localization sequence from residues 585-605, and is proposed to allow Amot130 to directly shuttle bound YAP into the nucleus. Thus, the overall hypothesis is that when YAP-Amot130 complex is dimerized with Amot80, the complex is brought into the vicinity of the nucleus, by the dominate redistribution via Amot80. Once surrounding the nucleus, the nuclear import via Amot130 nuclear localization sequence can occur, likely shuttling both YAP and Amot80 into the nucleus. This hypothesis helps explain data where Amot130, under conditions of low cell confluence, significantly promotes TEAD transcription across mammary epithelial cells (Figure 6-3A). At first, this seems counter to Amot130 as a tumor suppressor protein, which is at the crux of this study. However, there appears to be a dual function of Amot130, which prior to this study has not been appreciated. The

promotion of nuclear YAP is likely a result of the dominate redistribution of Amot130 to surrounding the nucleus by Amot80. Thus, in cells with low Amot80, this phenotype goes largely unnoticed. In fact, most cells examined in this thesis were at high cell confluence and had lower levels of Amot80 compared to Amot130. Thus, Amot130 was largely inhibiting cell growth by keeping YAP out of the nucleus by various mechanisms. However, it is possible that under low cell confluence conditions, Amot80 levels are increased, and thus phenotypically could outweigh the growth suppressive properties of Amot130, which is classically witnessed upon Amot80 overexpression (Ranahan et al., 2011). Secondly, in support of Amot130 promoting growth via its nuclear import, the Angiomotins have been differentially seen in nucleus. For instance, in cells grown to low confluence, cell fractionation experiments revealed Amot80 and Amot130, but not AmotL1, are primarily seen in a nuclear fraction (Figure 6-3B). Amot130 appears to be almost exclusively seen in a nuclear fraction, whereas Amot80 appears almost equally in both fractions. These findings encourage Amot130 having functions in the nuclei of cells.

In order for Amot130 to have polarizing roles in control of YAP, it likely requires an upstream signal as a switch. This thesis focused on the role of Hippo signaling in the functions of the Angiomotins. It is believed that the functions of serum factors and LATS phosphorylation of Amot130 are likely switches influencing Amot130 control of YAP nuclear activity. In investigation of this, the mutant of Amot130, which cannot be phosphorylated by LATS at Ser-175 (S175A), was used to determine a possible switch in Amot130 control of YAP. Interestingly, Amot130 (S175A) presents a similar phenotype as witnessed with Amot80 expression in MCF10A acini (Ranahan et al., 2011), unlike wild-type Amot130 which was growth suppressive. Further, stable expression of Amot130 (S175A) promotes increased Amot80 protein steady state levels beyond that seen with stable expression of wild-type Amot130 (Figure 6-3C). Based upon the role of Amot80 in increasing growth in mammary epithelial cells, this may in part explain why the mutant Amot130 (S175A) is able to activate growth and *CTGF* transcription beyond that seen in control cells. It is unknown how the unphosphorylated Ser-175 Amot130 could increase

Amot80 levels; however, by doing so it would impact YAP nuclear activity. Overall, based upon this work, it is hypothesized that a majority of the inhibition of Amot130 is through its ability to be phosphorylated by LATS. Thus, a final proposed mechanism for the nuclear import of YAP in response to the serum factors in the microenvironment of the cell occurs via specific binding of YAP to the unphosphorylated Amot130 dimerized with Amot80, resulting in a nuclear import mechanism for YAP. Upon upstream phosphorylation of Amot130 at Ser-175 by LATS, this complex breaks down and Amot130 promotes the degradation or cytosolic sequestration of YAP. In support of these theories, Amot130 has recently been shown to activate YAP by bringing it into the nucleus in cells grown to low confluence (Yi et al., 2013); however, how it is triggered and the mechanism of action remains to be investigated. Importantly, the results of this study could be an important link between the cellular microenvironment and the nuclear import of YAP. Future studies will likely uncover how Amot130 and Amot80 get into the nucleus and what their precise roles are there. Further, it is likely that the nuclear control of Angiotensin II is through a switch that is regulated by Hippo signaling and the microenvironment of the cell.

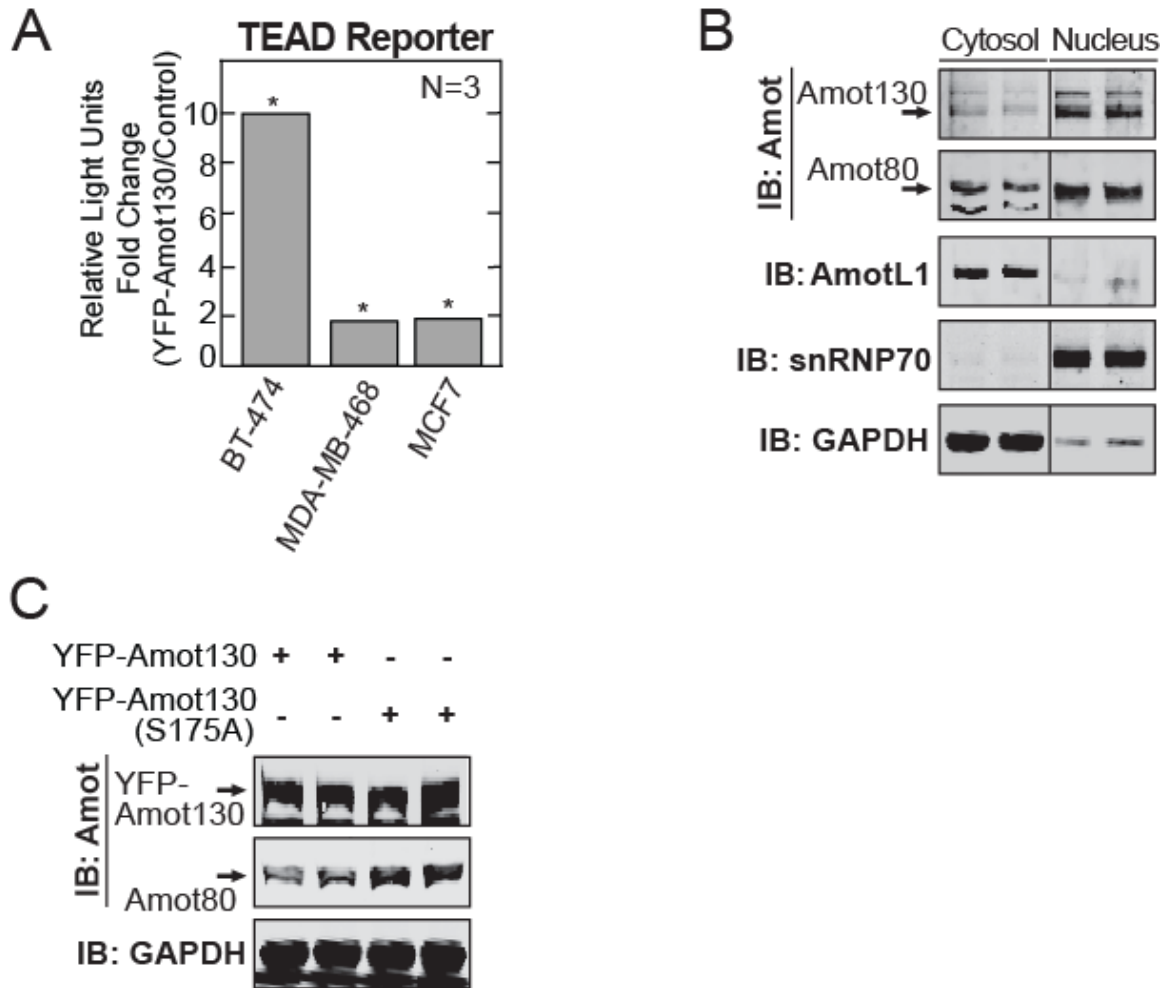


Figure 6-3 The Role of Nuclear Amot130 in YAP-Dependent Transcription.

(A) Indicated breast cancer cells were transfected with TEAD luciferase reporter constructs. Luminescence was measured using a dual-luminometer measuring TEAD luciferase activity in these cells harvested at low confluence. Relative fold changes of TEAD luciferase in YFP-tagged Amot130 expressing cells over TEAD levels in control cells are presented. (B) MDA-MB-468 cells were subjected to nuclear fractionation. Immunoblot of lysates from both fractions for two independent experiments are shown for proteins indicated. GAPDH and snRNP70 were used to determine quality of nuclear fractionation. Blots were cut from a larger experiment. (C) Immunoblot analysis of lysates from HEK 293T cells expressing YFP-tagged wild-type Amot130 or Amot130 (S175A) examining Angiomotin and GAPDH protein levels.

6.3. The Dual Role of AIP4 in Mammary Epithelial Cell Growth

Generally, the Nedd4 family ligases have diverse roles in cell signaling including the ubiquitination and regulation of proteins that control cell growth (Chen and Matesic, 2007; Rotin and Kumar, 2009). For example, AIP4 has dual roles in cell growth. Little is known regarding the means by which AIP4 is switched between the opposing roles of growth arrest and pro-growth signaling. AIP4, which localizes to the trans-Golgi network and recycling endosomes (Angers et al., 2004; Marchese and Benovic, 2001), promotes cell growth by inhibiting apoptosis through polyubiquitination and signaling the degradation of the transcription factor p73 (Rossi et al., 2005) and the pro-apoptotic factor tBid (Azakir et al., 2010). AIP4 also promotes cell proliferation more directly by similarly inducing the degradation of LATS1 (Salah et al., 2011). This degradation of LATS1 results in YAP and TAZ being less restricted from activating cellular growth. Conversely, AIP4 induces both poly- and mono-ubiquitination of Notch1 (Qiu et al., 2000) and inhibits hematopoietic stem cell proliferation by promoting its degradation (Rathinam et al., 2011). Further, this study highlights how binding of AIP4 to the adapter protein Amot130 can mediate the changeover of AIP4 from a pro-growth to an anti-growth role. Specifically, the binding of Amot130 to AIP4 prevents AIP4 association with LATS1 and increases AIP4 recruitment into a complex with YAP. The consequence is a functional reversal of AIP4, which no longer is able to degrade LATS1 and now works with Amot130 to induce inhibition of YAP nuclear activity.

The Nedd4 ligases are a family of proteins that bind diverse adapter proteins and thus likely have a diversity of functions within cells. Future studies examining the other Nedd4 ligases and their roles in growth regulation in mammary epithelial cells will likely uncover dual roles for all Nedd4 ligases and move them away from their previously assumed roles as proto-oncogenes. It is likely that there are many new substrates that the Nedd4 ligases interact with that are

involved in growth signaling, and the Angiomotins will likely play important roles in determining these new substrates.

6.4. The Multiple Mechanisms of YAP Ubiquitination

The canonical inhibition of YAP involves phosphorylation at Ser-127 by LATS1/2, which induces cytosolic sequestration via 14-3-3 and marks it for recognition and targeting for ubiquitination by the ubiquitin ligase SCF-(β)-TRCP (Zhao et al., 2010). An array of studies yields that YAP inhibition by Amot130 could be dependent or independent on the phosphorylation of YAP at Ser-127 by LATS1/2 (Chan et al., 2011; Zhao et al., 2011a). Here, this study describes a possible Ser-127 phosphorylation-independent mechanism involving the Amot130-AIP4 complex. Similar multiple ubiquitin ligases for proteins exist throughout the literature, including another transcriptional co-activator BCL10 that is targeted for ubiquitination and degradation by both AIP4 (Scharschmidt et al., 2004) and SCF-(β)-TRCP (Lobry et al., 2007), similarly to YAP. Thus, it is likely that YAP can be ubiquitinated and degraded by multiple approaches. Overall, this promotes an environment whereby the cells can inhibit its cellular growth via inhibition of YAP by multiple upstream signals. Specifically, the upstream signal of serum deprivation induces the ubiquitination of YAP, primarily upon expression of AIP4 and requiring Amot130 phosphorylation at Ser-175. Thus, this would argue that the ubiquitination, in response to serum changes, is largely through the Amot130-AIP4 complex and not via promoting degradation of YAP via SCF-(β)-TRCP. However, future studies will be needed to provide in depth analysis of the upstream signaling which differentiates which ligase, AIP4 or SCF-(β)-TRCP ubiquitinates YAP and the significance of this specificity.

6.5. Conclusion

The entirety of this work lays the foundation for understanding the roles of post-translational modifications on Amot130 in growth signaling in mammary epithelial cells. Mammary epithelial cells grow, divide, and die through physiological processes of the woman's life cycle. Understanding how cells initiate and promote cellular division versus growth inhibition during these processes is important for the overall understanding of a functioning healthy breast. Further, examination of these pathways may lead to insights in how this same regulation goes awry in breast cancers. Importantly, Amot130 appears to play a dominant role in the inhibition of YAP in response to depriving cells of serum. Further, this dominant role is under control of the tumor suppressor protein kinases, LATS1/2. While Amot130 appears to be regulated via LATS1/2, the effects on the other Angiomotins are less pronounced. Amot130 appears to be supersensitive to the effects of LATS1/2 more so than the other Angiomotin family members. Interesting the only other family member impacted by serum deprivation was Amot80, although this finding is difficult to pinpoint how this fits in with overall growth control. Regardless, Amot130, via its induced ability to bind AIP4, plays a primary role in the inhibition of YAP-dependent transcription. Future studies will likely uncover new post-translational modifications, which regulate the ability of Angiomotin to impact cellular growth control in mammary epithelial cells. Further, Angiomotin is a key determinate in the activity of YAP and is likely a transmitter of multiple microenvironmental signals. The presented alternative mechanism of YAP inhibition likely underlies a critical control pathway present in most cell types across mammals. Because of the important nature of Hippo signaling, future work will likely reveal that this alternative mechanism for YAP inhibition is an important way that cells respond to growth inhibition signals within the microenvironment.

APPENDIX – NUCLEOTIDE SEQUENCES AND CLONING STRATEGIES

qRT-PCR Primers

CTGF Forward: AGGAGTGGGTGTGTGACGA (Dupont et al., 2011)

CTGF Reverse: CCAGGCAGTTGGCTCTAATC (Dupont et al., 2011)

Cyr61 Forward: AAGGAGCTGGGATTCGATG (Wolf et al., 2010)

Cyr61 Reverse: TCTGGCCTTGTAAGGGTTG (Wolf et al., 2010)

AMOT Forward: CTCAGACTCAGGCACCAACT (RealTimePrimers.com validated)

AMOT Reverse: CTTGTCCCAGGATCTGAATG (RealTimePrimers.com validated)

GAPDH Forward: CTCCTGCACCACCAACTGCT (Dupont et al., 2011)

GAPDH Reverse: GGGCCATCCACAGTCTTCTG (Dupont et al., 2011)

shRNA Sequences

AIP4 shRNA:

CCGGCCAGAAGGTCAAGGTCAATTAAGTTCGAGTTAATTGACCTTGACTTCTCTGGTTT
TT in pLKO.1 (Sigma, TRCN000002087)

Angiotensin shRNA:

CCGGGAGGAGAATGTGATGAGACATCTCGAGATGTCTCATCACATTCTCCTCTTTTTT
G in pLKO.1 (Sigma, TRCN0000162009)

LATS1 shRNA:

CCGGCACGGCAAGATAGCATGGATTCTCGAGAATCCATGCTATCTTGCCGTGTTTTT
in pLKO.1 (Sigma, TRCN000001777)

Scramble shRNA: shControl pLKO.1 plasmid #1864 (Addgene)

Cloning Primers

Amot130 Forward: ACGTGGCGCGCCATGAGAAATTCTGAAGAACAG

Amot130 Reverse: ACGTTTAATTAATTAGATGAGATATTCCACC

Amot130 (P-Y1F) Forward: GAGGAGCTGCCCACCTTCGAGGAGGCCAAAGCCC

Amot130 (P-Y1F) Reverse: GGGCTTTGGCCTCCTCGAAGGTGGGCAGCTCCTC

Amot130 (P-Y2F) Forward: GGCCCCCAGAAATTTCCCTTCAAGGGC

Amot130 (P-Y2F) Reverse: GCCCTTGAAGGAAATTCTGGTGGGGGGCC

Amot130 (P-Y3F) Forward: CAGCATCCCCCTGAGTTTGGAGCCAGG

Amot130 (P-Y3F) Reverse: CCTGGCTGCTCCAACTCAGGGGGATGCTG

Amot80 Forward: TTCCCCAGGGGCGCGCCATGCCTCGGGCTCAGCCATC

Amot80 Reverse: CTAGGAACCTACCTGGTTAATTAATTAGATGAGATATTCCACCATC

AmotL1 Forward: TTCCCCAGGGGCGCGCCATGTGGAGGGCAAAGTTG

AmotL1 Reverse: CTAGGACTTACCTGGTTAATTAATTAGATGAGGACTTCCATCATC

AmotL2 Forward: TTCCCCAGGGGCGCGCATGAGGACACTGGAAGAC

AmotL2 Reverse: CTAGGAACTTACCTGGTTAATTAATTAGATCAGTATCTCCACCATG

AIP4 Forward: ATCGGGCGCGCCATGTCTGACAGTGGATCACAGCTTGGT

AIP4 Reverse: ATCGTTAATTAACTCTTGTCCAAATCCTTCTGTTTCTTCTAT

Nedd4-1 Forward: ATCGGGCGCGCCATGGCAACTTGC GCGGTGGAGGTGTTCCGGG

Nedd4-1 Reverse: ATCGTTAATTAATCAACTCCATCAAAGCCCTGGGTGTTTTC

WWP1 Forward: ATCGGGCGCGCCATGGCCACTGCTTCACCAAGGTCTGATACT

WWP1 Reverse: ATCGTTAATTAATTCTTGTCCAAATCCCTCTGTCTCTTCTAT

WWP2 Forward: ATCGGGCGGCCATGGCATCTGCCAGCTCTAGCCGGGCAGGA

WWP2 Reverse: ATCGTTAATTAACTCCTGTCCAAAGCCCTCGGTCTCCTCAAT

Smurf2 Forward:

ATCGGGCGCGCCATGTCTAACCCCGGAGGCCGGAGGAACGGGCCGTCAAGCTGCGC

Smurf2 Reverse: ATCGTTAATTAATTCCACAGCAAATCCACATGTTTCTTCAAT

NEDL2 Forward: ATCGGGCGCGCCATGGCTAGTTCAGCCCGGGAGCACCTGCTT

NEDL2 Reverse: ATCGTTAATTAACTCAAGTCCAAAAGTACTGGTTTCTTCAAC

NEDL1 Forward: ATCGGGCGCGCCATGGCGTCTCCTTCTAGAACTCCAGAGC

NEDL1 Reverse: ATCGTTAATTAACTCAAGTCCAAAGGTGCTGGTTTCTCTAC

YAP2 Forward: ACGTGGCGCGCCATGGATCCCGGGCAGCAGCCGCC

YAP2 Reverse: ACGTTTAATTAACTATAACCATGTAAGAAAGC

AIP4 WW1 Forward: ACGTGGCGCGCCGTA ACTCAAGCTCCCTTGCC

AIP4 WW1 Reverse: ACGTTTAATTAATCAGCCCCGTTCCAGCCAGGAGGTAG

AIP4 WW2 Forward: ACGTGGCGCGCCGATAGACCAGAACCTCTACC

AIP4 WW2 Reverse: ACGTTTAATTAATTATTCATAGTTCCGGACGGATTCC

AIP4 WW3 Forward: ACGTGGCGCGCCGATCCTCTTGGTCCATTGCC

AIP4 WW3 Reverse: ACGTTTAATTAATCACTTTTTCATTTAATTGACCTTG

AIP4 WW4 Forward: ACGTGGCGCGCCCAATTAATGAAAAGCCC

AIP4 WW4 Reverse: ACGTTTAATTAATCAGTCTAGGGCAGATTTTCTCTGTG

YAP2 WW1 Forward: ACGTTTAATTAACTACGAGTTCATCATATTCTGCTG

YAP2 WW1 Reverse: ACGTGGCGCGCCTCTTTTGAGATACCTGATGATG

YAP2 WW2 Forward: ACGTTTAATAATCAGTTCATGGCAAACGAGGGTC

YAP2 WW2 Reverse: ACGTGGCGCGCCCTGTCCCAGATGAACGTCAC

YAP2 WW1 & WW2 Forward: ACGTGGCGCGCCTCTTTTGAGATACCTGATGATG

YAP2 WW1 & WW2 Reverse: ACGTTTAATTAATCAGTTCATGGCAAACGAGGGTC

Cloning Strategies

Amot130 was cloned with primers described above and inserted into the following vectors via restriction enzyme PCR: pLP 3X Flag SD, pLP 2X Myc SD, pLP EYFP C1, and pLP monomeric Citrine YFP.

Amot130 (P-Y1F), (P-Y2F), and (P-Y3F) were all mutated via site directed mutagenesis utilizing primers from above then inserted into the following vectors via restriction enzyme PCR: pLP 3X Flag SD, pLP 2X Myc SD, pLP EYFP C1, and pLP monomeric Citrine YFP.

Amot130 (K481R) was designed by Eurofins then subcloned into Bluescript. Then this piece was inserted into the following vectors via restriction enzyme PCR: pLP EYFP C1 and pLP monomeric Citrine YFP.

Amot80 was cloned with primers described above and inserted into the following vector via restriction enzyme PCR: pLP EYFP C1.

AmotL1 was cloned with primers described above and inserted into the following vector via restriction enzyme PCR: pLP 3X Flag SD.

AmotL2 was cloned with primers described above and inserted into the following vector via restriction enzyme PCR: pLP 3X Flag SD.

AIP4, Nedd4-1, WWP1, WWP2, Smurf2, NEDL2, and NEDL1 were cloned with primers described above and inserted into the following vector via restriction enzyme PCR: pRETRO 3X Flag SD and AIP4 into pLP monomeric Cherry.

YAP2 was cloned with primers described above and inserted into the following vector via restriction enzyme PCR: pLP monomeric Cerulean CFP.

AIP4 WW1, WW2, WW3, and WW4 were cloned with primers described above and inserted into the following vector via restriction enzyme PCR: pGEX 6p-1 AscI/PacI.

YAP2 WW1 and WW2 were cloned with primers described above and inserted into the following vector via restriction enzyme PCR: pGEX 6p-1 AscI/PacI.

REFERENCES

- Aase, K., Ernkvist, M., Ebarasi, L., Jakobsson, L., Majumdar, A., Yi, C., Birot, O., Ming, Y., Kvanta, A., Edholm, D., *et al.* (2007). Angiotensin regulates endothelial cell migration during embryonic angiogenesis. *Genes Dev* 21, 2055-2068.
- Adler, J.J., Heller, B.L., Bringman, L.R., Ranahan, W.P., Cocklin, R.R., Goebel, M.G., Oh, M., Lim, H.S., Ingham, R.J., and Wells, C.D. (2013a). Amot130 adapts atrophin-1 interacting protein 4 to inhibit yes-associated protein signaling and cell growth. *J Biol Chem* 288, 15181-15193.
- Adler, J.J., Johnson, D.E., Heller, B.L., Bringman, L.R., Ranahan, W.P., Conwell, M.D., Sun, Y., Hudmon, A., and Wells, C.D. (2013b). Serum deprivation inhibits the transcriptional co-activator YAP and cell growth via phosphorylation of the 130-kDa isoform of Angiotensin by the LATS1/2 protein kinases. *Proc Natl Acad Sci U S A* 110, 17368-17373.
- Adler, J.J., Judd, M.V., Bringman, L.R., Wells, C.D., and Marrs, K.A. (2013c). Day as a Pathologist: Utilization of Technology to Guide Students in Exploring Careers in Breast Cancer Pathology. *The American Biology Teacher* 75, 559-565.
- Allen, J.J., Li, M., Brinkworth, C.S., Paulson, J.L., Wang, D., Hubner, A., Chou, W.-H., Davis, R.J., Burlingame, A.L., Messing, R.O., *et al.* (2007). A semisynthetic epitope for kinase substrates. *Nat Meth* 4, 511-516.
- Angers, A., Ramjaun, A.R., and McPherson, P.S. (2004). The HECT Domain Ligase Itch Ubiquitinates Endophilin and Localizes to the trans-Golgi Network and Endosomal System. *Journal of Biological Chemistry* 279, 11471-11479.
- Aragona, M., Panciera, T., Manfrin, A., Giullitti, S., Michielin, F., Elvassore, N., Dupont, S., and Piccolo, S. (2013). A Mechanical Checkpoint Controls Multicellular Growth through YAP/TAZ Regulation by Actin-Processing Factors. *Cell* 154, 1047-1059.
- Assémat, E., Bazellières, E., Pallezi-Pocachard, E., Le Bivic, A., and Massey-Harroche, D. (2008). Polarity complex proteins. *Biochimica et Biophysica Acta (BBA) - Biomembranes* 1778, 614-630.
- Avruch, J., Zhou, D., Fitamant, J., Bardeesy, N., Mou, F., and Barruffet, L.R. (2012). Protein kinases of the Hippo pathway: regulation and substrates. *Seminars in cell & developmental biology* 23, 770-784.
- Azakhir, B.A., Desrochers, G., and Angers, A. (2010). The ubiquitin ligase Itch mediates the antiapoptotic activity of epidermal growth factor by promoting the ubiquitylation and degradation of the truncated C-terminal portion of Bid. *FEBS Journal* 277, 1319-1330.
- Baker, D.L., Desiderio, D.M., Miller, D.D., Tolley, B., and Tigyi, G.J. (2001). Direct Quantitative Analysis of Lysophosphatidic Acid Molecular Species by Stable Isotope Dilution Electrospray Ionization Liquid Chromatography–Mass Spectrometry. *Analytical Biochemistry* 292, 287-295.
- Banks, L., Pim, D., and Thomas, M. (2012). Human tumour viruses and the deregulation of cell polarity in cancer. *Nat Rev Cancer* 12, 877-886.

- Barcellos-Hoff, M.H., Aggeler, J., Ram, T.G., and Bissell, M.J. (1989). Functional differentiation and alveolar morphogenesis of primary mammary cultures on reconstituted basement membrane. *Development* 105, 223-235.
- Bissell, M.J., Hall, H.G., and Parry, G. (1982). How does the extracellular matrix direct gene expression? *Journal of Theoretical Biology* 99, 31-68.
- Bissell, M.J., Rizki, A., and Mian, I.S. (2003). Tissue architecture: the ultimate regulator of breast epithelial function. *Current Opinion in Cell Biology* 15, 753-762.
- Bonifacino, J.S., and Traub, L.M. (2003). SIGNALS FOR SORTING OF TRANSMEMBRANE PROTEINS TO ENDOSOMES AND LYSOSOMES *. *Annual Review of Biochemistry* 72, 395-447.
- Bossuyt, W., Chen, C.L., Chen, Q., Sudol, M., McNeill, H., Pan, D., Kopp, A., and Halder, G. (2013). An evolutionary shift in the regulation of the Hippo pathway between mice and flies. *Oncogene*.
- Bratt, A., Birot, O., Sinha, I., Veitonmäki, N., Aase, K., Ernkvist, M., and Holmgren, L. (2005). Angiotensin Regulates Endothelial Cell-Cell Junctions and Cell Motility. *Journal of Biological Chemistry* 280, 34859-34869.
- Bratt, A., Wilson, W.J., Troyanovsky, B., Aase, K., Kessler, R., Meir, E.G.V., and Holmgren, L. (2002). Angiotensin belongs to a novel protein family with conserved coiled-coil and PDZ binding domains. *Gene* 298, 69-77.
- Bridges, D., and Moorhead, G.B.G. (2005). 14-3-3 Proteins: A Number of Functions for a Numbered Protein. *Sci STKE* 2005, re10-.
- Bundred, N.J., Chan, K., and Anderson, N.G. (2001). Studies of epidermal growth factor receptor inhibition in breast cancer. *Endocrine-Related Cancer* 8, 183-189.
- Cai, H., and Xu, Y. (2013). The role of LPA and YAP signaling in long-term migration of human ovarian cancer cells. *Cell Communication and Signaling* 11, 31.
- Cailleau, R., Olivé, M., and Cruciger, Q.J. (1978). Long-term human breast carcinoma cell lines of metastatic origin: Preliminary characterization. *In Vitro* 14, 911-915.
- Calvo, F., Ege, N., Grande-Garcia, A., Hooper, S., Jenkins, R.P., Chaudhry, S.I., Harrington, K., Williamson, P., Moendarbary, E., Charras, G., *et al.* (2013). Mechanotransduction and YAP-dependent matrix remodelling is required for the generation and maintenance of cancer-associated fibroblasts. *Nat Cell Biol* 15, 637-646.
- Castor, L.N. (1972). CONTACT INHIBITIONS OF CELL DIVISION AND CELL MOVEMENT. *J Invest Dermatol* 59, 27-32.
- Chan, E.H.Y., Nousiainen, M., Chalamalasetty, R.B., Schafer, A., Nigg, E.A., and Sillje, H.H.W. (2005). The Ste20-like kinase Mst2 activates the human large tumor suppressor kinase Lats1. *24*, 2076-2086.

- Chan, K.C., Knox, W.F., Gandhi, A., Slamon, D.J., Potten, C.S., and Bundred, N.J. (2001). Blockade of growth factor receptors in ductal carcinoma in situ inhibits epithelial proliferation. *British Journal of Surgery* 88, 412-418.
- Chan, S.W., Lim, C.J., Chong, Y.F., Pobbati, A.V., Huang, C., and Hong, W. (2011). Hippo Pathway-independent Restriction of TAZ and YAP by Angiomotin. *J Biol Chem* 286, 7018-7026.
- Chen, C.-C., and Lau, L.F. (2009). Functions and mechanisms of action of CCN matricellular proteins. *The International Journal of Biochemistry & Cell Biology* 41, 771-783.
- Chen, C., and Matesic, L. (2007). The Nedd4-like family of E3 ubiquitin ligases and cancer. *Cancer and Metastasis Reviews* 26, 587-604.
- Chen, C., Zhou, Z., Sheehan, C.E., Slodkowska, E., Sheehan, C.B., Boguniewicz, A., and Ross, J.S. (2009). Overexpression of WWP1 is associated with the estrogen receptor and insulin-like growth factor receptor 1 in breast carcinoma. *International Journal of Cancer* 124, 2829-2836.
- Chen, H.I., and Sudol, M. (1995). The WW domain of Yes-associated protein binds a proline-rich ligand that differs from the consensus established for Src homology 3-binding modules. *Proceedings of the National Academy of Sciences* 92, 7819-7823.
- Chiyoda, T., Sugiyama, N., Shimizu, T., Naoe, H., Kobayashi, Y., Ishizawa, J., Arima, Y., Tsuda, H., Ito, M., Kaibuchi, K., *et al.* (2012). LATS1/WARTS phosphorylates MYPT1 to counteract PLK1 and regulate mammalian mitotic progression. *The Journal of Cell Biology* 197, 625-641.
- Colwill, K., Wells, C., Elder, K., Goudreault, M., Hersi, K., Kulkarni, S., Hardy, W.R., Pawson, T., and Morin, G. (2006). Modification of the Creator recombination system for proteomics applications - improved expression by addition of splice sites. *BMC Biotechnology* 6, 13.
- Cordenonsi, M., Zanconato, F., Azzolin, L., Forcato, M., Rosato, A., Frasson, C., Inui, M., Montagner, M., Parenti, Anna R., Poletti, A., *et al.* (2011). The Hippo Transducer TAZ Confers Cancer Stem Cell-Related Traits on Breast Cancer Cells. *Cell* 147, 759-772.
- de Waard, F. (1969). The epidemiology of breast cancer; Review and prospects. *International Journal of Cancer* 4, 577-586.
- Debnath, J., and Brugge, J.S. (2005). Modelling glandular epithelial cancers in three-dimensional cultures. *Nat Rev Cancer* 5, 675-688.
- Debnath, J., Muthuswamy, S.K., and Brugge, J.S. (2003). Morphogenesis and oncogenesis of MCF-10A mammary epithelial acini grown in three-dimensional basement membrane cultures. *Methods* 30, 256-268.
- Dong, J., Feldmann, G., Huang, J., Wu, S., Zhang, N., Comerford, S.A., Gayyed, Mariana F., Anders, R.A., Maitra, A., and Pan, D. (2007). Elucidation of a Universal Size-Control Mechanism in *Drosophila* and Mammals. *Cell* 130, 1120-1133.
- Du, J., Sun, C., Hu, Z., Yang, Y., Zhu, Y., Zheng, D., Gu, L., and Lu, X. (2010). Lysophosphatidic Acid Induces MDA-MB-231 Breast Cancer Cells Migration through Activation of PI3K/PAK1/ERK Signaling. *PLoS ONE* 5, e15940.

- DuBridge, R.B., Tang, P., Hsia, H.C., Leong, P.M., Miller, J.H., and Calos, M.P. (1987). Analysis of mutation in human cells by using an Epstein-Barr virus shuttle system. *Molecular and Cellular Biology* 7, 379-387.
- Dupont, S., Morsut, L., Aragona, M., Enzo, E., Giulitti, S., Cordenonsi, M., Zanconato, F., Le Digabel, J., Forcato, M., Bicciato, S., *et al.* (2011). Role of YAP/TAZ in mechanotransduction. *Nature* 474, 179-183.
- Endicott, J.A., Noble, M.E.M., and Johnson, L.N. (2012). The Structural Basis for Control of Eukaryotic Protein Kinases. *Annual Review of Biochemistry* 81, 587-613.
- Erbas, B., Provenzano, E., Armes, J., and Gertig, D. (2006). The natural history of ductal carcinoma in situ of the breast: a review. *Breast Cancer Res Treat* 97, 135-144.
- Ernkvist, M., Aase, K., Ukomadu, C., Wohlschlegel, J., Blackman, R., Veitonmäki, N., Bratt, A., Dutta, A., and Holmgren, L. (2006). p130-Angiomotin associates to actin and controls endothelial cell shape. *FEBS Journal* 273, 2000-2011.
- Ernkvist, M., Birot, O., Sinha, I., Veitonmaki, N., Nyström, S., Aase, K., and Holmgren, L. (2008). Differential roles of p80- and p130-angiomotin in the switch between migration and stabilization of endothelial cells. *Biochimica et Biophysica Acta (BBA) - Molecular Cell Research* 1783, 429-437.
- Fan, R., Kim, N.-G., and Gumbiner, B.M. (2013). Regulation of Hippo pathway by mitogenic growth factors via phosphoinositide 3-kinase and phosphoinositide-dependent kinase-1. *Proceedings of the National Academy of Sciences* 110, 2569-2574.
- Ferlay, J., Autier, P., Boniol, M., Heanue, M., Colombet, M., and Boyle, P. (2007). Estimates of the cancer incidence and mortality in Europe in 2006. *Annals of Oncology* 18, 581-592.
- Ferlay, J., Shin, H.-R., Bray, F., Forman, D., Mathers, C., and Parkin, D.M. (2010). Estimates of worldwide burden of cancer in 2008: GLOBOCAN 2008. *International Journal of Cancer* 127, 2893-2917.
- Gagné, V., Moreau, J., Plourde, M., Lapointe, M., Lord, M., Gagnon, É., and Fernandes, M.J.G. (2009). Human angiomotin-like 1 associates with an angiomotin protein complex through its coiled-coil domain and induces the remodeling of the actin cytoskeleton. *Cell Motility and the Cytoskeleton* 66, 754-768.
- Genevet, A., and Tapon, N. (2011). The Hippo pathway and apico-basal cell polarity. *Biochemical Journal* 436, 213-224.
- Glickman, M.H., and Ciechanover, A. (2002). The Ubiquitin-Proteasome Proteolytic Pathway: Destruction for the Sake of Construction. *Physiological Reviews* 82, 373-428.
- Going, J.J., and Moffat, D.F. (2004). Escaping from Flatland: clinical and biological aspects of human mammary duct anatomy in three dimensions. *The Journal of Pathology* 203, 538-544.
- Graham, F.L., Smiley, J., Russell, W.C., and Nairn, R. (1977). Characteristics of a Human Cell Line Transformed by DNA from Human Adenovirus Type 5. *Journal of General Virology* 36, 59-72.

- Guo, C., Tang, T.-S., Bienko, M., Parker, J.L., Bielen, A.B., Sonoda, E., Takeda, S., Ulrich, H.D., Dikic, I., and Friedberg, E.C. (2006). Ubiquitin-Binding Motifs in REV1 Protein Are Required for Its Role in the Tolerance of DNA Damage. *Mol Cell Biol* 26, 8892-8900.
- Hao, Y., Chun, A., Cheung, K., Rashidi, B., and Yang, X. (2008). Tumor Suppressor LATS1 Is a Negative Regulator of Oncogene YAP. *Journal of Biological Chemistry* 283, 5496-5509.
- Hartmann, P.E. (2007). The Lactating Breast: An Overview from Down Under Breastfeeding Medicine 2, 3-9.
- Harvey, K.F., Pflieger, C.M., and Hariharan, I.K. (2003). The Drosophila Mst Ortholog, hippo, Restricts Growth and Cell Proliferation and Promotes Apoptosis. *Cell* 114, 457-467.
- Harvey, K.F., Zhang, X., and Thomas, D.M. (2013). The Hippo pathway and human cancer. *Nat Rev Cancer* 13, 246-257.
- Hassiotou, F., and Geddes, D. (2013). Anatomy of the human mammary gland: Current status of knowledge. *Clinical Anatomy* 26, 29-48.
- Heller, B., Adu-Gyamfi, E., Smith-Kinnaman, W., Babbey, C., Vora, M., Xue, Y., Bittman, R., Stahelin, R.V., and Wells, C.D. (2010). Amot recognizes a juxtannuclear endocytic recycling compartment via a novel lipid binding domain. *J Biol Chem* 285, 12308-12320.
- Hicke, L. (2001). A New Ticket for Entry into Budding Vesicles—Ubiquitin. *Cell* 106, 527-530.
- Hicke, L., and Riezman, H. (1996). Ubiquitination of a Yeast Plasma Membrane Receptor Signals Its Ligand-Stimulated Endocytosis. *Cell* 84, 277-287.
- Ho, K.C., Zhou, Z., She, Y.-M., Chun, A., Cyr, T.D., and Yang, X. (2011). Itch E3 ubiquitin ligase regulates large tumor suppressor 1 stability. *Proceedings of the National Academy of Sciences* 108, 4870-4875.
- Hodge, D.R., Hurt, E.M., and Farrar, W.L. (2005). The role of IL-6 and STAT3 in inflammation and cancer. *European Journal of Cancer* 41, 2502-2512.
- Hooper, C., Puttamadappa, S., Loring, Z., Shekhtman, A., and Bakowska, J. (2010). Spartin activates atrophin-1-interacting protein 4 (AIP4) E3 ubiquitin ligase and promotes ubiquitination of adipophilin on lipid droplets. *BMC Biology* 8, 72.
- Hoshijima, M., Hattori, T., Inoue, M., Araki, D., Hanagata, H., Miyauchi, A., and Takigawa, M. (2006). CT domain of CCN2/CTGF directly interacts with fibronectin and enhances cell adhesion of chondrocytes through integrin $\alpha 5 \beta 1$. *FEBS Letters* 580, 1376-1382.
- Hu, M., Yao, J., Carroll, D.K., Weremowicz, S., Chen, H., Carrasco, D., Richardson, A., Violette, S., Nikolskaya, T., Nikolsky, Y., *et al.* (2008). Regulation of In Situ to Invasive Breast Carcinoma Transition. *Cancer cell* 13, 394-406.
- Huang, J., Wu, S., Barrera, J., Matthews, K., and Pan, D. (2005). The Hippo Signaling Pathway Coordinately Regulates Cell Proliferation and Apoptosis by Inactivating Yorkie, the Drosophila Homolog of YAP. *Cell* 122, 421-434.

- Huibregtse, J.M., Scheffner, M., and Howley, P.M. (1993a). Cloning and expression of the cDNA for E6-AP, a protein that mediates the interaction of the human papillomavirus E6 oncoprotein with p53. *Molecular and Cellular Biology* 13, 775-784.
- Huibregtse, J.M., Scheffner, M., and Howley, P.M. (1993b). Localization of the E6-AP regions that direct human papillomavirus E6 binding, association with p53, and ubiquitination of associated proteins. *Molecular and Cellular Biology* 13, 4918-4927.
- Hussein, M.R., and Hassan, H.I. (2006). Analysis of the mononuclear inflammatory cell infiltrate in the normal breast, benign proliferative breast disease, in situ and infiltrating ductal breast carcinomas: preliminary observations. *Journal of Clinical Pathology* 59, 972-977.
- Hustad, C.M., Perry, W.L., Siracusa, L.D., Rasberry, C., Cobb, L., Cattanaach, B.M., Kovatch, R., Copeland, N.G., and Jenkins, N.A. (1995). Molecular genetic characterization of six recessive viable alleles of the mouse agouti locus. *Genetics* 140, 255-265.
- Ingham, R.J., Colwill, K., Howard, C., Dettwiler, S., Lim, C.S.H., Yu, J., Hersi, K., Raaijmakers, J., Gish, G., Mbamalu, G., *et al.* (2005). WW Domains Provide a Platform for the Assembly of Multiprotein Networks. *Mol Cell Biol* 25, 7092-7106.
- Ingham, R.J., Gish, G., and Pawson, T. (2004). The Nedd4 family of E3 ubiquitin ligases: functional diversity within a common modular architecture. *Oncogene* 23, 1972-1984.
- Ishii, I., Fukushima, N., Ye, X., and Chun, J. (2004). LYSOPHOSPHOLIPID RECEPTORS: Signaling and Biology. *Annual Review of Biochemistry* 73, 321-354.
- Jia, J., Zhang, W., Wang, B., Trinko, R., and Jiang, J. (2003). The Drosophila Ste20 family kinase dMST functions as a tumor suppressor by restricting cell proliferation and promoting apoptosis. *Genes Dev* 17, 2514-2519.
- Jiang, W., Watkins, G., Douglas-Jones, A., Holmgren, L., and Mansel, R. (2006). Angiomotin and angiomotin like proteins, their expression and correlation with angiogenesis and clinical outcome in human breast cancer. *BMC Cancer* 6, 16.
- Jin, J., Smith, F.D., Stark, C., Wells, C.D., Fawcett, J.P., Kulkarni, S., Metalnikov, P., O'Donnell, P., Taylor, P., Taylor, L., *et al.* (2004). Proteomic, Functional, and Domain-Based Analysis of In Vivo 14-3-3 Binding Proteins Involved in Cytoskeletal Regulation and Cellular Organization. *Current Biology* 14, 1436-1450.
- Justice, R.W., Zilian, O., Woods, D.F., Noll, M., and Bryant, P.J. (1995). The Drosophila tumor suppressor gene warts encodes a homolog of human myotonic dystrophy kinase and is required for the control of cell shape and proliferation. *Genes Dev* 9, 534-546.
- Kanai, F., Marignani, P.A., Sarbassova, D., Yagi, R., Hall, R.A., Donowitz, M., Hisaminato, A., Fujiwara, T., Ito, Y., Cantley, L.C., *et al.* (2000). TAZ: a novel transcriptional co-activator regulated by interactions with 14-3-3 and PDZ domain proteins. *EMBO J* 19, 6778-6791.
- Kang, Y., Siegel, P.M., Shu, W., Drobnjak, M., Kakonen, S.M., Cordon-Cardo, C., Guise, T.A., and Massagué, J. (2003). A multigenic program mediating breast cancer metastasis to bone. *Cancer Cell* 3, 537-549.

- Kango-Singh, M., and Singh, A. (2009). Regulation of organ size: Insights from the Drosophila Hippo signaling pathway. *Developmental Dynamics* 238, 1627-1637.
- Kao, J., Salari, K., Bocanegra, M., Choi, Y.-L., Girard, L., Gandhi, J., Kwei, K.A., Hernandez-Boussard, T., Wang, P., Gazdar, A.F., *et al.* (2009). Molecular Profiling of Breast Cancer Cell Lines Defines Relevant Tumor Models and Provides a Resource for Cancer Gene Discovery. *PLoS ONE* 4, e6146.
- Kenny, P.A., Lee, G.Y., Myers, C.A., Neve, R.M., Semeiks, J.R., Spellman, P.T., Lorenz, K., Lee, E.H., Barcellos-Hoff, M.H., Petersen, O.W., *et al.* (2007). The morphologies of breast cancer cell lines in three-dimensional assays correlate with their profiles of gene expression. *Molecular Oncology* 1, 84-96.
- Key, T.J., Verkasalo, P.K., and Banks, E. (2001). Epidemiology of breast cancer. *The Lancet Oncology* 2, 133-140.
- Khammanit, R., Chantakru, S., Kitiyanant, Y., and Saikhun, J. (2008). Effect of serum starvation and chemical inhibitors on cell cycle synchronization of canine dermal fibroblasts. *Theriogenology* 70, 27-34.
- Khokha, R., and Werb, Z. (2011). Mammary Gland Reprogramming: Metalloproteinases Couple Form with Function. *Cold Spring Harbor Perspectives in Biology* 3.
- Knopf, J.L., Lee, M.-H., Sultzman, L.A., Kriz, R.W., Loomis, C.R., Hewick, R.M., and Bell, R.M. (1986). Cloning and expression of multiple protein kinase C cDNAs. *Cell* 46, 491-502.
- Lai, D., Ho, K.C., Hao, Y., and Yang, X. (2011). Taxol Resistance in Breast Cancer Cells Is Mediated by the Hippo Pathway Component TAZ and Its Downstream Transcriptional Targets Cyr61 and CTGF. *Cancer Research* 71, 2728-2738.
- Lai, Z.-C., Wei, X., Shimizu, T., Ramos, E., Rohrbaugh, M., Nikolaidis, N., Ho, L.-L., and Li, Y. (2005). Control of Cell Proliferation and Apoptosis by Mob as Tumor Suppressor, Mats. *Cell* 120, 675-685.
- Lamb, R.A., Mahy, B.W.J., and Choppin, P.W. (1976). The synthesis of Sendai virus polypeptides in infected cells. *Virology* 69, 116-131.
- Lasfargues, E.Y., Coutinho, W.G., and Redfield, E.S. (1978). Isolation of Two Human Tumor Epithelial Cell Lines From Solid Breast Carcinomas. *Journal of the National Cancer Institute* 61, 967-978.
- Lei, Q.-Y., Zhang, H., Zhao, B., Zha, Z.-Y., Bai, F., Pei, X.-H., Zhao, S., Xiong, Y., and Guan, K.-L. (2008). TAZ Promotes Cell Proliferation and Epithelial-Mesenchymal Transition and Is Inhibited by the Hippo Pathway. *Molecular and Cellular Biology* 28, 2426-2436.
- Leung, C.Y., and Zernicka-Goetz, M. (2013). Angiomotin prevents pluripotent lineage differentiation in mouse embryos via Hippo pathway-dependent and -independent mechanisms. *Nat Commun* 4.

- Levin, V.A., Panchabhai, S.C., Shen, L., Kornblau, S.M., Qiu, Y., and Baggerly, K.A. (2009). Different Changes in Protein and Phosphoprotein Levels Result from Serum Starvation of High-Grade Glioma and Adenocarcinoma Cell Lines. *Journal of Proteome Research* 9, 179-191.
- Li, Y., Pei, J., Xia, H., Ke, H., Wang, H., and Tao, W. (2003). Lats2, a putative tumor suppressor, inhibits G1/S transition. *Oncogene* 22, 4398-4405.
- Li, Z., Zhao, B., Wang, P., Chen, F., Dong, Z., Yang, H., Guan, K.-L., and Xu, Y. (2010). Structural insights into the YAP and TEAD complex. *Genes Dev* 24, 235-240.
- Lieblein, J., Ball, S., Hutzen, B., Sasser, A.K., Lin, H.-J., Huang, T., Hall, B., and Lin, J. (2008). STAT3 can be activated through paracrine signaling in breast epithelial cells. *BMC Cancer* 8, 302.
- Lim, K.L., Chew, K.C.M., Tan, J.M.M., Wang, C., Chung, K.K.K., Zhang, Y., Tanaka, Y., Smith, W., Engelender, S., Ross, C.A., *et al.* (2005). Parkin Mediates Nonclassical, Proteasomal-Independent Ubiquitination of Synphilin-1: Implications for Lewy Body Formation. *The Journal of Neuroscience* 25, 2002-2009.
- Lin, M.-T., Chang, C.-C., Chen, S.-T., Chang, H.-L., Su, J.-L., Chau, Y.-P., and Kuo, M.-L. (2004). Cyr61 Expression Confers Resistance to Apoptosis in Breast Cancer MCF-7 Cells by a Mechanism of NF- κ B-dependent XIAP Up-Regulation. *Journal of Biological Chemistry* 279, 24015-24023.
- Liu, C.-Y., Zha, Z.-Y., Zhou, X., Zhang, H., Huang, W., Zhao, D., Li, T., Chan, S.W., Lim, C.J., Hong, W., *et al.* (2010). The Hippo Tumor Pathway Promotes TAZ Degradation by Phosphorylating a Phosphodegron and Recruiting the SCF β -TrCP E3 Ligase. *Journal of Biological Chemistry* 285, 37159-37169.
- Lo, D., Dai, M.-S., Sun, X.-X., Zeng, S.X., and Lu, H. (2012). Ubiquitin- and MDM2 E3 Ligase-independent Proteasomal Turnover of Nucleostemin in Response to GTP Depletion. *Journal of Biological Chemistry* 287, 10013-10020.
- Lobry, C., Lopez, T., Israel, A., and Weil, R. (2007). Negative feedback loop in T cell activation through I(κ)B kinase-induced phosphorylation and degradation of Bcl10. *Proceedings of the National Academy of Sciences* 104, 908-913.
- Macias, M.J., Wiesner, S., and Sudol, M. (2002). WW and SH3 domains, two different scaffolds to recognize proline-rich ligands. *FEBS Letters* 513, 30-37.
- Marchese, A., and Benovic, J.L. (2001). Agonist-promoted Ubiquitination of the G Protein-coupled Receptor CXCR4 Mediates Lysosomal Sorting. *Journal of Biological Chemistry* 276, 45509-45512.
- Martin-Serrano, J., Eastman, S.W., Chung, W., and Bieniasz, P.D. (2005). HECT ubiquitin ligases link viral and cellular PPXY motifs to the vacuolar protein-sorting pathway. *The Journal of Cell Biology* 168, 89-101.
- Matakatsu, H., and Blair, S.S. (2004). Interactions between Fat and Dachshous and the regulation of planar cell polarity in the Drosophila wing. *Development* 131, 3785-3794.

- Miller, E., Yang, J., DeRan, M., Wu, C., Su, A.I., Bonamy, G.M., Liu, J., Peters, E.C., and Wu, X. (2012). Identification of serum-derived sphingosine-1-phosphate as a small molecule regulator of YAP. *Chem Biol* *19*, 955-962.
- Mohankumar, K.M., Perry, J.K., Kannan, N., Kohno, K., Gluckman, P.D., Emerald, B.S., and Lobie, P.E. (2008). Transcriptional Activation of Signal Transducer and Activator of Transcription (STAT) 3 and STAT5B Partially Mediate Homeobox A1-Stimulated Oncogenic Transformation of the Immortalized Human Mammary Epithelial Cell. *Endocrinology* *149*, 2219-2229.
- Moolenaar, W.H. (2000). Development of Our Current Understanding of Bioactive Lysophospholipids. *Annals of the New York Academy of Sciences* *905*, 1-10.
- Moore, P.S., and Chang, Y. (2010). Why do viruses cause cancer? Highlights of the first century of human tumour virology. *Nat Rev Cancer* *10*, 878-889.
- Moreau, J., Lord, M., Boucher, M., Belleau, P., and Fernandes, M.J.G. (2005). Protein diversity is generated within the motin family of proteins by alternative pre-mRNA splicing. *Gene* *350*, 137-148.
- Mund, T., and Pelham, H.R.B. (2009). Control of the activity of WW-HECT domain E3 ubiquitin ligases by NDFIP proteins. *EMBO Rep* *10*, 501-507.
- Muslin, A.J., Tanner, J.W., Allen, P.M., and Shaw, A.S. (1996). Interaction of 14-3-3 with Signaling Proteins Is Mediated by the Recognition of Phosphoserine. *Cell* *84*, 889-897.
- Muthuswamy, S.K., Li, D., Lelievre, S., Bissell, M.J., and Brugge, J.S. (2001). ErbB2, but not ErbB1, reinitiates proliferation and induces luminal repopulation in epithelial acini. *Nat Cell Biol* *3*, 785-792.
- Muthuswamy, S.K., Siegel, P.M., Dankort, D.L., Webster, M.A., and Muller, W.J. (1994). Mammary tumors expressing the neu proto-oncogene possess elevated c-Src tyrosine kinase activity. *Molecular and Cellular Biology* *14*, 735-743.
- Nalefski, E.A., and Falke, J.J. (1996). The C2 domain calcium-binding motif: Structural and functional diversity. *Protein Science* *5*, 2375-2390.
- Neve, R.M., Chin, K., Fridlyand, J., Yeh, J., Baehner, F.L., Fevr, T., Clark, L., Bayani, N., Coppe, J.-P., Tong, F., *et al.* (2006). A collection of breast cancer cell lines for the study of functionally distinct cancer subtypes. *Cancer Cell* *10*, 515-527.
- Neville MC, M.T., Forsyth I. (2002). Hormonal regulation of mammary differentiation and milk secretion. *J Mammary Gland Biol Neoplasia* *7*, 49-66.
- Nguyen, H.B., Babcock, J.T., Wells, C.D., and Quilliam, L.A. (2012). LKB1 tumor suppressor regulates AMP kinase/mTOR-independent cell growth and proliferation via the phosphorylation of Yap. *Oncogene*.
- O'Shea, J.J., and Murray, P.J. (2008). Cytokine Signaling Modules in Inflammatory Responses. *Immunity* *28*, 477-487.

- Oka, T., Mazack, V., and Sudol, M. (2008). Mst2 and Lats Kinases Regulate Apoptotic Function of Yes Kinase-associated Protein (YAP). *Journal of Biological Chemistry* 283, 27534-27546.
- Oka, T., Remue, E., Meerschaert, K., Vanloo, B., Boucherie, C., Gfeller, D., Bader, G.D., Sidhu, S.S., Vandekerckhove, J., Gettemans, J., *et al.* (2010). Functional complexes between YAP2 and ZO-2 are PDZ domain-dependent, and regulate YAP2 nuclear localization and signalling1. *Biochemical Journal* 432, 461-472.
- Oka, T., Schmitt, A.P., and Sudol, M. (2012). Opposing roles of angiomin-1 and zona occludens-2 on pro-apoptotic function of YAP. *Oncogene* 31, 128-134.
- Ota, M., and Sasaki, H. (2008). Mammalian Tead proteins regulate cell proliferation and contact inhibition as transcriptional mediators of Hippo signaling. *Development* 135, 4059-4069.
- Overholtzer, M., Zhang, J., Smolen, G.A., Muir, B., Li, W., Sgroi, D.C., Deng, C.-X., Brugge, J.S., and Haber, D.A. (2006). Transforming properties of YAP, a candidate oncogene on the chromosome 11q22 amplicon. *Proceedings of the National Academy of Sciences* 103, 12405-12410.
- Pan, D. (2007). Hippo signaling in organ size control. *Genes Dev* 21, 886-897.
- Pang, W., and Hartmann, P. (2007). Initiation of Human Lactation: Secretory Differentiation and Secretory Activation. *J Mammary Gland Biol Neoplasia* 12, 211-221.
- Pantalacci, S., Tapon, N., and Leopold, P. (2003). The Salvador partner Hippo promotes apoptosis and cell-cycle exit in *Drosophila*. *Nat Cell Biol* 5, 921-927.
- Paramasivam, M., Sarkeshik, A., Yates, J.R., Fernandes, M.J.G., and McCollum, D. (2011). Angiomin family proteins are novel activators of the LATS2 kinase tumor suppressor. *Mol Biol Cell* 22, 3725-3733.
- Pardee, A.B. (1974). A Restriction Point for Control of Normal Animal Cell Proliferation. *Proceedings of the National Academy of Sciences* 71, 1286-1290.
- Patrie, K.M. (2005). Identification and characterization of a novel tight junction-associated family of proteins that interacts with a WW domain of MAGI-1. *Biochimica et Biophysica Acta (BBA) - Molecular Cell Research* 1745, 131-144.
- Pei, Z., Bai, Y., and Schmitt, A.P. (2010). PIV5 M protein interaction with host protein angiomin-like 1. *Virology* 397, 155-166.
- Perry, W.L., Hustad, C.M., Swing, D.A., O'Sullivan, T.N., Jenkins, N.A., and Copeland, N.G. (1998). The itchy locus encodes a novel ubiquitin protein ligase that is disrupted in a18H mice. *Nat Genet* 18, 143-146.
- Pervin, S., Tran, A., Tran, L., Urman, R., Braga, M., Chaudhuri, G., and Singh, R. (2011). Reduced association of anti-apoptotic protein Mcl-1 with E3 ligase Mule increases the stability of Mcl-1 in breast cancer cells. *Br J Cancer* 105, 428-437.
- Petersen, O.W., Ronnov-Jessen, L., Howlett, A.R., and Bissell, M.J. (1992). Interaction with Basement Membrane Serves to Rapidly Distinguish Growth and Differentiation Pattern of

Normal and Malignant Human Breast Epithelial Cells. *Proceedings of the National Academy of Sciences* 89, 9064-9068.

Pickart, C.M. (2001). MECHANISMS UNDERLYING UBIQUITINATION. *Annual Review of Biochemistry* 70, 503-533.

Plant, P.J., Yeager, H., Staub, O., Howard, P., and Rotin, D. (1997). The C2 Domain of the Ubiquitin Protein Ligase Nedd4 Mediates Ca²⁺-dependent Plasma Membrane Localization. *Journal of Biological Chemistry* 272, 32329-32336.

Qiu, L., Joazeiro, C., Fang, N., Wang, H.-Y., Elly, C., Altman, Y., Fang, D., Hunter, T., and Liu, Y.-C. (2000). Recognition and Ubiquitination of Notch by Itch, a Hect-type E3 Ubiquitin Ligase. *Journal of Biological Chemistry* 275, 35734-35737.

Ranahan, W.P., Han, Z., Smith-Kinnaman, W., Nabinger, S.C., Heller, B., Herbert, B.-S., Chan, R., and Wells, C.D. (2011). The Adaptor Protein AMOT Promotes the Proliferation of Mammary Epithelial Cells via the Prolonged Activation of the Extracellular Signal-Regulated Kinases. *Cancer Research* 71, 2203-2211.

Rasband, W.S. (2011). ImageJ (U.S. National Institutes of Health, Bethesda, Maryland, USA).

Rathinam, C., Matesic, L.E., and Flavell, R.A. (2011). The E3 ligase Itch is a negative regulator of the homeostasis and function of hematopoietic stem cells. *Nat Immunol* 12, 399-407.

Rauch, S., and Martin-Serrano, J. (2011). Multiple Interactions between the ESCRT Machinery and Arrestin-Related Proteins: Implications for PPXY-Dependent Budding. *Journal of Virology* 85, 3546-3556.

Rossi, M., De Laurenzi, V., Munarriz, E., Green, D.R., Liu, Y.-C., Vousden, K.H., Cesareni, G., and Melino, G. (2005). The ubiquitin-protein ligase Itch regulates p73 stability. *EMBO J* 24, 836-848.

Roth, A.F., and Davis, N.G. (1996). Ubiquitination of the yeast a-factor receptor. *The Journal of Cell Biology* 134, 661-674.

Rotin, D., and Kumar, S. (2009). Physiological functions of the HECT family of ubiquitin ligases. *Nat Rev Mol Cell Biol* 10, 398-409.

Rotin, D., Staub, O., and Haguenauer-Tsapis, R. (2000). Ubiquitination and Endocytosis of Plasma Membrane Proteins: Role of Nedd4/Rsp5p Family of Ubiquitin-Protein Ligases. *J Membrane Biol* 176, 1-17.

Roudier, E., Chapados, N., Decary, S., Gineste, C., Le Bel, C., Lavoie, J.-M., Bergeron, R., and Birot, O. (2009). Angiotensin p80/p130 ratio: a new indicator of exercise-induced angiogenic activity in skeletal muscles from obese and non-obese rats? *The Journal of Physiology* 587, 4105-4119.

Russo J, R.I. (1992). The pathology of breast cancer: staging and prognostic indicators. *J Am Med Womens Assoc* 47, 181-187.

Russo, J., and Russo, I.H. (2004). Development of the human breast. *Maturitas* 49, 2-15.

Rutherford, R.B., and Ross, R. (1976). Platelet factors stimulate fibroblasts and smooth muscle cells quiescent in plasma serum to proliferate. *The Journal of Cell Biology* 69, 196-203.

Salah, Z., Melino, G., and Aqeilan, R.I. (2011). Negative Regulation of the Hippo Pathway by E3 Ubiquitin Ligase ITCH Is Sufficient to Promote Tumorigenicity. *Cancer Research* 71, 2010-2020.

Sano, T., Baker, D., Virag, T., Wada, A., Yatomi, Y., Kobayashi, T., Igarashi, Y., and Tigyi, G. (2002). Multiple Mechanisms Linked to Platelet Activation Result in Lysophosphatidic Acid and Sphingosine 1-Phosphate Generation in Blood. *Journal of Biological Chemistry* 277, 21197-21206.

Sansores-Garcia, L., Bossuyt, W., Wada, K., Yonemura, S., Tao, C., Sasaki, H., and Halder, G. (2011). Modulating F-actin organization induces organ growth by affecting the Hippo pathway. *EMBO J* 30, 2325-2335.

Scharschmidt, E., Wegener, E., Heissmeyer, V., Rao, A., and Krappmann, D. (2004). Degradation of Bcl10 Induced by T-Cell Activation Negatively Regulates NF- κ B Signaling. *Mol Cell Biol* 24, 3860-3873.

Scheffner, M., Nuber, U., and Huibregtse, J.M. (1995). Protein ubiquitination involving an E1-E2-E3 enzyme ubiquitin thioester cascade. *Nature* 373, 81-83.

Schlegelmilch, K., Mohseni, M., Kirak, O., Pruszk, J., Rodriguez, J.R., Zhou, D., Kreger, Bridget T., Vasioukhin, V., Avruch, J., Brummelkamp, Thijn R., *et al.* (2011). Yap1 Acts Downstream of α -Catenin to Control Epidermal Proliferation. *Cell* 144, 782-795.

Scialpi, F., Malatesta, M., Peschiaroli, A., Rossi, M., Melino, G., and Bernassola, F. (2008). Itch self-polyubiquitylation occurs through lysine-63 linkages. *Biochemical Pharmacology* 76, 1515-1521.

Silvis, M.R., Kreger, B.T., Lien, W.-H., Klezovitch, O., Rudakova, G.M., Camargo, F.D., Lantz, D.M., Seykora, J.T., and Vasioukhin, V. (2011). α -Catenin Is a Tumor Suppressor That Controls Cell Accumulation by Regulating the Localization and Activity of the Transcriptional Coactivator Yap1. *Sci Signal* 4, ra33-.

Skouloudaki, K., and Walz, G. (2012). YAP1 recruits c-Abl to protect angiotensin-like 1 from Nedd4-mediated degradation. *PLoS ONE* 7, e35735.

Soetens, O., De Craene, J.-O., and André, B. (2001). Ubiquitin Is Required for Sorting to the Vacuole of the Yeast General Amino Acid Permease, Gap1. *Journal of Biological Chemistry* 276, 43949-43957.

Soule, H.D., Maloney, T.M., Wolman, S.R., Peterson, W.D., Brenz, R., McGrath, C.M., Russo, J., Pauley, R.J., Jones, R.F., and Brooks, S.C. (1990). Isolation and Characterization of a Spontaneously Immortalized Human Breast Epithelial Cell Line, MCF-10. *Cancer Research* 50, 6075-6086.

Soule, H.D., Vazquez, J., Long, A., Albert, S., and Brennan, M. (1973). A Human Cell Line From a Pleural Effusion Derived From a Breast Carcinoma. *Journal of the National Cancer Institute* 51, 1409-1416.

- St John, M.A. (1999). Mice deficient of Lats1 develop soft-tissue sarcomas, ovarian tumours and pituitary dysfunction. *Nature Genet* 21, 182-186.
- Stawiecka-Mirota, M., Kamińska, J., Urban-Grimal, D., Haines, D.S., and Żołądek, T. (2008). Nedd4, a human ubiquitin ligase, affects actin cytoskeleton in yeast cells. *Experimental Cell Research* 314, 3318-3325.
- Stein, T., Salomonis, N., and Gusterson, B. (2007). Mammary Gland Involution as a Multi-step Process. *J Mammary Gland Biol Neoplasia* 12, 25-35.
- Stein, T., Salomonis, N., Nuyten, D.A., Vijver, M., and Gusterson, B. (2009). A Mouse Mammary Gland Involution mRNA Signature Identifies Biological Pathways Potentially Associated with Breast Cancer Metastasis. *J Mammary Gland Biol Neoplasia* 14, 99-116.
- Sternlicht, M. (2006). Key stages in mammary gland development: The cues that regulate ductal branching morphogenesis. *Breast Cancer Research* 8, 201.
- Strano, S., Munarriz, E., Rossi, M., Castagnoli, L., Shaul, Y., Sacchi, A., Oren, M., Sudol, M., Cesareni, G., and Blandino, G. (2001). Physical Interaction with Yes-associated Protein Enhances p73 Transcriptional Activity. *Journal of Biological Chemistry* 276, 15164-15173.
- Sudol, M., Chen, H.I., Bougeret, C., Einbond, A., and Bork, P. (1995). Characterization of a novel protein-binding module — the WW domain. *FEBS Letters* 369, 67-71.
- Sugihara-Mizuno, Y., Adachi, M., Kobayashi, Y., Hamazaki, Y., Nishimura, M., Imai, T., Furuse, M., and Tsukita, S. (2007). Molecular characterization of angiomin/IEAP family proteins: interaction with MUPP1/Patj and their endogenous properties. *Genes to Cells* 12, 473-486.
- Tao, W., Zhang, S., Turenchalk, G.S., Stewart, R.A., St John, M.A.R., Chen, W., and Xu, T. (1999). Human homologue of the *Drosophila melanogaster* lats tumour suppressor modulates CDC2 activity. *Nat Genet* 21, 177-181.
- Thrower, J.S., Hoffman, L., Rechsteiner, M., and Pickart, C.M. (2000). Recognition of the polyubiquitin proteolytic signal. *EMBO J* 19, 94-102.
- Tonelli, Q.J., and Sorof, S. (1980). Epidermal growth factor requirement for development of cultured mammary gland. *Nature* 285, 250-252.
- Troyanovsky, B., Levchenko, T., Månsson, G., Matvijenko, O., and Holmgren, L. (2001). Angiomin: An Angiostatin Binding Protein That Regulates Endothelial Cell Migration and Tube Formation. *The Journal of Cell Biology* 152, 1247-1254.
- Udan, R.S., Kango-Singh, M., Nolo, R., Tao, C., and Halder, G. (2003). Hippo promotes proliferation arrest and apoptosis in the Salvador/Warts pathway. *Nat Cell Biol* 5, 914-920.
- Ullrich, A., and Schlessinger, J. (1990). Signal transduction by receptors with tyrosine kinase activity. *Cell* 61, 203-212.

- Ushiro, H., and Cohen, S. (1980). Identification of phosphotyrosine as a product of epidermal growth factor-activated protein kinase in A-431 cell membranes. *Journal of Biological Chemistry* 255, 8363-8365.
- Vargo-Gogola, T., and Rosen, J.M. (2007). Modelling breast cancer: one size does not fit all. *Nat Rev Cancer* 7, 659-672.
- Vassilev, A., Kaneko, K.J., Shu, H., Zhao, Y., and DePamphilis, M.L. (2001). TEAD/TEF transcription factors utilize the activation domain of YAP65, a Src/Yes-associated protein localized in the cytoplasm. *Genes Dev* 15, 1229-1241.
- Visser-Grieve, S., Zhou, Z., She, Y.-M., Huang, H., Cyr, T.D., Xu, T., and Yang, X. (2011). LATS1 tumor suppressor is a novel actin-binding protein and negative regulator of actin polymerization. *Cell Res* 21, 1513-1516.
- Vitolo, M.I., Anglin, I.E., Mahoney, W.M., Jr., Renoud, K.J., Gartenhaus, R.B., Bachman, K.E., and Passaniti, A. (2007). The RUNX2 transcription factor cooperates with the YES-associated protein, YAP65, to promote cell transformation. *Cancer Biol Ther* 6, 856-863.
- Wada, K.-I., Itoga, K., Okano, T., Yonemura, S., and Sasaki, H. (2011). Hippo pathway regulation by cell morphology and stress fibers. *Development* 138, 3907-3914.
- Wang, C., An, J., Zhang, P., Xu, C., Gao, K., Wu, D., Wang, D., Yu, H., Liu, J.O., and Yu, L. (2012). The Nedd4-like ubiquitin E3 ligases target angiomin/p130 to ubiquitin-dependent degradation. *The Biochemical journal* 444, 279-289.
- Wang, J., Peng, Q., Lin, Q., Childress, C., Carey, D., and Yang, W. (2010). Calcium Activates Nedd4 E3 Ubiquitin Ligases by Releasing the C2 Domain-mediated Auto-inhibition. *Journal of Biological Chemistry* 285, 12279-12288.
- Wang, W., Huang, J., and Chen, J. (2011). Angiomin-like Proteins Associate with and Negatively Regulate YAP1. *Journal of Biological Chemistry* 286, 4364-4370.
- Wang, X., Trotman, L.C., Koppie, T., Alimonti, A., Chen, Z., Gao, Z., Wang, J., Erdjument-Bromage, H., Tempst, P., Cordon-Cardo, C., *et al.* (2007). NEDD4-1 Is a Proto-Oncogenic Ubiquitin Ligase for PTEN. *Cell* 128, 129-139.
- Wells, A. (1999). EGF receptor. *The International Journal of Biochemistry & Cell Biology* 31, 637-643.
- Wells, C.D., Fawcett, J.P., Traweger, A., Yamanaka, Y., Goudreault, M., Elder, K., Kulkarni, S., Gish, G., Virag, C., Lim, C., *et al.* (2006). A Rich1/Amot Complex Regulates the Cdc42 GTPase and Apical-Polarity Proteins in Epithelial Cells. *Cell* 125, 535-548.
- Welsh, C.F., Roovers, K., Villanueva, J., Liu, Y., Schwartz, M.A., and Assoian, R.K. (2001). Timing of cyclin D1 expression within G1 phase is controlled by Rho. *Nat Cell Biol* 3, 950-957.
- Wolf, N., Yang, W., Dunk, C.E., Gashaw, I., Lye, S.J., Ring, T., Schmidt, M., Winterhager, E., and Gellhaus, A. (2010). Regulation of the Matricellular Proteins CYR61 (CCN1) and NOV (CCN3) by Hypoxia-Inducible Factor-1 α and Transforming-Growth Factor- β 3 in the Human Trophoblast. *Endocrinology* 151, 2835-2845.

- Wren, B.G. (2007). The origin of breast cancer. *Menopause* 14, 1060-1068.
- Wu, S., Huang, J., Dong, J., and Pan, D. (2003). Hippo Encodes a Ste-20 Family Protein Kinase that Restricts Cell Proliferation and Promotes Apoptosis in Conjunction with salvador and warts. *Cell* 114, 445-456.
- Xie, D., Nakachi, K., Wang, H., Elashoff, R., and Koeffler, H.P. (2001). Elevated Levels of Connective Tissue Growth Factor, WISP-1, and CYR61 in Primary Breast Cancers Associated with More Advanced Features. *Cancer Research* 61, 8917-8923.
- Xie, Y., Gibbs, T.C., and Meier, K.E. (2002). Lysophosphatidic acid as an autocrine and paracrine mediator. *Biochimica et Biophysica Acta (BBA) - Molecular and Cell Biology of Lipids* 1582, 270-281.
- Xu, R., Boudreau, A., and Bissell, M. (2009). Tissue architecture and function: dynamic reciprocity via extra- and intra-cellular matrices. *Cancer and Metastasis Reviews* 28, 167-176.
- Xu, T., Wang, W., Zhang, S., Stewart, R.A., and Yu, W. (1995a). Identifying tumor suppressors in genetic mosaics: the *Drosophila* *lats* gene encodes a putative protein kinase. *Development* 121, 1053-1063.
- Xu, Y., Gaudette, D.C., Boynton, J.D., Frankel, A., Fang, X.J., Sharma, A., Hurteau, J., Casey, G., Goodbody, A., and Mellors, A. (1995b). Characterization of an ovarian cancer activating factor in ascites from ovarian cancer patients. *Clinical Cancer Research* 1, 1223-1232.
- Yabuta, N., Fujii, T., Copeland, N.G., Gilbert, D.J., Jenkins, N.A., Nishiguchi, H., Endo, Y., Toji, S., Tanaka, H., Nishimune, Y., *et al.* (2000). Structure, Expression, and Chromosome Mapping of LATS2, a Mammalian Homologue of the *Drosophila* Tumor Suppressor Gene *lats/warts*. *Genomics* 63, 263-270.
- Yagi, R., Chen, L.-F., Shigesada, K., Murakami, Y., and Ito, Y. (1999). A WW domain-containing Yes-associated protein (YAP) is a novel transcriptional co-activator. *EMBO J* 18, 2551-2562.
- Yang, J., Liao, X., Agarwal, M.K., Barnes, L., Auron, P.E., and Stark, G.R. (2007). Unphosphorylated STAT3 accumulates in response to IL-6 and activates transcription by binding to NFκB. *Genes Dev* 21, 1396-1408.
- Yang, X., Yu, K., Hao, Y., Li, D.-m., Stewart, R., Insogna, K.L., and Xu, T. (2004). LATS1 tumour suppressor affects cytokinesis by inhibiting LIMK1. *Nat Cell Biol* 6, 609-617.
- Yatomi, Y., Ohmori, T., Rile, G., Kazama, F., Okamoto, H., Sano, T., Satoh, K., Kume, S., Tigyi, G., Igarashi, Y., *et al.* (2000). Sphingosine 1-phosphate as a major bioactive lysophospholipid that is released from platelets and interacts with endothelial cells. *Blood* 96, 3431-3438.
- Yeung, B., Ho, K.-C., and Yang, X. (2013). WWP1 E3 Ligase Targets LATS1 for Ubiquitin-Mediated Degradation in Breast Cancer Cells. *PLoS ONE* 8, e61027.
- Yi, C., Shen, Z., Stemmer-Rachamimov, A., Dawany, N., Troutman, S., Showe, L.C., Liu, Q., Shimono, A., Sudol, M., Holmgren, L., *et al.* (2013). The p130 Isoform of Angiomotin Is

Required for Yap-Mediated Hepatic Epithelial Cell Proliferation and Tumorigenesis. *Sci Signal* 6, ra77-.

Yi, C., Troutman, S., Fera, D., Stemmer-Rachamimov, A., Avila, Jacqueline L., Christian, N., Persson, Nathalie L., Shimono, A., Speicher, David W., Marmorstein, R., *et al.* (2011). A Tight Junction-Associated Merlin-Angiomotin Complex Mediates Merlin's Regulation of Mitogenic Signaling and Tumor Suppressive Functions. *Cancer Cell* 19, 527-540.

Yu, F.-X., Zhao, B., Panupinthu, N., Jewell, Jenna L., Lian, I., Wang, Lloyd H., Zhao, J., Yuan, H., Tumaneng, K., Li, H., *et al.* (2012). Regulation of the Hippo-YAP Pathway by G-Protein-Coupled Receptor Signaling. *Cell* 150, 780-791.

Yuh, I.S. (2011). Lysophosphatidic acid (LPA) stimulates mouse mammary epithelial cell growth. *Cell Biology International* 35, 875-881.

Zender, L., Spector, M.S., Xue, W., Flemming, P., Cordon-Cardo, C., Silke, J., Fan, S.-T., Luk, J.M., Wigler, M., Hannon, G.J., *et al.* (2006). Identification and Validation of Oncogenes in Liver Cancer Using an Integrative Oncogenomic Approach. *Cell* 125, 1253-1267.

Zhao, B. (2012). Cell detachment activates the Hippo pathway via cytoskeleton reorganization to induce anoikis. *Genes Dev* 26, 54-68.

Zhao, B., Lei, Q.-Y., and Guan, K.-L. (2008a). The Hippo-YAP pathway: new connections between regulation of organ size and cancer. *Current Opinion in Cell Biology* 20, 638-646.

Zhao, B., Li, L., Lu, Q., Wang, L.H., Liu, C.-Y., Lei, Q., and Guan, K.-L. (2011a). Angiomotin is a novel Hippo pathway component that inhibits YAP oncoprotein. *Genes Dev* 25, 51-63.

Zhao, B., Li, L., Tumaneng, K., Wang, C.-Y., and Guan, K.-L. (2010). A coordinated phosphorylation by Lats and CK1 regulates YAP stability through SCF β -TRCP. *Genes Dev* 24, 72-85.

Zhao, B., Li, L., Wang, L., Wang, C.-Y., Yu, J., and Guan, K.-L. (2012). Cell detachment activates the Hippo pathway via cytoskeleton reorganization to induce anoikis. *Genes Dev* 26, 54-68.

Zhao, B., Tumaneng, K., and Guan, K.-L. (2011b). The Hippo pathway in organ size control, tissue regeneration and stem cell self-renewal. *Nat Cell Biol* 13, 877-883.

Zhao, B., Wei, X., Li, W., Udan, R.S., Yang, Q., Kim, J., Xie, J., Ikenoue, T., Yu, J., Li, L., *et al.* (2007). Inactivation of YAP oncoprotein by the Hippo pathway is involved in cell contact inhibition and tissue growth control. *Genes Dev* 21, 2747-2761.

Zhao, B., Ye, X., Yu, J., Li, L., Li, W., Li, S., Yu, J., Lin, J.D., Wang, C.-Y., Chinnaiyan, A.M., *et al.* (2008b). TEAD mediates YAP-dependent gene induction and growth control. *Genes Dev* 22, 1962-1971.

CURRICULUM VITAE

Jacob J. Adler

EDUCATION:

- 2013 Ph.D. Indiana University, Indianapolis, IN
Department of Biochemistry and Molecular Biology
Dissertation: The Inhibition of Mammary Epithelial Cell Growth by the Long Isoform of Angiotensin II
- 2008 B.S. Purdue University, West Lafayette, IN,
Biochemistry (summa cum laude)

RESEARCH POSITIONS:

- 2009-2013 Doctoral Research: Breast Cancer Researcher, Indiana University School of Medicine
Researched the implications of the protein Angiotensin II in breast cancer signaling in relationship to polarity of epithelial cells and cellular growth; mentored 5 students
- 2009 Doctoral Research: Cancer Biomarker Researcher, Indiana University School of Medicine
Investigated the development of cisplatin resistance in breast cancer treatments
- 2008 Doctoral Research: Diabetes Researcher, Indiana University School of Medicine
Researched the effects of chromium supplements on insulin sensitivity
- 2007-2008 Undergraduate Research: Proteomics Researcher, Purdue University
Probed the use of N-terminal labeling reagents for use with quantitative proteomics studies; mentored 2 students
- 2007 Industry Research: Intern Researcher for Cargill Incorporated, Dayton, OH
Researched improvements and quality assurance in the production of high fructose corn syrup and filtration of fiber from corn starch

TEACHING POSITIONS:

- 2011-2013 National Science Foundation GK-12 Fellow, Indiana University-Purdue University Indianapolis
Instructed 15 hours weekly in Biomedical Project Lead the Way, Advanced Placement Biology and Introductory Biology courses. Mentored over 50 individual student's research projects for scientific inquiry. Incorporated cancer research into the classroom including entire units devoted to cancer biology.
- 2006-2008 Resident Assistant, Purdue University

Provided paraprofessional advising and mentoring for 60 undergraduate students. Created and presented hall programs to educate residents about critical issues in diversity, personal development, engagement, and lifelong learning.

- 2008 Biology Teaching Assistant, Purdue University
Taught two laboratory classes each week throughout the semester in introductory biology. Managed sessions improving students understanding of lab material. Student evaluations gave 99 % approval rating and 93 % of students giving a good or higher rating.
- 2005 Animal Science Teaching Assistant, Purdue University
Taught study sessions for Animal Science, Introduction to Companion Animals. Developed a discussion-based teaching environment in classes typically taught in lecture format. Recorded notes during lectures for students with disabilities.

GRANTS, AWARDS AND HONORS (selected):

- 2013 Keystone Symposia Future of Science Fund Travel Grant, \$1200
2013 Indiana University Student Spotlight for *Inside IU*
2011-2013 National Science Foundation (NSF) GK-12 Fellowship Grant, \$30,000/year
2012 Indiana University School of Medicine Graduate Student Travel Grant, \$500
2010 NSF Graduate Research Fellowship Honorable Mention
2010 Biology Concepts Exam Praxis II - Top 15 % of all test takers, Indianapolis, IN
2009-2013 Preparing Future Faculty Program Participant, Indianapolis, IN
2009-2013 Indiana University School of Medicine Graduate Student Mentor
2008 Summer Undergraduate Research, Best Senior Researcher, Purdue University
2008 Agricultural Research Scholarship Recipient, Purdue University
2006 Multicultural Coordinator, Meredith Hall, Purdue University
2006 Department of Biochemistry Outstanding Sophomore Award, Purdue University

PUBLICATIONS:

Jacob J. Adler, Johnson DE, Heller BL, Bringman LR, Ranahan WP, Conwell MD, Yang S, Hudmon A and Wells CD (2013) Serum deprivation inhibits the transcriptional co-activator YAP and cell growth via the phosphorylation of the 130-kDa isoform of Angiotensin II type 1 receptor by the LATS1/2 protein kinases, *Proceedings of the National Academy of Sciences*, Vol. 110, 43: 17368-17373.

Jacob J. Adler, Heller BL, Bringman LR, Ranahan WP, Cocklin RR, Goebel MG, Oh M, Lim H, Ingham RJ and Wells CD (2013) Amot130 Adapts Atrophen-1 Interacting Protein 4 to Inhibit Yes-associated Protein signaling and Cell Growth, *Journal of Biological Chemistry*, Vol. 288, 25: 15181-15193.

Jacob J. Adler, Judd MV, Bringman LR, Wells CD and Marrs KA (2013) Day as a Pathologist: Utilization of Technology to Guide Students in Exploring Careers in Breast Cancer Pathology, *The American Biology Teacher*, Vol. 75, 8: 559-565.

Galan JA, Paris LL, Zhang H, Jacob J. Adler, Geahlen RL and Tao WA (2011) Proteomic Studies of Syk-Interacting Proteins Using a Novel Amine-Specific Isotope Tag and GFP Nanotrap, *Journal of The American Society for Mass Spectrometry*, Vol. 22, 319-328.

PROFESSIONAL PRESENTATIONS:

Jacob J. Adler, Invited Seminar Speaker: “Balancing the Control of Breast Cancer” (2013) Department of Biological Sciences, Butler University, Indianapolis, IN

Jacob J. Adler, Invited Speaker: “The Properties of Cancer Cells” (2013) Department of Biochemistry and Molecular Biology, University of Georgia, Athens, GA

Jacob J. Adler, Invited Speaker: “The Role of Angiomotin in Hippo Signaling and Cellular Growth” (2013) Department of Cell Biology, University of Virginia School of Medicine, Charlottesville, VA

Jacob J. Adler, Platform Invited Speaker: “Amot adapts the ubiquitin ligase AIP4 to inhibit YAP signaling and cell growth” (2013) Keystone Symposia: The Hippo Tumor Suppressor Network Conference, Monterey, CA

Jacob J. Adler, Heller BL, Bringman LR and Wells CD, Poster: “Amot130 adapts the ubiquitin ligase AIP4 to inhibit YAP signaling and cell growth” (2013) Keystone Symposia: The Hippo Tumor Suppressor Network Conference, Monterey, CA

Ranahan WP, Jacob J. Adler, Heller BL and Wells CD, Poster: “Amot Family Members underlie a switch that both activates and inhibits Hippo Signaling and Cell Growth” (2013) Keystone Symposia: The Hippo Tumor Suppressor Network Conference, Monterey, CA

Jacob J. Adler, McAdams A.J., Judd MV, and Marrs KA, Poster: “Research in the Classroom: The Art of Bringing Experts into Your Classroom” (2013) Edward C. Moore Symposium on Excellence in Teaching, Indianapolis, IN

Jacob J. Adler, McAdams A.J., Judd MV, and Marrs KA, Poster: “Research in the Classroom: The Art of Bringing Experts into Your Classroom” (2013) Indiana University-Purdue University Indianapolis Research Day, Indianapolis, IN

Jacob J. Adler and Palacio L, Workshop: “Scientists in the classroom: A driving force in project centered courses” (2013) International Teacher-Scientist Partnership Conference AAAS, Boston, MA

Jacob J. Adler, Carpenter M, Manring K and Meissner D, Poster: “IUPUI GK-12 Urban Educators Program” (2013) AAAS Annual Meeting, Boston, MA

Jacob J. Adler, Cooper GL, Judd MV, Wells CD and Marrs KA, Poster: “Breast cancer analysis in the advanced placement biology classroom” (2012) 60th NSTA National Conference on Science Education, Indianapolis, IN

Judd MV, Jacob J. Adler and Marrs KA, Workshop: “Thinking like a scientist: Lessons learned in the NSF-funded K-12 experience” (2012) 60th NSTA National Conference on Science Education, Indianapolis, IN

Jacob J. Adler, Heller BL, Tucheck CA and Wells CD, Poster: “The Amot family of proteins binds and activates Nedd4 family ligases to promote the ubiquitination of LATS and YAP” (2012)

National Science Foundation Graduate STEM Fellows in K-12 Education Annual Conference, Washington D.C.

Judd MV, Jacob J. Adler, Cooper GL and Marrs KA, Workshop: “The power of the pair: Taking an innovative approach to optimizing mentorship through creating strong GK-12 partners” (2012) National Science Foundation Graduate STEM Fellows in K-12 Education Annual Conference, Washington D.C.

Jacob J. Adler, Heller BL, Tucheck CA and Wells CD, Poster: “The Amot family of proteins binds and activates Nedd4 family ligases to promote the ubiquitination of LATS and YAP” (2012) Indiana University-Purdue University Indianapolis Research Day, Indianapolis, IN

Jacob J. Adler, Cooper GL, Judd MV, Wells CD and Marrs KA, Poster: “Breast cancer analysis in the advanced placement biology classroom” (2012) Indiana University-Purdue University Indianapolis Research Day, Indianapolis, IN

Jacob J. Adler, Platform Presentation: “The Amot family of proteins binds and activates Nedd4 family ligases to promote the ubiquitination of YAP” (2012) Department of Biochemistry Research Seminar, Indianapolis, IN

Jacob J. Adler, Guo M, Paris LL, Geahlen RL and Tao WA, Poster: “Identification of phosphorylation-dependent proteins in B cells using novel quantitative proteomics strategy” (2008) Summer Undergraduate Research Fellowship Program, Purdue University, West Lafayette, IN

Jacob J. Adler, Guo M, Paris LL, Geahlen RL and Tao WA, Poster: “Stable isotopic labeling utilizing SILAG reagents: Identification of phosphorylation-dependent proteins in B cells using novel quantitative proteomics strategy” (2007) Department of Biochemistry Research Retreat, Purdue University, West Lafayette, IN

MEMBERSHIP IN PROFESSIONAL SOCIETIES (Current Only):

2013-Present American Society for Cell Biology, National
2012-Present The Business of Life Sciences Collaboration, Indianapolis, IN
2011-Present Graduate STEM Fellows in K-12 Education, National
2007-Present Phi Beta Kappa Honorary Fraternity, National

RESEARCH BASED SKILLS:

Protein immunoprecipitation and pull-down techniques
SDS-PAGE, Western Blot and other biochemical techniques
Cloning techniques: primer design, gene amplification and plasmid modification
Mammalian tissue culture (primary, stable cell lines, 3D Matrigel)
Lentivirus/Retrovirus production and transduction
Confocal microscopy of immunofluorescence staining and live cells
Real time PCR and mRNA isolation
LC-MS, Thermo LTQ
MALDI-TOF
Statistical analysis
Research and model testing
Problem solving

Hypothesis testing
Innovation utilizing limited resources
Resourceful and effective work ethic
Approach unfamiliar problems and recognize the underlying connections
Microsoft: Word, Excel, PowerPoint
Adobe: Photoshop, Illustrator, Acrobat Pro
Scientific: Blast, ClustalW, pDRAW32, ImageJ, LightCycler, SEQUEST, Institute of Systems
Biology Protein/Peptide Prophet

TEACHING BASED SKILLS:

Course design and curriculum management
Blackboard Learning
Education manuscript publication
Lesson plan development
Instructional design, delivery and assessment
Differentiated instruction
Mentor independent research
Website preparation and design
Non-technical summaries of my research for distribution
Press releases
Public lectures to non-scientists
Website aimed for general public
Science fair competition judge
Journalist interviews for Internet, TV, newspaper and magazines
Scientific blog publication
Dean and Faculty Search

Specific Topics Include: The Scientific Method, Biostatistics, Cell Theory and Properties, pH and Buffers, Enzymes, Cancer Biology, Breast Cancer, Lipids, Metabolism, Membrane Biology, Photosynthesis, Protein Biology, Lab Skills and Report Documentation, Peer-Review, Collaboration, Scientific Writing, Scientific Presentations, Personalized Medicine, Cell Cycle